

Generalized free energy and excess entropy production for active systems

Artemy Kolchinsky,^{1,2} Andreas Dechant,³ Kohei Yoshimura,⁴ and Sosuke Ito^{2,4}

¹ICREA-Complex Systems Lab, Universitat Pompeu Fabra, 08003 Barcelona, Spain

²Universal Biology Institute, The University of Tokyo, 7-3-1 Hongo, Bunkyo-ku, Tokyo 113-0033, Japan

³Department of Physics No. 1, Graduate School of Science, Kyoto University, Kyoto 606-8502, Japan

⁴Department of Physics, The University of Tokyo, 7-3-1 Hongo, Bunkyo-ku, Tokyo 113-0033, Japan

We propose a generalized free energy potential for active systems, including both stochastic master equations and deterministic nonlinear chemical reaction networks. Our generalized free energy is defined variationally as the “most irreversible” state observable. This variational principle is motivated from several perspectives, including large deviations theory, thermodynamic uncertainty relations, Onsager theory, and information-theoretic optimal transport. In passive systems, the most irreversible observable is the usual free energy potential and its irreversibility is the entropy production rate (EPR). In active systems, the most irreversible observable is the generalized free energy and its irreversibility gives the excess EPR, the nonstationary contribution to dissipation. The remaining “housekeeping” EPR is a genuine nonequilibrium contribution that quantifies the nonconservative nature of the forces. We derive far-from-equilibrium thermodynamic speed limits for excess EPR, applicable to both linear and nonlinear systems. Our approach overcomes several limitations of the steady-state potential and the Hatano-Sasa (adiabatic/nonadiabatic) decomposition, as we demonstrate in several examples.

I. INTRODUCTION

Thermodynamics is one of the most far-reaching and useful theoretical frameworks in the physical sciences. Traditionally, this framework was mainly used to study “passive” systems, which tend to detail-balanced equilibrium states when allowed to relax freely. Many of the thermodynamic, dynamical, and statistical properties of passive systems are governed by the free energy potential. For instance, passive systems have conservative thermodynamic forces, which can be written as the gradient of this potential. In addition, the free energy determines the availability of extractable work [1, 2], guarantees the stability of equilibrium states [3], and governs steady-state fluctuations [4, 5].

In nonequilibrium thermodynamics, dissipation is quantified using the entropy production rate (EPR), the rate of entropy increase in a system and its environment. In passive systems, EPR is proportional to the decrease of free energy over time, and it vanishes in then equilibrium steady state, where free energy remains constant. The connection between dissipation and nonstationarity also appears in the Clausius equality, which states that overall dissipation vanishes in the limit of slow evolution. More recently, this connection has been used to derive “thermodynamic speed limits”, which relate the time and dissipation needed to transform a system between two states [6–10]. In fact, the minimal dissipation required to go between two states in a given time defines a thermodynamic notion of distance. In the near-equilibrium regime, this distance leads to the geometry of “thermodynamic length” [11–14]. Far from equilibrium, it leads to the Wasserstein geometry of thermodynamic optimal transport [15–22].

Recently, research interest has shifted to active systems that undergo continuous driving and do not relax toward equilibrium. Active systems may be driven by nonequilibrium boundary conditions, applied mechanical forces (e.g., stirring), or internal fuel sources (e.g., active matter [23]). For example, living cells maintain nonequilibrium concentration of ATP, which then drives active molecular machines like ribosomes. Active systems exhibit nonconservative forces that cannot be

written as the gradient of any free energy potential. Moreover, they relax to nonequilibrium steady states, or even limit cycles and chaos in the case of nonlinear dynamics. Because there is no direct relationship between dissipation and speed of evolution in active systems, standard inequalities that relate entropy production and nonstationarity, such as the Clausius inequality and thermodynamic speed limits, become very weak, or simply inapplicable, in active systems.

Nonetheless, there has long been interest in identifying a generalized free energy potential for active systems [24–27], as well as a renormalized notion of *excess EPR* [20, 28–36]. In general terms, excess EPR is the nonstationary component of dissipation that is associated with the generalized free energy and vanishes in steady state. Among other applications, excess EPR may lead to bounds — such as thermodynamic speed limits [6, 8, 10, 37] and generalized Clausius inequalities [35, 38, 39] — that are tight even in active systems. The remaining non-excess contribution, which does not vanish even in steady state, is called the *housekeeping EPR*. It is a genuine nonequilibrium contribution associated with nonconservative forces and cyclic fluxes that cause steady-state dissipation.

The best-known definition of the generalized free energy is based on nonequilibrium steady states. Here, the generalized free energy is defined as the relative entropy between the actual state and the steady state, and the excess EPR is defined as the decrease of this generalized free energy over time. This leads to the Hatano-Sasa (HS) decomposition into excess and housekeeping EPR, also called the nonadiabatic/adiabatic decomposition [31, 32, 40–42]. The steady-state approach is useful in many applications, especially for studying stability and fluctuations near steady states. However, as we discuss below, it has several drawbacks for studying nonstationary systems, such lacking a clear physical interpretation, not being “local in time”, and having a limited domain of applicability.

In this paper, we propose a new notion of the generalized free energy and excess/housekeeping for active systems. Our approach applies to a broad class of linear and nonlinear discrete systems, including stochastic master equations and deterministic chemical reaction networks (CRNs). Moreover, it avoids

	Generalized free energy potential ϕ^*	Section	Steady-state potential ϕ^{ss}
Applicability	All MJPs and CRNs	§II	MJPs w/o odd variables, CRNs with complex balance
Definition	$\dot{x} = -\nabla^\top (j \circ e^{\nabla\phi^*})$	§IV-V	$\phi^{ss} = \ln \frac{x}{x^{ss}}$
Excess/housekeeping decomposition	Information-geometric decomposition	§VD	Hatano-Sasa a.k.a. adiabatic/nonadiabatic
Linear response transport coefficients	Mean-squared displacement	§VF	Green-Kubo relations
Large deviations	Dynamical fluctuations	§VI	Steady-state fluctuations
Thermodynamic speed limit	Wasserstein speed	§VII	Total variation speed

Table I. Summary of our main definitions and results, and comparison with the steady-state/Hatano-Sasa approach.

several drawbacks of the steady-state approach. For one, all relevant quantities are physically meaningful, being directly related to measurable properties of a system at a given point in time. In addition, our formulation does not make explicit reference to the steady state, or any other special state. For this reason, it generalizes to a broad class of systems, including general nonlinear CRNs without steady states and stochastic systems with odd variables. A brief summary of our main results, as well as a comparison with the steady-state approach, is provided in Table I.

The central idea of this work is that the generalized free energy and excess EPR can be derived from a variational principle — that is, as the solution to an optimization problem. The free energy potential is defined as the “most irreversible” state observable, while the excess EPR is its degree of irreversibility. The irreversibility of an observable can be understood as its rate of change relative to its dynamical fluctuations. This measure of irreversibility is experimentally accessible and, as we show below, it has natural interpretations in terms of large deviations theory, thermodynamic uncertainty relations, Onsager theory, and information-theoretic optimal transport.

In passive systems, the most irreversible observable is the usual free energy potential, and its degree of irreversibility is the EPR. In active systems, the most irreversible observable is the generalized free energy potential, and its degree of irreversibility is the excess EPR. Excess EPR vanishes in steady state, when all state observables are constant, thus it quantifies the nonstationary contribution to dissipation. This leads to an excess/housekeeping decomposition, where the housekeeping EPR (the non-excess contribution) is shown to quantify the nonconservative nature of the thermodynamic forces. Our decomposition is universally applicable, and it has an appealing interpretation in terms of the Pythagorean relation from information geometry.

By exploiting the relationship between excess EPR and non-stationarity, we derive a set of thermodynamic speed limits for excess entropy production. In particular, we derive a speed limit based on 1-Wasserstein distance, an optimal-transport

distance that is sensitive to the system’s topology [10, 43]. Our speed limits can be tight even in the far-from-equilibrium regime, and they apply to both linear and nonlinear systems.

The paper is laid out as follows. In the next section, we describe our physical setup and formalism. Background Section III discusses free energy in passive systems, and its generalization to active systems based on nonequilibrium steady states. We introduce our variational principle for passive systems in Section IV and for active systems in Section V. There we also introduce our excess/housekeeping decomposition and propose an important “coarse-graining” principle. We also consider the linear-response regime, making important connections to Onsager theory and thermodynamic length, and compare with the HS approach. In Section VI, we discuss operational interpretations of our measures based on dynamical large deviations and thermodynamic uncertainty relations. In Section VII, we derive several thermodynamic speed limits for excess entropy production.

In Section VIII, we illustrate our results on two examples: a unicyclic master equation and the Brusselator, a nonlinear chemical oscillator.

We finish with a summary and suggestions for future work in Section IX. In addition, Appendices A and B discuss generalizations to systems with external flows and odd variables. Supporting derivations are found in the Supplemental Material (SM) [44]. The SM also includes comparisons with some recent proposals, such as EPR decompositions based on Euclidean geometry [20] and so-called “Hessian geometry” [45, 46].

II. SETUP AND PRELIMINARIES

Before proceeding, we introduce notation. Vectors are written in bold, $\mathbf{a} = (a_1, a_2, \dots) \in \mathbb{R}^d$, including the special vectors $\mathbf{0} = (0, 0, 0, \dots)$ and $\mathbf{1} = (1, 1, 1, \dots)$. We use $e^{\mathbf{a}}, \mathbf{a}^2, |\mathbf{a}| \dots$ to indicate element-wise operations, for

example $e^{\mathbf{a}} := (e^{a_1}, e^{a_2}, \dots)$. The notation $\mathbf{a} \circ \mathbf{b} := (a_1 b_1, a_2 b_2, \dots)$ indicates element-wise multiplication, while $\mathbf{a}/\mathbf{b} := (a_1/b_1, a_2/b_2, \dots)$ indicates element-wise division. As discussed below, ∇ refers to the stoichiometric matrix (which acts like the discrete gradient operator). To avoid confusion, we write the usual gradient of a function $f : \mathbb{R}^d \rightarrow \mathbb{R}$ as $\text{grad}_{\mathbf{x}} f = (\partial_{x_1} f, \dots, \partial_{x_d} f)$.

A. States, reactions, and dynamics

We focus on discrete Markovian systems with linear and nonlinear dynamics. This includes Markov jump processes (MJP) with linear dynamics that represent the transport of probability between microstates. It also includes deterministic chemical reaction networks (CRNs), often used for modeling biological and chemical systems in the large-volume limit [41, 47, 48]. CRNs have nonlinear dynamics that represent macroscopic transport of matter between chemical species. Extensions to continuous-state systems are briefly mentioned in Section VF and non-Markovian systems in Section IX.

The system's thermodynamic *state* at time t is specified by a nonnegative vector $\mathbf{x}(t) = (x_1(t), \dots, x_d(t)) \in \mathbb{R}_+^d$. We often simply write the state \mathbf{x} , leaving dependence on time implicit. In an MJP, the state is a normalized probability distribution over d microstates (or, more generally, “mesostates”). In a deterministic chemical reaction network (CRN), the state is the unnormalized vector of concentrations of d chemical species.

We always use the term *state* to refer to the system's thermodynamic state \mathbf{x} ; when referring to the microstates or species, we do so explicitly. The term *state function* refers to functions of the state, $f : \mathbb{R}^d \rightarrow \mathbb{R}$. The term *state observable* refers to functions over microstates/species, represented by a vector $\phi \in \mathbb{R}^d$.

The system is also associated with m one-way *reactions* indexed by $\rho \in \{1, \dots, m\}$. These reactions corresponds to transitions between microstates in an MJP, or one-way chemical reactions in a CRN. We use the term *reaction observable* to refer to functions of individual reactions, represented by a vector $\theta \in \mathbb{R}^m$.

The one-way *flux* $j_\rho(\mathbf{x}, t)$ of reaction ρ is the expected number of reactions per unit time and volume. The dependence of the fluxes $j_\rho(\mathbf{x}, t)$ on the state \mathbf{x} reflects system-specific kinetics. Explicit dependence of $j_\rho(\mathbf{x}, t)$ on time t reflects external driving, i.e., changing control parameters. Except where otherwise noted, we make no assumptions about the kinetics or external driving. The entire set of one-way fluxes is represented by the vector $\mathbf{j}(\mathbf{x}, t) = (j_1(\mathbf{x}, t), \dots, j_m(\mathbf{x}, t)) \in \mathbb{R}_+^m$. Where clear from context, we often write $\mathbf{j}(\mathbf{x})$, $\mathbf{j}(t)$ or \mathbf{j} , leaving dependence on state and/or time implicit.

The system's state evolves according to

$$\dot{\mathbf{x}} = \nabla^\top \mathbf{j}, \quad (1)$$

where $\nabla \in \mathbb{Z}^{m \times d}$ is matrix whose entries $\nabla_{\rho i}$ indicate the number of i created or destroyed by reaction ρ . This matrix acts like the discrete gradient operator: the net increase of any state observable ϕ due to reaction ρ is $[\nabla \phi]_\rho = \sum_i \nabla_{\rho i} \phi_i$.

The transpose ∇^\top acts as the negative discrete divergence operator, so Eq. (1) can be interpreted as a discrete continuity equation. The matrix ∇^\top is often called the “incidence matrix” in MJPs and the “stoichiometric matrix” in CRNs.

B. Thermodynamic forces and entropy production

In order to define thermodynamic quantities, each one-way reaction ρ is associated with a *reverse flux* \tilde{j}_ρ , where $\tilde{\mathbf{j}} = (\tilde{j}_1, \dots, \tilde{j}_m)$ indicates the vector of reverse fluxes. We sometimes refer to \mathbf{j} as the *forward fluxes* to distinguish them from the reverse fluxes $\tilde{\mathbf{j}}$. Each reaction ρ is associated with a (*thermodynamic*) *force*, also called “reaction affinity”. It is defined as the log-ratio of the forward and reverse fluxes,

$$f_\rho := \ln \frac{j_\rho}{\tilde{j}_\rho}. \quad (2)$$

We represent the forces across all reactions using the vector

$$\mathbf{f} = \ln \frac{\mathbf{j}}{\tilde{\mathbf{j}}} = (f_1, \dots, f_m) \in \mathbb{R}^m.$$

Like the fluxes, the forces may depend on the current state \mathbf{x} and on time t , although we leave this dependence implicit in our notation.

For simplicity, we mainly focus on systems without odd variables (such as velocity or momenta). However, many of our results generalize to systems with odd variables. See Appendix B for more details, including a detailed example and comparison with the HS decomposition.

In systems without odd variables, each reaction $\rho \in \{1, \dots, m\}$ is associated one-to-one with a reverse reaction $\tilde{\rho} \in \{1, \dots, m\}$ with opposite stoichiometry ($\nabla_{\rho i} = -\nabla_{\tilde{\rho} i}$). The reverse flux \tilde{j}_ρ of reaction ρ is the forward flux of reaction $\tilde{\rho}$,

$$\tilde{j}_\rho = j_{\tilde{\rho}}. \quad (3)$$

Because reversal is one-to-one, forward and reverse fluxes have the same sum,

$$\sum_\rho j_\rho = \sum_\rho \tilde{j}_\rho. \quad (4)$$

Also, since reverse reactions have opposite stoichiometry, the continuity equation (1) can be written as

$$\dot{\mathbf{x}} = \nabla^\top \mathbf{j} = \frac{1}{2} \nabla^\top (\mathbf{j} - \tilde{\mathbf{j}}). \quad (5)$$

Our main thermodynamic quantity of interest is the entropy production rate (EPR). For systems without odd variables, the EPR is written as

$$\sigma = \sum_\rho j_\rho \ln \frac{j_\rho}{\tilde{j}_\rho} = \mathbf{j}^\top \mathbf{f}. \quad (6)$$

Using Eq. (3), we may also write it as

$$\sigma = \frac{1}{2} \sum_\rho (j_\rho - \tilde{j}_\rho) \ln \frac{j_\rho}{\tilde{j}_\rho} \geq 0. \quad (7)$$

Example: 2-level Markov jump process (MJP)

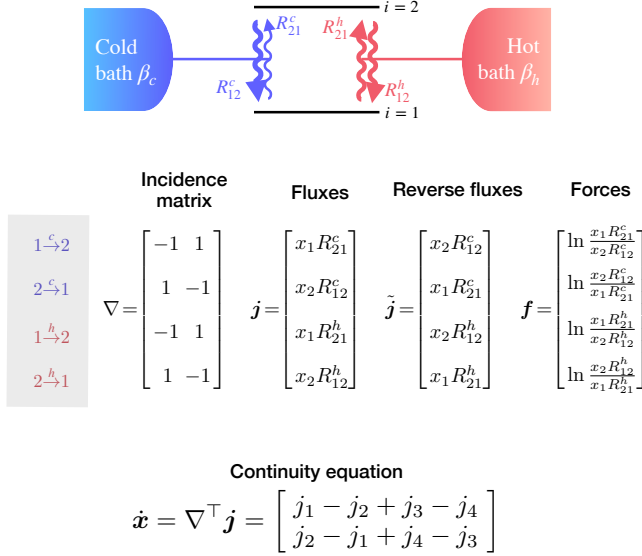


Figure 1. **Formalism illustrated on a simple MJP, a two-level system coupled to a pair of heat baths.** Transitions between the two levels occur with rates R_{21}^c and R_{12}^c when exchanging energy with the cold bath (at inverse temperature β_c), and with rates R_{21}^h and R_{12}^h when exchanging energy with the hot bath (at inverse temperature β_h). This gives four one-way transitions, here characterized by the incidence matrix, forward and reverse flux vectors, and force vector.

The total entropy production (EP) incurred over time $0 \leq t \leq T$ is given by the time integral

$$\Sigma = \int_0^T \sigma(t) dt, \quad (8)$$

where $\sigma(t)$ is the EPR incurred by the fluxes at time t , $\mathbf{j}(t)$. In the following, we usually write thermodynamic quantities such as EPR, free energy, chemical potentials, etc. in dimensionless units (i.e., units are chosen so that k_B , $k_B T$, RT , etc. are equal to unity).

Eq. (7) implies that EPR vanishes only when the reverse and forward fluxes are equal ($\mathbf{j} = \tilde{\mathbf{j}}$), equivalently when the forces vanish ($\mathbf{f} = \mathbf{0}$). Thus, EPR quantifies the difference between forward and reverse flux vectors, being a measure of dynamical irreversibility. EPR acquires additional thermodynamic meaning when *local detailed balance* (LDB) holds, which says that the force f_ρ associated with each reaction ρ is equal to the increase of thermodynamic entropy of the system and its environment due to that reaction [48–50]. When LDB holds, EPR is equal to the expected rate of increase of the thermodynamic entropy of the system and its environment.

C. Example: Markov jump process (MJP)

To illustrate our formalism, consider an MJP that represents a stochastic system with d microstates, coupled to one or more thermodynamic reservoirs indexed by α . The probability dis-

tribution \mathbf{x} evolves according to a master equation,

$$\dot{x}_i = \sum_{\alpha} \sum_{j=1}^d (x_j R_{ij}^{\alpha} - x_i R_{ji}^{\alpha}), \quad (9)$$

where R_{ji}^{α} is the transition rate from microstate i to microstate j mediated by reservoir α .

In our formalism, each transition $i \rightarrow j$ mediated by reservoir α is associated with a one-way reaction ρ , with corresponding incidence matrix entries

$$\nabla_{\rho k} = \delta_{kj} - \delta_{ki}, \quad (10)$$

and flux $j_\rho = x_i R_{ji}^{\alpha}$. The reverse flux $\tilde{j}_\rho = x_j R_{ij}^{\alpha}$ is the flux across the reverse reaction $\tilde{\rho}$, which corresponds to the transition $j \rightarrow i$ mediated by α . Given these definitions, the continuity equation (1) is equivalent to the master equation (9). The force across each reaction is

$$f_\rho = \ln \frac{j_\rho}{\tilde{j}_\rho} = \ln \frac{R_{ji}^{\alpha} x_i}{R_{ij}^{\alpha} x_j}, \quad (11)$$

In Figure 1, we illustrate our formalism on a simple MJP, representing a two-level system coupled to a pair of heat baths. We consider this example again in Section VB below.

D. Example: chemical reaction network (CRNs)

Consider a CRN with d chemical species, where the state $\mathbf{x} \in \mathbb{R}_+^d$ is the concentration vector. Suppose that the CRN contains k reversible reactions,

$$\sum_{i=1}^d \nu_{ri} X_i \rightleftharpoons \sum_{i=1}^d \kappa_{ri} X_i \quad \forall r \in \{1, \dots, k\}, \quad (12)$$

where ν_{ri} and κ_{ri} specify the stoichiometry of species i as reactant and product in reaction r . The forward and reverse fluxes across each reversible reaction r are indicated as j_r^+ and j_r^- . These fluxes will depend on the concentration vector \mathbf{x} , possibly in a nonlinear manner. For instance, for mass-action kinetics, the forward flux for reaction r is

$$j_r^+ = k_r^+ \prod_{i=1}^d x_i^{\nu_{ri}}, \quad (13)$$

where k_r^+ is the forward rate constant of reaction r . However, except where otherwise noted, we do not assume mass-action kinetics.

In our formalism, each reversible reaction $r \in \{1, \dots, k\}$ is treated as two one-way reactions $\rho, \tilde{\rho}$, with fluxes $j_\rho = j_r^+$, $\tilde{j}_\rho = j_r^-$ and stoichiometry $\nabla_{\rho i} = \kappa_{ri} - \nu_{ri} = -\nabla_{\tilde{\rho} i}$. The concentration vector \mathbf{x} evolves according to Eq. (1), sometimes called the “reaction rate equation” in the CRN literature.

Importantly, the CRN may be open in that reactions involve exchanges of external species, beyond the d species represented by the concentration vector. In such cases, the concentrations of external species may influence the (pseudo) rate constants

Example: Chemical Reaction Network (CRN)

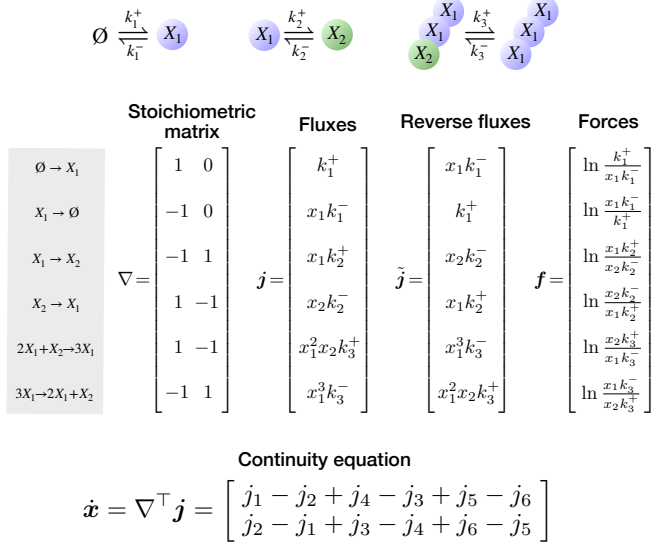


Figure 2. **Formalism illustrated on the Brusselator, a non-linear CRN that can exhibit oscillations.** There are three reversible reactions: $\emptyset \rightleftharpoons X_1$ (inflow), $X_1 \rightleftharpoons X_2$ (conversion), and $2X_1 + X_2 \rightleftharpoons 3X_1$ (second-order autocatalysis). There are six one-way reactions, here characterized by the stoichiometric matrix, forward and reverse flux vectors, and thermodynamic forces.

of the reactions. In particular, this allows us to account for *chemostatted* species, often used to study active CRNs in the literature [41]. For simplicity, we assume that there are no external inflows/outflows, so that the concentrations evolve only due to reactions. See Appendix A for a generalization of our formalism that accounts for external flows.

In Figure 2, we illustrate our formalism on the Brusselator [51], a simple CRN that can exhibit oscillations. We also consider this example in Section VIII B below.

E. Relative entropy

Relative entropy is an information-theoretic measure of divergence that plays a central role in our work.

The relative entropy between a pair of states $\mathbf{x}, \mathbf{y} \in \mathbb{R}_+^d$ is defined as

$$D(\mathbf{x} \parallel \mathbf{y}) := \sum_{i=1}^d \left(x_i \ln \frac{x_i}{y_i} - x_i + y_i \right). \quad (14)$$

This is a nonnegative quantity that vanishes only when $\mathbf{x} = \mathbf{y}$. Observe that we use a generalized version of relative entropy, appropriate for unnormalized states that do not have to sum to unity (e.g., concentration vectors in CRNs). For normalized probability distribution, it reduces to the well-known Kullback-Leibler divergence, $D(\mathbf{x} \parallel \mathbf{y}) := \sum_{i=1}^d x_i \ln \frac{x_i}{y_i}$.

We will also use the relative entropy between flux vectors.

Given a pair of flux vectors $\mathbf{j}, \mathbf{j}' \in \mathbb{R}_+^m$, it is

$$\mathcal{D}(\mathbf{j} \parallel \mathbf{j}') := \sum_{\rho=1}^m \left(j_\rho \ln \frac{j_\rho}{j'_\rho} - j_\rho + j'_\rho \right). \quad (15)$$

We use the calligraphic \mathcal{D} (rather than D) to distinguish the relative entropy defined over fluxes.

Importantly, the EPR can be written as the relative entropy between the forward and reverse flux vectors,

$$\sigma = \mathcal{D}(\mathbf{j} \parallel \tilde{\mathbf{j}}) = \sum_{\rho} \left(j_\rho \ln \frac{j_\rho}{\tilde{j}_\rho} - j_\rho + \tilde{j}_\rho \right) \geq 0. \quad (16)$$

For systems without odd variables, this follows Eqs. (6) and (4). However, Eq. (16) also correctly captures EPR for systems with odd variables, where Eq. (6) may not apply (see Appendix B).

III. BACKGROUND ON FREE ENERGY

In this section, we review the concept of free energy in passive systems. We then discuss a proposed generalization to active systems based on nonequilibrium steady states.

A. Free energy in passive systems

We use the term *passive* to refer to a system that is governed by a free energy function $\mathcal{F}(\mathbf{x}, t)$. Formally, this means that the thermodynamic forces can be expressed in terms of the chemical potential $\boldsymbol{\mu} = \text{grad}_{\mathbf{x}} \mathcal{F}(\mathbf{x}, t)$ as

$$\mathbf{f} = -\nabla \boldsymbol{\mu}. \quad (17)$$

Here, $\nabla \in \mathbb{R}^{m \times d}$ is the discrete gradient operator defined above and we consider \mathcal{F} and $\boldsymbol{\mu}$ in dimensionless units. Forces that have the form (17) are termed *conservative forces*.

The dynamic evolution of a passive system is a gradient flow for the free energy function. To show this, we rewrite the continuity equation (5) as

$$\dot{\mathbf{x}} = \frac{1}{2} \nabla^\top (\mathbf{j} - \tilde{\mathbf{j}}) = \nabla^\top L \mathbf{f} = -\nabla^\top L \nabla \boldsymbol{\mu}, \quad (18)$$

where L is a diagonal matrix with entries $L_{\rho\rho} = \frac{1}{2} j_\rho (1 - e^{-f_\rho}) / f_\rho \geq 0$. Given the definition of $\boldsymbol{\mu}$, the continuity equation can be written as a gradient flow:

$$\dot{\mathbf{x}} = -(\nabla^\top L \nabla) \text{grad}_{\mathbf{x}} \mathcal{F}. \quad (19)$$

Observe that $\nabla^\top L \nabla$ is a positive-semidefinite matrix. Therefore, if there is no external driving (\mathcal{F} does not depend explicitly on time), the free energy function decreases monotonically over time, until the system reaches an equilibrium state \mathbf{x}^{eq} of minimal free energy. Thus, if a passive system is allowed to relax freely, it tends toward equilibrium.

In fact, the above relations imply that the EPR (6) is the rate of decrease of free energy,

$$\sigma = -\mathbf{j}^\top \nabla \boldsymbol{\mu} = -\dot{\mathbf{x}}^\top \boldsymbol{\mu} = -\partial_t \mathcal{F}(\mathbf{x}(t), s)|_{s=t}. \quad (20)$$

Once the system reaches equilibrium \mathbf{x}^{eq} and the free energy stops decreasing, the forces vanish:

$$\mathbf{f} = -\nabla \mu^{\text{eq}} = \mathbf{0} \quad \mu^{\text{eq}} = \text{grad}_{\mathbf{x}} \mathcal{F}(\mathbf{x}^{\text{eq}}, t).$$

Thus, in equilibrium, the forward and backward fluxes obey the condition of *detailed balance*,

$$\mathbf{j}(\mathbf{x}^{\text{eq}}) = \tilde{\mathbf{j}}(\mathbf{x}^{\text{eq}}). \quad (21)$$

The equilibrium state is stationary, as follows from Eq. (5).

The expression of conservative forces (17) is invariant if μ is shifted by any null vector of ∇ . Such null vectors represent conserved quantities that do not affect thermodynamic forces. For our purposes, it will be convenient to consider the equilibrium chemical potential μ^{eq} as the null vector, then define $\phi^{\text{eq}} = \mu - \mu^{\text{eq}}$ as the nonequilibrium contribution to the chemical potential. Using $-\nabla \mu^{\text{eq}} = \mathbf{0}$, we have

$$\mathbf{f} = -\nabla \phi^{\text{eq}} \quad (22)$$

We will refer to ϕ^{eq} simply as the “free energy potential”.

So far, our statements apply to general passive systems. However, for MJPs and ideal CRNs with mass-action kinetics, things become less abstract. In that case, the free energy potential ϕ^{eq} has an explicit form, as the gradient of the relative entropy between the current state and the equilibrium state:

$$\phi^{\text{eq}} = \text{grad}_{\mathbf{x}} D(\mathbf{x} \parallel \mathbf{x}^{\text{eq}}) \quad \phi_i^{\text{eq}} = \ln \frac{x_i}{x_i^{\text{eq}}}. \quad (23)$$

As a concrete example, consider a passive MJP governed by the master equation (9). Suppose there is a single reservoir and that each transition $\rho = (i \rightarrow j)$ has a conservative force,

$$f_\rho = \ln \frac{x_i}{x_i^{\text{eq}}} - \ln \frac{x_j}{x_j^{\text{eq}}} = [-\nabla \phi^{\text{eq}}]_\rho. \quad (24)$$

Recall that $f_\rho = \ln(x_i R_{ji}/x_j R_{ij})$ by the definition of the forces. Combining shows that \mathbf{x}^{eq} is an equilibrium state that obeys detailed balance,

$$x_i^{\text{eq}} R_{ji} = x_j^{\text{eq}} R_{ij}. \quad (25)$$

Conversely, if there is some equilibrium state \mathbf{x}^{eq} that obeys detailed balance, it follows from the definition of the forces that they have the conservative form (24).

The relative entropy in Eq. (23) quantifies the nonequilibrium contribution to the free energy [2],

$$D(\mathbf{x} \parallel \mathbf{x}^{\text{eq}}) = \mathcal{F}(\mathbf{x}) - \mathcal{F}(\mathbf{x}^{\text{eq}}). \quad (26)$$

This relative entropy appears under many names in the literature, including “pseudo-Helmholtz function” [41], “shear Lyapunov function” [41], negative “nonequilibrium Massieu potential” [52], or simply “free energy” [5, 25, 53, 54]. Moreover, it plays many roles in the thermodynamics of passive MJPs and ideal CRNs. For instance, it is proportional to the maximal work that can be extracted by bringing the system from \mathbf{x} to \mathbf{x}^{eq} in a controlled manner [1, 2, 41]. Conversely, the loss of relative entropy due to relaxation is equal to EPR,

$$\sigma = -\dot{\mathbf{x}}^\top \phi^{\text{eq}} = -\partial_t D(\mathbf{x}(t) \parallel \mathbf{x}^{\text{eq}}(s))|_{s=t} \geq 0. \quad (27)$$

This follows from Eq. (20) since \mathcal{F} and the relative entropy differ by an equilibrium contribution that does not depend on \mathbf{x} . Thus, we may also consider the dynamics (19) as a gradient flow for the relative entropy.

This relative entropy also has a statistical interpretation in large deviations theory. To introduce this interpretation, consider an MJP in equilibrium and let the random variable $\mathbf{X}_n^{\text{eq}} \in \mathbb{R}_+^d$ represent the empirical occupation frequencies of microstates, as measured from n independent and identical copies of the system (or n independent and identical measurements performed on a single system). For large n , the probability of observing some state \mathbf{x} as a statistical fluctuation is governed by a large deviations principle [4, 5, 55],

$$P(\mathbf{X}_n^{\text{eq}} \approx \mathbf{x}) \asymp e^{-nD(\mathbf{x} \parallel \mathbf{x}^{\text{eq}})}. \quad (28)$$

In this notation, \approx indicates equality up to an arbitrarily small fixed error, while \asymp indicates equality up to sub-exponential factors in n (see Ref. [56] for details). Eq. (28) implies that states with higher free energy are exponentially more unlikely to appear as statistical fluctuations in equilibrium. A similar expression can be derived for concentration fluctuations in ideal stochastic chemical systems, where the scaling parameter n indicates reactor volume [57].

B. The steady-state approach to active systems

Recent work in thermodynamics has focused on *active* systems. In active systems, the thermodynamic forces are not conservative, meaning that they cannot be expressed in the form of Eq. (22) for any ϕ . Such systems are not governed by a free energy function and the steady state does not satisfy detailed balance.

Nonetheless, it has been suggested that it may be possible to define a “generalized” free energy for active systems. A related idea is that the EPR in active systems may be decomposed into an excess term and a housekeeping term, as in

$$\sigma = \sigma_{\text{ex}} + \sigma_{\text{hk}}. \quad (29)$$

The excess term is usually associated with the generalized free energy, while the housekeeping term is the genuine nonequilibrium contribution that cannot be associated with any potential.

The best-known generalized free energy and excess/housekeeping decomposition is based on nonequilibrium steady states [31, 58, 59]. Here, the role of the equilibrium state is played by the steady state \mathbf{x}^{ss} , which is determined by the control parameters at a given instant in time. By definition, the steady state satisfies the condition of stationarity, $\nabla^\top \mathbf{j}(\mathbf{x}^{\text{ss}}) = \mathbf{0}$. However, the steady-state fluxes $\mathbf{j}(\mathbf{x}^{\text{ss}})$ generally do not satisfy detailed balance (21), so the system will incur EPR even in stationarity.

Usually, the steady-state approach is applied to MJPs and ideal CRNs that satisfy *complex balance* [3, 57, 58]. Complex balance is a strong dynamical constraint which guarantees the existence of steady states, while ruling out nonlinear behavior like oscillations and chaos [42]. For such systems, a generalized free energy potential may be defined in analogy

to Eq. (23), as the gradient of the relative entropy between the system's actual state and the steady state [58],

$$\phi^{\text{ss}} := \text{grad}_{\mathbf{x}} D(\mathbf{x} \parallel \mathbf{x}^{\text{ss}}) \quad \phi_i^{\text{ss}} = \ln \frac{x_i}{x_i^{\text{ss}}}. \quad (30)$$

In active systems, the relative entropy does not have a simple interpretation in terms of work. However, as for passive systems, it still governs steady-state fluctuations, meaning that the probability of observing state \mathbf{x} as a fluctuation scales as [57, 58]

$$P(\mathbf{X}_n^{\text{ss}} \approx \mathbf{x}) \asymp e^{-nD(\mathbf{x} \parallel \mathbf{x}^{\text{ss}})}. \quad (31)$$

Here, the random variable \mathbf{X}_n^{ss} indicates the empirical distribution measured from n independent and identical copies of a stationary system.

In general, the dynamics of active systems cannot be written as a gradient flow. Nonetheless, in MJPs and complex-balanced CRNs, the relative entropy between the actual state and the steady state decreases under relaxation dynamics [3], therefore it serves as a Lyapunov function that guarantees convergence to steady state [29, 60]. This leads to the Hatano-Sasa (HS) decomposition of EP, also called the nonadiabatic/adiabatic decomposition [31, 32, 61, 62]. The HS excess EPR is defined in analogy to Eq. (27), as the decrease of the relative entropy due to relaxation:

$$\sigma_{\text{ex}}^{\text{HS}} := -\dot{\mathbf{x}}^\top \phi^{\text{ss}} = -\partial_t D(\mathbf{x}(t) \parallel \mathbf{x}^{\text{ss}}(s))|_{s=t} \geq 0. \quad (32)$$

The HS housekeeping EPR is defined as the remainder,

$$\sigma_{\text{hk}}^{\text{HS}} := \sigma - \sigma_{\text{ex}}^{\text{HS}}. \quad (33)$$

For CRNs without complex balance, the situation is more complicated. First, a steady state \mathbf{x}^{ss} may not exist — there may not be a stable fixed point for the deterministic dynamics (1) — in which case the steady-state approach is not applicable. Even if a steady state \mathbf{x}^{ss} exists, and even if it is unique, the relative entropy $D(\mathbf{x} \parallel \mathbf{x}^{\text{ss}})$ does not always decrease under free relaxation. Thus, the HS decomposition may fail for systems without complex balance, either by being undefined or by giving unphysical negative values.

A related issue is that, in systems without complex balance, the rate function of steady-state fluctuations is no longer the relative entropy $D(\mathbf{x} \parallel \mathbf{x}^{\text{ss}})$, as in Eq. (31). It has been proposed to define the generalized potential as the gradient of the rate function [24, 55, 57, 63–65]. Sometimes, this leads to useful Lyapunov functions, although it can run into difficulties, including in systems with coexisting attractors [24]. The approach also runs into difficulties due to ambiguities in the definition of macroscopic steady states, such as non-commutativity of the large-volume and long-time limits [66].

The steady-state approach and the HS decomposition are useful for studying fluctuations and stability of steady states. Nonetheless, the approach also has limitations. First, the HS decomposition cannot be applied to many cases of interest. As discussed above, this includes CRNs without complex balance. It also includes MJPs with odd variables [67–69] and non-Markovian stochastic processes, where stationarity cannot be defined purely in terms of states [70].

Second, the physical meaning of the steady-state potential and the HS decomposition is unclear. In passive systems, the free energy potential ϕ^{eq} is directly related to the forces and fluxes at a given point in time, via Eq. (22). In active systems, however, the steady-state potential ϕ^{ss} does not have this “local in time” property. Rather, it is defined in terms of the steady state \mathbf{x}^{ss} that would be reached in the long-time limit of a free relaxation, which may never be approached in practice [35, 71, 72]. Thus, there is no simple way to relate the steady-state potential and the HS decomposition to measurable properties of a nonstationary system at given point in time.

Finally, although the HS decomposition has been used to derive thermodynamic speed limits [6, 8, 10, 73], it is not always sensitive to system topology or the speed of state evolution. This is most easily shown with a concrete example, such as the unicyclic MJP considered in Section VIII A.

IV. VARIATIONAL APPROACH: PASSIVE SYSTEMS

We now propose an alternative approach to derive the free energy potential. Our approach is based on a variational principle that — even in passive systems — makes no explicit reference to equilibrium states, stationary states, or the free energy function \mathcal{F} . Nonetheless, this variational principle recovers the usual free energy potential and the EPR in passive systems. We extend our variational principle to active systems in the subsequent Section V.

Before proceeding, recall from Eq. (16) that, in both active and passive systems, the EPR can be expressed as the relative entropy between forward and backward fluxes, $\sigma = \mathcal{D}(\mathbf{j} \parallel \tilde{\mathbf{j}})$. This allows us to express the EPR in a variational way, as the solution to the following optimization over reaction observables:

$$\sigma = \max_{\boldsymbol{\theta} \in \mathbb{R}^m} \left[\mathbf{j}^\top \boldsymbol{\theta} - \tilde{\mathbf{j}}^\top (e^\boldsymbol{\theta} - \mathbf{1}) \right]. \quad (34)$$

To derive this expression, note that $\min_{\boldsymbol{\theta}} \mathcal{D}(\mathbf{j} \parallel \tilde{\mathbf{j}} \circ e^\boldsymbol{\theta}) = 0$, where the minimizer is given by the forces, $\boldsymbol{\theta}^* = \ln(\mathbf{j}/\tilde{\mathbf{j}}) = \mathbf{f}$. We can then write the EPR as

$$\begin{aligned} \sigma &= \mathcal{D}(\mathbf{j} \parallel \tilde{\mathbf{j}}) - \min_{\boldsymbol{\theta}} \mathcal{D}(\mathbf{j} \parallel \tilde{\mathbf{j}} \circ e^\boldsymbol{\theta}) \\ &= \max_{\boldsymbol{\theta}} \left[\mathcal{D}(\mathbf{j} \parallel \tilde{\mathbf{j}}) - \mathcal{D}(\mathbf{j} \parallel \tilde{\mathbf{j}} \circ e^\boldsymbol{\theta}) \right]. \end{aligned}$$

Eq. (34) follows by expanding the relative entropy terms and simplifying. The optimal observable is $\boldsymbol{\theta}^* = \mathbf{f}$, and it is unique due to the strict concavity of the objective.

Eq. (34) provides a family of bounds on the EPR, one for each reaction observable. The EPR is achieved by maximizing over the choice of observable, while the thermodynamic forces are recovered as the optimal observables. This optimization problem was recently proposed as a technique for thermodynamic inference in MJPs [74, 75].

The expression (34) applies to both passive and active systems. However, in passive systems, the forces have the conservative form $\mathbf{f} = -\nabla \phi^{\text{eq}}$, as in Eq. (22). Therefore, we

may restrict the optimization to reaction observables having the form $\theta = -\nabla\phi$ for various state observables $\phi \in \mathbb{R}^d$,

$$\sigma = \max_{\phi \in \mathbb{R}^d} \left[-\mathbf{j}^\top \nabla\phi - \tilde{\mathbf{j}}^\top (e^{-\nabla\phi} - \mathbf{1}) \right]. \quad (35)$$

This expression may be simplified and written in terms of forward fluxes as

$$\sigma = \max_{\phi \in \mathbb{R}^d} \left[-\dot{\mathbf{x}}^\top \phi - \mathbf{j}^\top (e^{\nabla\phi} - \mathbf{1}) \right] \quad (36)$$

where we used $\mathbf{j}^\top \nabla\phi = \dot{\mathbf{x}}^\top \phi$ from Eq. (1) and $\tilde{\mathbf{j}}^\top e^{-\nabla\phi} = \mathbf{j}^\top e^{\nabla\phi}$ from Eq. (3).

Eq. (36) provides a variational expression of the EPR in passive systems. Taking derivatives shows that the optimal ϕ^* obeys

$$\dot{\mathbf{x}} = -\nabla^\top (\mathbf{j} \circ e^{\nabla\phi^*}). \quad (37)$$

The free energy potential ϕ^{eq} satisfies this relation, as can be verified using Eq. (22). Moreover, the objective (36) is strictly concave in $\nabla\phi$, so the free energy potential ϕ^{eq} is the unique ϕ^* , up to the nullspace of ∇ , representing conserved quantities.

In case it is useful to identify the precise value of ϕ^{eq} , ϕ^* may be chosen so that the corresponding canonical state, $\mathbf{x}^* := \mathbf{x} \circ e^{-\phi^*}$, has the same conserved quantities as the actual state \mathbf{x} , therefore also as the (physically relevant) equilibrium state \mathbf{x}^{eq} . Formally, ϕ^* may be chosen to satisfy

$$P_\emptyset \mathbf{x}^* \equiv P_\emptyset (\mathbf{x} \circ e^{-\phi^*}) = P_\emptyset \mathbf{x}, \quad (38)$$

where P_\emptyset is the projector onto the nullspace of ∇ . For example, for an MJP with an irreducible rate matrix, the nullspace is spanned by the vector $\mathbf{1}$ (representing conservation of probability) and ϕ^* is determined by Eq. (37) up to an additive constant. Since $P_\emptyset \propto \mathbf{1}\mathbf{1}^\top$, Eq. (38) implies that \mathbf{x}^* is a valid probability distribution,

$$\mathbf{1}^\top \mathbf{x}^* \equiv \mathbf{1}^\top (\mathbf{x} \circ e^{-\phi^*}) = \mathbf{1}^\top \mathbf{x} = 1. \quad (39)$$

In SM1 [44], we show how to find the ϕ^* that satisfies (38) by solving an information-theoretic convex optimization.

Next, we consider our variational principle from the ‘‘dual’’ perspective. Observe that Eq. (36) involves the maximization of a concave objective over state observables. Using convex duality [76], it has an equivalent formulation as the minimization of a convex objective over flux vectors:

$$\sigma = \min_{\mathbf{j}' \in \mathbb{R}^m} \mathcal{D}(\mathbf{j}' \parallel \tilde{\mathbf{j}}) \quad \text{where} \quad \nabla^\top \mathbf{j}' = \dot{\mathbf{x}}. \quad (40)$$

To show the equivalence, we write Eq. (40) in its Lagrangian dual form [76, Ch. 5],

$$\sigma = \max_{\phi \in \mathbb{R}^d} \min_{\mathbf{j}' \in \mathbb{R}^m} \left[\mathcal{D}(\mathbf{j}' \parallel \tilde{\mathbf{j}}) + \phi^\top (\nabla^\top \mathbf{j}' - \dot{\mathbf{x}}) \right], \quad (41)$$

where $\phi \in \mathbb{R}^d$ indicates the Lagrangian multipliers. The inner optimization can be solved by taking derivatives; with a

bit of algebra, this shows that the optimal fluxes have the form $\tilde{\mathbf{j}} \circ e^{-\nabla\phi}$. Plugging back into (41) and simplifying shows equivalence to Eq. (36). The optimal Lagrange multipliers are equal to the free energy potential ϕ^{eq} , while the optimal fluxes are equal to the actual forward fluxes $\mathbf{j}^* = \mathbf{j} = \tilde{\mathbf{j}} \circ e^{-\nabla\phi^{\text{eq}}}$.

The dual formulation (40) allows us to interpret our variational principle as an information-theoretic optimal transport problem [77]. Generally, optimal transport considers the minimum cost required to transform a system between a given initial and final state [78]. This minimal cost can be used to define operational notions of distance and speed [78]. In our case, the relative entropy $\mathcal{D}(\mathbf{j}' \parallel \tilde{\mathbf{j}})$ gives the information-theoretic cost for flux vector \mathbf{j}' , reflecting the breaking of symmetry between \mathbf{j}' and the reverse fluxes \mathbf{j} . Eq. (40) implies that the EPR is the minimal cost necessary to achieve a given dynamical evolution $\dot{\mathbf{x}}$. We discuss the relation to another optimal-transport distance (Wasserstein distance) in Section VII.

The variational expressions (36)-(40) comprise our first set of results. These expressions allow one to compute the EPR and the free energy potential ϕ^{eq} as a function of the fluxes, without any explicit reference to equilibrium states.

V. VARIATIONAL APPROACH: ACTIVE SYSTEMS

This section contains the bulk of our main results. We begin by extending our variational principle to active systems, in this way defining the generalized free energy and the excess EPR. We then show that our variational principle satisfies an important consistency condition under coarse-graining. We introduce the excess/housekeeping decomposition of EPR, and then provide a comparison with the HS decomposition. Finally, we consider the linear-response regime of slow evolution.

A. Overview

Consider an active system that, in general, may not have conservative forces. In direct analogy to (36), we propose the following variational principle

$$\sigma_{\text{ex}} = \max_{\phi \in \mathbb{R}^d} \left[-\dot{\mathbf{x}}^\top \phi - \mathbf{j}^\top (e^{\nabla\phi} - \mathbf{1}) \right]. \quad (42)$$

As we will show, the value of σ_{ex} defines the excess EPR, the nonstationary contribution to dissipation. The generalized free energy potential is defined as the optimal state observable ϕ^* in Eq. (42). This observable satisfies the optimality condition

$$\dot{\mathbf{x}} = -\nabla^\top (\mathbf{j} \circ e^{\nabla\phi^*}), \quad (43)$$

which is the analogue of Eq. (37). The optimality condition (43) determines ϕ^* up to the nullspace of ∇ (representing conserved quantities). Although it is not necessary for most of our results, comparison with ϕ^{eq} and ϕ^{ss} can be facilitated by choosing ϕ^* to satisfy conservation laws (38) (see SM1 [44]).

Excess EPR is always nonnegative, $\sigma_{\text{ex}} \geq 0$, since $\phi = \mathbf{0}$ achieves the objective value 0. Moreover, when the system

is in steady state, this null observable satisfies the optimality condition (43):

$$-\nabla^\top(\mathbf{j}(\mathbf{x}^{\text{ss}}) \circ e^{\nabla\phi}) = -\nabla^\top \mathbf{j}(\mathbf{x}^{\text{ss}}) = \mathbf{0} = \dot{\mathbf{x}}.$$

Plugging into Eq. (42) shows that the generalized free energy and the excess EPR vanish ($\phi^* = \mathbf{0}$ and $\sigma_{\text{ex}} = 0$) in steady state.

The variational expression (42) is a central result of this paper. Its physical meaning is explored further below in this section, as well as in Section VI where we show that the generalized free energy ϕ^* is the ‘‘most irreversible’’ state observable and σ_{ex} quantifies its degree of irreversibility.

To our knowledge, this variational expression is largely unknown in stochastic thermodynamics, for either passive or active systems. One exception is Ref. [79], which proposed a different variational expression for EPR in passive MJPs. In Section VII C, we show that the expression of Ref. [79] can be recovered as a special case of Eq. (36), and we generalize their main result to active systems. In addition, some related (but distinct) variational principles have been explored in the literature on large deviations and macroscopic fluctuation theory. We discuss the relation with large deviations in Section VI.

We note a few important aspects. First, Eq. (42) can be rearranged as

$$\sigma_{\text{ex}} = \max_{\phi \in \mathbb{R}^d} [-2\dot{\mathbf{x}}^\top \phi - \mathbf{j}^\top (e^{\nabla\phi} - \nabla\phi - \mathbf{1})]. \quad (44)$$

The first term is (twice) the average change of ϕ . The second term, as we show below, quantifies the fluctuations of ϕ , and it is always nonnegative (since $e^x - x - 1 \geq 0$ for all x). Therefore, since excess EPR is nonnegative, the generalized free energy must obey

$$-\dot{\mathbf{x}}^\top \phi^* \geq 0. \quad (45)$$

This suggests that the system evolves down the direction of the generalized free energy. This is analogous to $-\dot{\mathbf{x}}^\top \phi^{\text{eq}} \geq 0$ from Eq. (27), which implies that passive systems lose free energy when relaxing. However, in active systems, ϕ^* does not have to be the gradient of any state function (like \mathcal{F}). Therefore, the dynamical evolution of an active system cannot always be expressed as a gradient flow, as it can for a passive system. This is consistent with the fact that some nonlinear active systems, such as oscillatory and chaotic systems, do not have global stability.

Second, our variational expression (42) can be put in its dual form,

$$\sigma_{\text{ex}} = \min_{\mathbf{j}' \in \mathbb{R}^m} \mathcal{D}(\mathbf{j}' \|\tilde{\mathbf{j}}) \quad \text{where} \quad \nabla^\top \mathbf{j}' = \dot{\mathbf{x}}, \quad (46)$$

which is derived in the same way as Eq. (40). The generalized free energy potential ϕ^* sets the optimal Lagrange multipliers for the constrained optimization, and the optimal fluxes are

$$\mathbf{j}^* = \tilde{\mathbf{j}} \circ e^{-\nabla\phi^*}. \quad (47)$$

The excess EPR can be written using these optimal fluxes as

$$\sigma_{\text{ex}} = \mathcal{D}(\mathbf{j}^* \|\tilde{\mathbf{j}}). \quad (48)$$

Unlike the case for passive systems, the optimal fluxes \mathbf{j}^* are not always the same as the forward fluxes \mathbf{j} .

Importantly, the dual principle (46) implies that $\sigma_{\text{ex}} \leq \sigma$, because the actual fluxes \mathbf{j} satisfy the feasibility constraint while achieving $\mathcal{D}(\mathbf{j} \|\tilde{\mathbf{j}}) = \sigma$. As for Eq. (40), the excess EPR can be understood as the cost of state evolution as measured by information-theoretic optimal transport.

Third, the precise values of excess EPR and the generalized free energy can be found by numerical optimization of Eq. (42). This is a convex optimization problem that can be solved efficiently by standard algorithms. In addition, as discussed below, these quantities can be found in closed-form for systems that have conservative coarse-grained forces. Furthermore, over an extended time interval, the generalized free energy potential can be found by solving an ordinary differential equation starting from a known initial condition. Specifically, the time derivative of $\phi^*(t)$ can be found by differentiating both sides of (43) and rearranging. With some algebra, this gives

$$\dot{\phi}^*(t) = -\frac{1}{2} \mathcal{H}_t^+ \nabla^\top (\dot{\mathbf{j}}(t) \circ (e^{\nabla\phi^*(t)} + \mathbf{1})), \quad (49)$$

where \mathcal{H}_t^+ refers to the pseudo-inverse of the symmetric positive-semidefinite matrix

$$\mathcal{H}_t := \frac{1}{2} \nabla^\top \text{diag}(\mathbf{j}(t) \circ e^{\nabla\phi^*(t)}) \nabla. \quad (50)$$

Thus, given an initial $\phi^*(0)$ and flux trajectory $\mathbf{j}(t)$, $\phi^*(t)$ can be found by numerical integration of Eq. (49).

B. Example: two-level MJP

To make things concrete, we illustrate our approach on a minimal example, the two-level MJP shown in Figure 1. More sophisticated examples are considered in Section VIII.

For this system, the dynamics obey

$$\dot{x}_2 = j_{21}^c + j_{21}^h - j_{12}^c - j_{12}^h,$$

where $\dot{x}_1 = -\dot{x}_2$ by conservation of probability. At the same time, the optimality condition (43) reduces to

$$\dot{x}_2 = -(j_{21}^c + j_{21}^h)e^{\phi_2^* - \phi_1^*} + (j_{12}^c + j_{12}^h)e^{\phi_1^* - \phi_2^*}.$$

This condition is satisfied by the potential

$$\phi^* = \left(0, \ln \frac{j_{12}^c + j_{12}^h}{j_{21}^c + j_{21}^h}\right) + \text{const}, \quad (51)$$

where const is an arbitrary constant that corresponds to the one-dimensional nullspace of ∇ (conservation of probability). If desired, this constant may be chosen so that the normalization condition (39) is satisfied. Plugging ϕ^* into Eq. (42) and simplifying gives

$$\sigma_{\text{ex}} = (j_{21}^c + j_{21}^h - j_{12}^c - j_{12}^h) \ln \frac{j_{21}^c + j_{21}^h}{j_{12}^c + j_{12}^h}. \quad (52)$$

In this example, the excess EPR is the same as the EPR incurred by a system with only two one-way transitions, with fluxes $j_{12}^c + j_{12}^h$ and $j_{12}^c + j_{12}^h$. We will see below that this is an instance of a more general “coarse-graining” principle. Furthermore, we can interpret Eq. (52) in terms of an effective force across the transition $1 \rightarrow 2$,

$$\ln \frac{j_{21}^c + j_{21}^h}{j_{12}^c + j_{12}^h} = \ln \frac{x_1}{x_2} + \beta^{\text{eff}} \Delta E,$$

where $\Delta E = E_1 - E_2$ indicates the energy gap and β^{eff} is an effective inverse temperature, $\beta^{\text{eff}} = (\ln \frac{R_{21}^h + R_{21}^c}{R_{12}^h + R_{12}^c}) / \Delta E$. Note that β^{eff} does not depend on the probability distribution \mathbf{x} , only on the energy gap and the kinetics.

C. Consistency under coarse-graining

We show that our generalized free energy and excess EPR satisfy an important consistency condition under coarse-graining.

To introduce this idea, observe that a system may have multiple different reactions with the same (net) stoichiometry. In fact, this is a common way to drive active systems. For example, in the two-level MJP discussed above and shown in Figure 1, the two reversible transitions between levels 1 and 2 have identical stoichiometry. As a result, the incidence matrix ∇ has duplicate rows: rows 1 and 3 are the same, as are 2 and 4. As another example, in the Brusselator CRN from Figure 2, the reversible reactions $X_1 \rightleftharpoons X_2$ and $2X_1 + X_2 \rightleftharpoons 3X_1$ have opposite stoichiometry. As a result, ∇ has duplicate rows: rows 3 and 6 are the same, as are 4 and 5.

We introduce a coarse-graining procedure that combines reactions with the same stoichiometry. Given a stoichiometric matrix ∇ , the coarse-grained stoichiometric matrix is defined as $\bar{\nabla} \in \mathbb{Z}^{m' \times d}$ ($m' \leq m$) where any duplicate rows (reactions with the same stoichiometry) are merged. We also define coarse-grained forward fluxes $\bar{\mathbf{j}} \in \mathbb{R}_+^{m'}$ by summing fluxes j_ρ from reactions with same stoichiometry. The coarse-grained reverse fluxes $\bar{\mathbf{j}} \in \mathbb{R}_+^{m'}$ are defined in the same way, except using the reverse fluxes $\tilde{\mathbf{j}}$. In the case of an MJP where the same transitions may be mediated by different reservoirs α , the coarse-graining procedure is equivalent to summing rate matrices corresponding to different reservoirs, $\bar{R} = \sum_\alpha R^\alpha$.

This coarse-graining preserves state dynamics,

$$\dot{\mathbf{x}} = \nabla^\top \mathbf{j} = \bar{\nabla}^\top \bar{\mathbf{j}}, \quad (53)$$

which means that reactions with the same stoichiometry have the same effect on the state evolution. The quantity $\mathbf{j}^\top (e^{\nabla \phi} - \mathbf{1})$, which appears in our variational principle (42), is also invariant under coarse-graining:

$$\mathbf{j}^\top (e^{\nabla \phi} - \mathbf{1}) = \bar{\mathbf{j}}^\top (e^{\bar{\nabla} \phi} - \mathbf{1}). \quad (54)$$

In Section VI, we will show that this quantities encode the statistics of dynamical fluctuations of ϕ , so Eq. (54) reflects

the fact that these statistics are invariant under coarse-graining. Finally, our variational principle (42) is also invariant, in the sense that the excess EPR and generalized free energy ϕ^* do not change due to merging of reactions with the same stoichiometry. We may write

$$\sigma_{\text{ex}}(\mathbf{j}) = \bar{\sigma}_{\text{ex}}(\bar{\mathbf{j}}) \quad (55)$$

where $\bar{\sigma}_{\text{ex}}$ is defined as in (42) but using the coarse-grained fluxes $\bar{\mathbf{j}}$ and stoichiometric matrix $\bar{\nabla}$.

The coarse-graining condition (55) implies that our generalized free energy and excess EPR do not distinguish between reactions that lead to the same state changes. Arguably, this property may be desired from any definition of a generalized free energy and excess EPR that aim to quantify the dissipation due to nonstationarity.

The consistency condition also has practical implications, because it sometimes allows the generalized free energy and excess EPR to be computed in closed-form. In particular, consider the class of systems that have conservative coarse-grained forces, meaning that

$$\bar{\mathbf{f}} = \ln(\bar{\mathbf{j}}/\tilde{\bar{\mathbf{j}}}) = -\nabla \phi \quad (56)$$

for some ϕ . Then, the excess EPR is given by the regular EPR at the level of the coarse-grained fluxes,

$$\sigma_{\text{ex}}(\mathbf{j}) = \bar{\sigma}_{\text{ex}}(\bar{\mathbf{j}}) = \sigma(\bar{\mathbf{j}}), \quad (57)$$

and the generalized free energy ϕ^* is equal to the potential ϕ in Eq. (56). In many cases, ϕ^* can be found directly by inspecting the linear system of equations (56), thus eliminating the need for numerical optimization. In essence, this technique was used to find ϕ^* for the two-level MJP in the previous example, as in Eq. (51). The same technique will be demonstrated in our analysis of the Brusselator in Section VIII B.

D. Excess vs. housekeeping entropy production

As discussed above, excess EPR quantifies the nonstationary contribution to EPR, vanishing for a system in steady state. In this section, we consider the non-excess remaining part of the EPR, typically called the *housekeeping EPR*:

$$\sigma_{\text{hk}} = \sigma - \sigma_{\text{ex}}.$$

Since the excess EPR satisfies $0 \leq \sigma_{\text{ex}} \leq \sigma$, the housekeeping EPR also obeys the bounds $0 \leq \sigma_{\text{hk}} \leq \sigma$. This gives a decomposition of the EPR into nonnegative excess and housekeeping terms,

$$\sigma = \sigma_{\text{ex}} + \sigma_{\text{hk}}. \quad (58)$$

For a temporally-extended processes, the overall excess EPR and housekeeping EP are given by the time-integrals $\Sigma_{\text{ex}} = \int \sigma_{\text{ex}}(t) dt$ and $\Sigma_{\text{hk}} = \int \sigma_{\text{hk}}(t) dt$.

The housekeeping EPR quantifies the “nonconservativeness” of the thermodynamic forces. Specifically, the housekeeping EPR has the following variational expression:

$$\sigma_{\text{hk}} = \min_{\phi \in \mathbb{R}^d} \mathcal{D}(\mathbf{j} \parallel \tilde{\mathbf{j}} \circ e^{-\nabla \phi}) = \mathcal{D}(\mathbf{j} \parallel \mathbf{j}^*), \quad (59)$$

where the optimal fluxes are given by $j^* = \tilde{j} \circ e^{-\nabla\phi^*}$ as in Eq. (47). This result can be derived by plugging Eq. (42) into $\sigma_{\text{hk}} = \mathcal{D}(j\|\tilde{j}) - \sigma_{\text{ex}}$, expanding the definition of \mathcal{D} , and rearranging. To clarify the meaning of Eq. (59), we define the notation

$$\mathcal{D}(\theta\|\theta') := \mathcal{D}(\tilde{j} \circ e^\theta\|\tilde{j} \circ e^{\theta'}) \quad (60)$$

to indicate the relative entropy between pairs of flux vectors in the exponentially-tilted parametric family

$$\theta \mapsto \tilde{j} \circ e^\theta. \quad (61)$$

Using this notation, the housekeeping EPR may be written as

$$\sigma_{\text{hk}} = \min_{\phi \in \mathbb{R}^d} \mathcal{D}(f\|-\nabla\phi) = \mathcal{D}(f\|-\nabla\phi^*). \quad (62)$$

Thus, the housekeeping EPR quantifies the information-geometric distance between the actual forces f and the closest conservative forces, which have the form $-\nabla\phi$. Clearly, it vanishes when the actual forces have the conservative form $f = -\nabla\phi^{\text{eq}}$. The generalized free energy potential ϕ^* , which achieves the minimum in Eq. (62), can be understood as the best ‘‘conservative approximation’’ of the nonconservative forces.

Interestingly, both the forces and fluxes can be decomposed into excess and housekeeping parts:

$$\begin{aligned} f &= -\nabla\phi^* + (f + \nabla\phi^*) \\ j &= j^* + (j - j^*) \end{aligned} \quad (63)$$

The excess contribution to the forces, $-\nabla\phi^*$, is conservative. The housekeeping contribution to the fluxes is stationary, $\nabla^\top(j^* - j) = 0$, since $\nabla^\top j^* = \nabla^\top j$ from Eq. (46). This stationary current represents the cyclic contribution to the fluxes, which leads to dissipation without changing the state.

Our excess/housekeeping decomposition can be interpreted in terms of information-geometry, as shown in Figure 3. In the space of fluxes, we may write our decomposition as

$$\underbrace{\mathcal{D}(j\|\tilde{j})}_\sigma = \underbrace{\mathcal{D}(j^*\|\tilde{j})}_{\sigma_{\text{ex}}} + \underbrace{\mathcal{D}(j\|j^*)}_{\sigma_{\text{hk}}}. \quad (64)$$

This expression is an instance of the Pythagorean relation from information geometry [80]. It is analogous to the Pythagorean relation from Euclidean geometry, except that squared Euclidean distance is replaced by relative entropy. Eq. (64), illustrated in Figure 3(a), shows that the excess/housekeeping terms provide an orthogonal decomposition of EPR. Orthogonality arises because excess EPR (46) is defined by the information-geometric projection of \tilde{j} onto the flat manifold of fluxes that generate the forward time evolution, $\nabla^\top j' = \dot{x}$.

Alternatively, the same decomposition can be expressed in the dual space of forces, as shown in Figure 3(b). Using the notation (60), this gives

$$\underbrace{\mathcal{D}(f\|0)}_\sigma = \underbrace{\mathcal{D}(-\nabla\phi^*\|0)}_{\sigma_{\text{ex}}} + \underbrace{\mathcal{D}(f\|-\nabla\phi^*)}_{\sigma_{\text{hk}}} \quad (65)$$

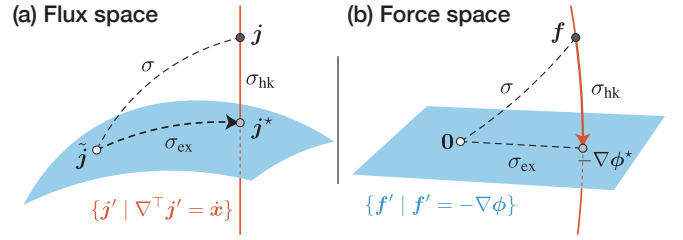


Figure 3. **Information-geometric interpretation of excess/housekeeping decomposition.** (a) The EPR $\sigma = \mathcal{D}(j\|\tilde{j})$ is the relative entropy from the forward fluxes j to the reverse fluxes \tilde{j} . Excess EPR σ_{ex} is defined by the projection of \tilde{j} onto the set of fluxes that give the correct time evolution (orange line), Eq. (46). Excess/housekeeping provide an orthogonal decomposition of the EPR in flux space, Eq. (64). (b) In the space of forces, the EPR $\sigma = \mathcal{D}(f\|0)$ is the relative entropy from the actual forces f to the origin 0 . Housekeeping EPR is defined by the (dual) projection of the forces onto the set of conservative forces (blue plane), Eq. (62). Excess/housekeeping provide an orthogonal decomposition of the EPR in force space, Eq. (65). The two projections meet at the same point, determined by the generalized free energy ϕ^* .

Here, orthogonality arises because the housekeeping EPR (62) is defined by the dual projection of the forces f onto the flat manifold of conservative forces, which have the form $f' = -\nabla\phi$. It is a central result of information geometry that these two projections meet at the same point [81], corresponding to the generalized free energy ϕ^* .

To our knowledge, there is little work on decompositions of entropy production using the information-geometric Pythagorean relation at the level of fluxes or trajectories. One exception is Ref. [82], where entropy production was decomposed into partial contributions from individual subsystems. More recently, Ref. [45] explored information-geometric decompositions using a different divergence (not relative entropy).

E. Comparison to Hatana-Sasa (HS) decomposition

As mentioned above, the HS excess/housekeeping decomposition is defined for systems where a steady state x^{ss} exists, and it is based on the steady-state potential $\phi^{\text{ss}} = \ln(x/x^{\text{ss}})$. For such systems, we may compare the HS decomposition to ours.

As we show in SM6 [44], the HS housekeeping EPR can be expressed as the relative entropy between the actual forces f and the conservative forces corresponding to the steady-state potential ϕ^{ss} . Using the notation of (60), it can be written as

$$\sigma_{\text{hk}}^{\text{HS}} = \mathcal{D}(f\|-\nabla\phi^{\text{ss}}),$$

In terms of Figure 3(b), the HS housekeeping EPR may be represented by a line from the actual forces f to the special point $-\nabla\phi^{\text{ss}}$ on the conservative manifold.

Since our housekeeping EPR satisfies the variational principle (62), it is always smaller than the HS housekeeping EPR:

$$\sigma_{\text{hk}} \leq \sigma_{\text{hk}}^{\text{HS}}, \quad \sigma_{\text{ex}} \geq \sigma_{\text{ex}}^{\text{HS}}. \quad (66)$$

The nonnegative difference $\sigma_{\text{hk}}^{\text{HS}} - \sigma_{\text{hk}} = \sigma_{\text{ex}} - \sigma_{\text{ex}}^{\text{HS}} \geq 0$ has been previously considered in the setting of Langevin dynamics, where it quantifies the gap between the HS and Maes-Netočný [35] definitions of housekeeping EPR [72].

For MJPs, there is an important special case in which the two decomposition agree. Recall Section V C, where we discuss coarse-graining of reactions with the same stoichiometry. Suppose that the resulting coarse-grained forces are conservative, as in Eq. (56). In that case, the “pseudo-canonical” state $\mathbf{x}^* = \mathbf{x} \circ e^{-\phi^*}$ obeys detailed balance for the coarse-grained rate matrix \bar{R} . In this case, the pseudo-canonical state is stationary ($\mathbf{x}^{\text{ss}} = \mathbf{x}^*$), the two potentials agree ($\phi^{\text{ss}} = \ln(\mathbf{x}/\mathbf{x}^{\text{ss}}) = \phi^*$), and the two excess/housekeeping decompositions are the same. This is the case, for instance, for the two-level MJP discussed in Section V B.

However, the same argument does not apply to nonlinear CRNs. That is, even if the coarse-grained forces are conservative, there is no simple relationship between the effective equilibrium state and the steady state. Thus, there is no simple relationship between our decomposition and the HS decomposition. In fact, it is possible for a CRN to have conservative coarse-grained forces but not have any steady states, and thus not have a well-defined HS decomposition, as is the case for the Brusselator example considered below.

F. Linear response

We now consider our variational principle in the linear-response regime of slow evolution. We show that our generalized free energy obeys Onsager relations, where the transport coefficients can be understood as diffusion coefficients. In this sense, our approach generalizes Onsager theory to far-from-equilibrium and active systems. We also compare with the linear-response regime of the HS decomposition, where the transport coefficients have been derived using a Green-Kubo relation from long-time steady-state correlations [39].

Recall that in a stationary system ($\dot{\mathbf{x}} = \mathbf{0}$), the generalized free energy can be chosen as $\phi^* = \mathbf{0}$. Therefore, for slow evolution ($\dot{\mathbf{x}} \approx \mathbf{0}$), we may restrict our variational principle (44) to $\phi \approx \mathbf{0}$. Expanding the objective to second order gives

$$\sigma_{\text{ex}} \approx \max_{\phi \in \mathbb{R}^d} \left[-2\dot{\mathbf{x}}^\top \phi - \phi^\top H \phi \right], \quad (67)$$

where we introduced the matrix

$$H := \frac{1}{2} \nabla^\top \text{diag}(\mathbf{j}) \nabla. \quad (68)$$

The optimal observable in Eq. (67) satisfies the linear-response version of (43),

$$\dot{\mathbf{x}} \approx -H \phi^* \quad \phi^* \approx -H^+ \dot{\mathbf{x}}, \quad (69)$$

where H^+ is the pseudo-inverse [83]. The linear-response approximation is consistent ($\phi^* \approx \mathbf{0}$) when H is much larger than $\dot{\mathbf{x}}$.

Eq. (69) recovers the usual linear form of Onsager phenomenological relations [84, Ch. 7], which relate a free energy potential to dynamical evolution. From this perspective,

the matrix H specifies the mobility coefficients, while H^+ specifies the friction coefficients. These matrices are positive-semidefinite and symmetric, meaning that Onsager’s reciprocal relations are satisfied.

Interestingly, our variational principle can be interpreted as a version of Onsager’s variational principle (OVP) [84–86], also called the “least dissipation principle”. OVP says that the system’s evolution $\dot{\mathbf{x}}$ is determined by an optimal balance between free energy input and dissipation due to friction. In our notation, this can be expressed as a variational principle for the state evolution, given a fixed potential ϕ^* :

$$\sigma_{\text{ex}} \approx \max_{\dot{\mathbf{y}} \in \text{im} \nabla^\top} \left[-2\dot{\mathbf{y}}^\top \phi^* - \dot{\mathbf{y}} H^+ \dot{\mathbf{y}} \right], \quad (70)$$

which recovers the actual evolution at optimality, $\dot{\mathbf{x}} \approx -H \phi^*$. However, we are usually interested in the “inverse” problem of inferring the generalized potential ϕ^* from the fixed state evolution $\dot{\mathbf{x}}$, as in Eq. (67) and $\phi^* \approx -H^+ \dot{\mathbf{x}}$. This inverse form of the OVP is sometimes called “Gyarmati’s variational principle” [86–88].

The excess EPR can be written as

$$\sigma_{\text{ex}} \approx \dot{\mathbf{x}}^\top H^+ \dot{\mathbf{x}}. \quad (71)$$

Although our results do not assume the existence of steady states, for systems that remain close to steady state ($\mathbf{x} \approx \mathbf{x}^{\text{ss}}$), we may further approximate the excess EPR as

$$\sigma_{\text{ex}} \approx \dot{\mathbf{x}}^{\text{ss}\top} H_{\text{ss}}^+ \dot{\mathbf{x}}^{\text{ss}}, \quad (72)$$

where $\dot{\mathbf{x}}^{\text{ss}}$ is change of the steady state due to driving and the steady-state mobility matrix H_{ss} is defined using Eq. (68) with steady-state fluxes $\mathbf{j}(\mathbf{x}^{\text{ss}})$. Importantly, Eq. (72) is quadratic in the speed of driving $\dot{\mathbf{x}}^{\text{ss}}$. Therefore, the total excess EP incurred over the course of a process, $\Sigma_{\text{ex}}(T) = \int_0^T \sigma_{\text{ex}}(t) dt$, vanishes in the limit of slow driving ($T \rightarrow \infty$ and $\dot{\mathbf{x}}^{\text{ss}} = O(1/T)$). This can be understood as a generalization of the Clausius equality to excess EP [33].

Our results show that excess EPR defines a Riemannian geometry over thermodynamic states. Specifically, σ_{ex} acts as the square of the line element and the friction tensor H^+ acts as the Riemannian metric. This can be used to define thermodynamic length for slowly-evolving active systems, thereby generalizing the thermodynamic geometry originally developed for passive systems [14].

The above results apply both to CRNs and MJPs. However, it is interesting to consider the special case of MJPs. For an MJP with rate matrix R , our mobility matrix H can be expressed as

$$H_{ji} = \frac{1}{2} \begin{cases} -x_i R_{ji} - x_j R_{ij} & i \neq j \\ \sum_{k(\neq i)} (x_i R_{ki} + x_k R_{ik}) & i = j \end{cases} \quad (73)$$

In this case, we may also compare with the linear-response regime of the steady-state potential and the HS decomposition [39]. Near steady state, $\mathbf{x} \approx \mathbf{x}^{\text{ss}}$, the steady-state potential can be approximated as $\phi_i^{\text{ss}} = \ln(x_i/x_i^{\text{ss}}) \approx (x_i - x_i^{\text{ss}})/x_i^{\text{ss}}$. Summing both sides across $R_{ji} x_i^{\text{ss}}$ gives

$$\dot{\mathbf{x}} \approx -G \phi^{\text{ss}}, \quad (74)$$

where $G_{ji} := -R_{ji}x_i^{\text{ss}}$ is the HS mobility matrix. In active systems, the matrix G may not symmetric, hence Eq. (74) does not satisfy Onsager's reciprocal relations. Interestingly, our steady-state mobility matrix is the additive symmetrization of the HS one, $H_{\text{ss}} = (G + G^{\text{T}})/2$, and the two agree for passive systems.

In Ref. [39], Eq. (74) was inverted to solve for ϕ^{ss} using a generalized inverse of the rate matrix R (the so-called ‘‘Drazin inverse’’ [89, 90]). This generalized inverse was also used to define a Riemannian geometry over thermodynamic states, which governs HS excess EP for slow driving between nonequilibrium steady states [39]. For active systems, the resulting geometry is different from the ours, because the two Riemannian metrics are different.

To understand the difference between the two approaches, note that there are (at least) two different methods for measuring transport coefficients [91]. The two methods are equivalent for passive systems, as result of the fluctuation-dissipation theorem, but for active systems they lead to different generalizations. The first method uses Green-Kubo relations, which express transport coefficients in terms of long-time decay of steady-state correlations [92]. This approach was used to justify the ‘‘thermodynamic length’’ metric for passive systems [14], and latter the linear-response HS transport coefficients in active systems [39]. The second method uses the Einstein relation, which shows that mean-squared displacement (MSD) grows over time in proportion to the diffusion coefficient. In fact, diffusion coefficients in practice are often estimated from the initial slope of the MSD [93, 94]. This second approach does not rely on steady-state statistics and it is local in time. In the next section (see Eq. (78)), we will see that H governs short-time MSD, thus our transport coefficients can be understood in terms of this second approach.

We finish by noting that our linear-response analysis also applies to far-from-equilibrium systems (i.e., the housekeeping EPR may be arbitrarily large). However, close to equilibrium, our framework becomes equivalent to the Euclidean decomposition of EPR proposed in Ref. [20]. Moreover, considering diffusive systems as the continuum limit of MJPs, both approaches become equivalent to the decomposition proposed by Maes and Netočný for Langevin systems [35, 71] (see SM6 [44] for details). In this sense, our approach generalizes the Maes-Netočný decomposition to systems that are far-from-equilibrium and far-from-stationarity.

VI. LARGE DEVIATIONS, THERMODYNAMIC UNCERTAINTY RELATIONS, AND THERMODYNAMIC INFERENCE

Above, we introduced our variational principle and used it to derive the generalized free energy and excess EPR. It is worth noting, however, that our variational principle is not unique. In fact, there are many variational principles that can be used to recover the free energy potential and EPR in passive systems, and which lead to different generalizations for active systems (we discuss two other principles in SM6 [44]).

At the same time, not all variational principles are equally

physically meaningful. Here we show that our principle has an intuitive physical interpretation in terms of statistical fluctuations. Using this interpretation, we show that our generalized free energy is the ‘‘most irreversible’’ state observable, and that the excess EPR reflects its degree of irreversibility. We discuss this idea in the context of two different (though closely related) settings: many-particle large deviations and thermodynamic uncertainty relations.

Before proceeding, we first discuss how our formalism, in both its MJP and CRN flavors, relates to the statistics of short-time dynamical fluctuations. Consider a Markovian stochastic system observed during a short time interval $[t, t + dt]$, and let the random variable N_{ρ} indicate the number of times that reaction ρ occurs during this interval [94]. If the system is described by an MJP, we assume that dt is short enough so that multiple jumps are unlikely, so that $N_{\rho} = 1$ with probability $\approx j_{\rho} dt$. Alternatively, the system may represent a unit volume of a stochastic chemical reaction system, whose mean reaction rates are specified by the fluxes of a deterministic CRN. In this latter case, we assume that reaction counts N_{ρ} are independent and Poisson distributed with mean $j_{\rho} dt$. This kind of description is standard for well-mixed chemical systems with large particle counts [95], assuming that dt is small enough so that reaction fluxes do not change appreciably.

Suppose we are interested in the change (i.e., displacement) of some fluctuating state observable ϕ over time $[t, t + dt]$, such as energy, position, etc. The displacement of this observable is given by the random variable

$$\Delta\phi = \sum_{\rho,i} N_{\rho} \nabla_{\rho i} \phi_i. \quad (75)$$

This random variable will exhibit dynamical fluctuations due to the stochasticity of reaction counts. Its statistics are encoded in the derivatives of the cumulant generated function (CGF) $\Lambda_{\phi}(\lambda) = \ln \mathbb{E} e^{\lambda \Delta\phi}$. For example, in an MJP where ϕ_i is the position of site i on a one-dimensional lattice, $\Delta\phi$ is the short-time displacement. The first derivative of the CGF gives the mean displacement, the second derivatives gives the mean square displacement, etc.

In SM2 [44], we show that, for both the MJP and CRN (Poisson) descriptions, the CGF is given by

$$\Lambda_{\phi}(\lambda) \approx \mathbf{j}^{\text{T}} (e^{\lambda \nabla \phi} - 1) dt \quad (76)$$

to first order in dt . Furthermore, although we omit it here for simplicity, a similar expression can be derived for joint outcomes of multiple observables. (For a set of k observables, the joint CGF (76) is a function of $\lambda \in \mathbb{R}^k$ and ϕ is replaced by an $d \times k$ matrix.). The cumulants are given by

$$K_{\phi}^{(k)} = \partial_{\lambda}^{(k)} \Lambda_{\phi}(0) \approx \mathbf{j}^{\text{T}} [\nabla \phi]^k dt. \quad (77)$$

For example, the mean and variance of the displacement are given by

$$\begin{aligned} K_{\phi}^{(1)} &= \mathbb{E}[\Delta\phi] \approx \sum_{\rho} j_{\rho} [\nabla \phi]_{\rho} dt = \dot{\mathbf{x}}^{\text{T}} \phi dt \\ K_{\phi}^{(2)} &= \mathbb{E}[(\Delta\phi)^2] - \mathbb{E}[\Delta\phi]^2 \approx \sum_{\rho} j_{\rho} [\nabla \phi]_{\rho}^2 dt. \end{aligned}$$

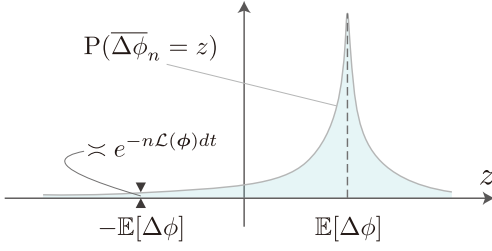


Figure 4. **Large deviations interpretation of the irreversibility measure $\mathcal{L}(\phi)$.** The change of state observable ϕ is measured in n independent stochastic systems over time $[t, t + dt]$. The empirical mean change is captured by the random variable $\overline{\Delta\phi}_n$. Here we show schematically the probability of different outcomes $\overline{\Delta\phi}_n = z \in \mathbb{R}$. For large n , the probability distribution is peaked at $z = \mathbb{E}[\Delta\phi]$. The probability that the empirical mean takes the opposite value, $z = -\mathbb{E}[\Delta\phi]$, decays exponentially as $\simeq e^{-n\mathcal{L}(\phi)dt}$. According to Eq. (80), the generalized free energy ϕ^* is the “most irreversible” observable, having the largest $\mathcal{L}(\phi)$.

Note that the variance is equal to the mean-squared displacement (MSD) $\mathbb{E}[(\Delta\phi)^2]$ to first order in dt . Note also that the MSD can be expressed using our mobility matrix H (68) as

$$K_\phi^{(2)} = 2\phi^\top H\phi. \quad (78)$$

In this sense, H is a diffusion matrix that governs the short-time MSD of all state observables.

In the following, we will exploit the close connection between the excess EPR (42) and the CGF (76) to provide a physical interpretation to our generalized free energy and excess EPR.

A. Large deviations

We now show that our generalized free energy potential and excess EPR have a natural interpretation in terms of large deviations. First, we rearrange our variational principle for excess EPR (42) as

$$\sigma_{\text{ex}} = \max_{\phi \in \mathbb{R}^d} \max_{\lambda \in \mathbb{R}} \left[-\lambda \dot{\mathbf{x}}^\top \phi - \mathbf{j}^\top (e^{\lambda \nabla \phi} - \mathbf{1}) \right], \quad (79)$$

which follows since the optimization is invariant under rescaling $\phi \rightarrow \lambda\phi$. With a bit of rearranging, we may write the excess EPR as

$$\sigma_{\text{ex}} = \max_{\phi \in \mathbb{R}^d} \mathcal{L}(\phi) = \mathcal{L}(\phi^*), \quad (80)$$

where for convenience we defined the function

$$\mathcal{L}(\phi) = \max_{\lambda \in \mathbb{R}} \left[\lambda(-\dot{\mathbf{x}}^\top \phi) - \mathbf{j}^\top (e^{\lambda \nabla \phi} - \mathbf{1}) \right]. \quad (81)$$

Importantly, for small dt , $\mathcal{L}(\phi)dt$ is the Legendre transform of the CGF $\Lambda_\phi(\lambda)$ (76) evaluated at $-\mathbb{E}[\Delta\phi] = -\dot{\mathbf{x}}^\top \phi dt$.

As we now explain using large deviations theory, and illustrate in Figure 4, $\mathcal{L}(\phi)$ is a fundamental measure of the irreversibility of observable ϕ . Suppose that we measure n

independent and identical copies of the system. These copies may represent independent particles, many unit volumes in a chemical reactor, or many trial runs of the same experiment. The empirical mean change of ϕ is

$$\overline{\Delta\phi}_n = \frac{1}{n} \sum_k \sum_{\rho,i} N_\rho^{(k)} \nabla_{\rho i} \phi_i, \quad (82)$$

where $N_\rho^{(k)}$ is the reaction count in system copy k . The empirical mean converges to $\mathbb{E}[\Delta\phi]$ for large n , but for finite n , it will exhibit fluctuations. According to Cramér’s theorem, a classic result from large deviations theory [p. 11, 96], the fluctuations of the empirical mean are governed by the Legendre transform of the CGF. Specifically, the probability that the empirical mean is equal to the negative of the true mean is

$$P(\overline{\Delta\phi}_n \approx -\mathbb{E}[\Delta\phi]) \simeq e^{-n\mathcal{L}(\phi)dt}. \quad (83)$$

Thus, $\mathcal{L}(\phi)$ governs the probability that ϕ appears to evolve “backwards in time” due to random fluctuations, in the sense that the empirical mean takes the opposite value of its large- n limit. $\mathcal{L}(\phi)$ is large when the observable ϕ evolves quickly, relative to the scale of its dynamical fluctuations.

Eq. (80) implies that the generalized free energy ϕ^* is the “most irreversible” observable, and that the excess EPR $\sigma_{\text{ex}} dt$ is its degree of irreversibility:

$$P(\overline{\Delta\phi}_n^* \approx -\mathbb{E}[\Delta\phi^*]) \simeq e^{-n\sigma_{\text{ex}} dt}. \quad (84)$$

The generalized free energy and the excess EPR vanish in stationarity, when it is impossible to tell whether the mean of any state observable is moving forward or backward in time.

Actually, the excess EPR can be shown to quantify the irreversibility of the entire state \mathbf{x} . Let the vector-valued random variable $[\Delta\mathbf{x}]_i = \sum_\rho N_\rho \nabla_{\rho i}$ represent the stochastic evolution of the state. The probability that the state evolves backward in time due to a random fluctuation is

$$P(\overline{\Delta\mathbf{x}}_n \approx -\dot{\mathbf{x}} dt) \simeq e^{-n\sigma_{\text{ex}} dt}. \quad (85)$$

Although we do not provide a derivation of this result here, it can be derived in a straightforward manner by combining the definition of σ_{ex} with existing results from large deviations [54][97]. Comparing (84) and (85) shows that the observable ϕ^* captures all of the irreversibility of the state evolution.

Note that a similar analysis could be performed by considering the fluctuations of an arbitrary reaction observable θ . In this case, we may define the random variable $\sum_\rho N_\rho \theta_\rho$ and consider its statistics. For antisymmetric observables ($\theta_\rho = -\theta_{\bar{\rho}}$), an expression analogous to Eq. (80) can be derived for EPR using Eq. (34) and SM2 [44]. In this expression, the force vector \mathbf{f} would be the most irreversible observable, and the EPR its degree of irreversibility. Thus, while the EPR bounds the irreversibility of all antisymmetric reaction observables, excess EPR bounds the irreversibility of changes of state observables.

We note that variational principles related to Eq. (42) have been explored in the literature on large deviations [54, 98–104]

and macroscopic fluctuation theory [36, 64, 65, 105]. Many of these results consider the large deviations of state trajectories, as in Eq. (85). However, most of these results focus on the steady-state rate function, or on the probability of rare fluctuations compatible with some constraints (e.g., escape probability from a meta-stable state). Our variational principle and our goals are somewhat different: we use large deviations to quantify the dynamical irreversibility of observables, with the aim of finding the generalized free energy ϕ^* (generalization of ϕ^{eq} , the nonequilibrium contribution to the free energy) and quantifying the excess EPR σ_{ex} (the nonstationary contribution to dissipation).

B. Thermodynamic uncertainty relation and thermodynamic inference

We now interpret our generalized free energy in terms of thermodynamic uncertainty relations (TURs), which relate dissipation, expected change of state observables, and dynamical fluctuations. This interpretation is closely related to large deviations, but there is an important difference. We considered the large deviations of fluctuations of the empirical mean change of ϕ ($\overline{\Delta\phi_n}$), averaged across many copies of the system of interest. This leads to elegant expressions for the generalized free energy and excess EPR in terms of statistical irreversibility, such as Eqs. (83) and (84). However, these expressions are often not useful in practice, because they involve the statistics of exponentially-rare events.

On the other hand, TURs are expressed in terms of the statistics of a single system, and do not refer to exponentially-rare events. Such statistics can be estimated from many copies of the system, which provides a practical method for performing thermodynamic inference — that is, for inferring the generalized free energy and excess EPR from experimental data.

Suppose one is interested in the change of some state observable ϕ over a short-time interval $[t, t + dt]$. The fluctuating change of ϕ in a single system is represented by the random variable $\Delta\phi$, Eq. (75). Furthermore, its cumulants were shown to be $K_\phi^{(k)} \approx \int \mathbf{j}^\top [\nabla\phi]^k dt$ in Eq. (77). By expanding the exponential, we can rewrite the excess EPR (44) in terms of these cumulants as

$$\sigma_{\text{ex}} = \max_{\phi \in \mathbb{R}^d} \left[-2\dot{\mathbf{x}}^\top \phi - \frac{1}{dt} \sum_{k=2} \frac{1}{k!} K_\phi^{(k)} \right]. \quad (86)$$

This gives a set of bounds on the excess EPR, each one involving empirically-accessible statistics of a single state observable ϕ . The objective in Eq. (86) quantifies the irreversibility of ϕ , defined as the difference between twice the expected change and the (nonnegative) fluctuation term. We may optimize these bounds by varying over ϕ , in this way recovering ϕ^* as the most irreversible observable and σ_{ex} at its degree of irreversibility.

Eq. (86) can be interpreted as a short-time TUR [106] for excess EPR. It is also a “higher-order” TUR [107], since it involves not only the mean and variance but also higher cumulants. Unlike traditional TURs, higher-order TURs can be

made tight by appropriate choice of observable, including in discrete systems and systems arbitrarily far from equilibrium and steady state.

We note that thermodynamic inference techniques proposed in Refs. [74, 75] for estimating EPR can also be used to estimate excess EPR using (86). Actually, estimation of excess EPR may be more practical, because it only involves measurements of state observables at two time points, rather than measurements of general reaction observables.

VII. THERMODYNAMIC SPEED LIMITS

In this section, we derive thermodynamic speed limits (TSLs). We consider both short-time TSL, which relate excess EPR to the instantaneous speed of evolution at a given time, and finite-time TSLs, which relate integrated excess EP to time and trajectory length. Because excess EPR is always smaller than EPR, our expressions also imply TSLs on the overall entropy production.

A. Short-time speed limits

We first derive a short-time TSL that bounds the rate of change of any state observable ϕ . Before proceeding, we note that our higher-order TUR (86) can already be understood as a kind of short-time TSL, since it controls the rate of change of all state observables. However, that bound involve all cumulants, which are not always accessible in practice. Here we derive weaker thermodynamic bounds that involve only a few simple statistics.

We introduce a bit of notation for convenience. We refer to the instantaneous rate of change of ϕ as

$$d_t \langle \phi \rangle := \dot{\mathbf{x}}^\top \phi. \quad (87)$$

In addition, we define the “activity of observable ϕ ” as

$$a(\phi) := \mathbf{j}^\top |\nabla\phi|. \quad (88)$$

This quantifies the rate of absolute (negative and positive) changes of observable ϕ across all reactions. It is as a nonnegative measure of the dynamical fluctuations of ϕ , vanishing only when ϕ is a conserved quantity ($\nabla\phi = \mathbf{0}$). Finally, we refer to the “dynamical activity”,

$$\mathfrak{a} := \|\mathbf{j}\|_1 = \sum_{\rho} j_{\rho}.$$

The dynamical activity, a well-known quantity in stochastic thermodynamics [6], measures the average number of reactions per unit time.

To derive our TSL, we assume without loss of generality that our observable of interest ϕ is normalized so its change across any reaction ρ is bounded as

$$\|\nabla\phi\|_{\infty} := \max_{\rho} \left| \sum_i \nabla_{\rho i} \phi_i \right| \leq 1. \quad (89)$$

The quantity $\|\nabla\phi\|_\infty$ is sometimes called the discrete Lipschitz constant in the literature.

Given assumption (89), we have the following TSL:

$$\sigma_{\text{ex}} \geq 2d_t\langle\phi\rangle \tanh^{-1} \frac{d_t\langle\phi\rangle}{a(\phi)}. \quad (90)$$

This result follows from (42) and a simple bound on the exponential function, with details provided in SM4 [44]. We can also derive a weaker, but simpler, TSL in terms of the dynamical activity \mathfrak{a} :

$$\sigma_{\text{ex}} \geq 2d_t\langle\phi\rangle \tanh^{-1} \frac{d_t\langle\phi\rangle}{\mathfrak{a}}. \quad (91)$$

This follows from (90) and $a(\phi) \leq \|\mathbf{j}\|_1 \|\nabla\phi\|_\infty = \mathfrak{a}$ using Hölder's inequality.

Eqs. (90) and (91) bound the excess EPR in terms of the change of ϕ and the activity. Unlike the higher-order TUR (86), these bounds cannot always be made tight by optimizing over ϕ . Nonetheless, these TSL can provide useful bounds, especially in the far-from-equilibrium regime. For instance, the bound (90) diverges in the absolutely irreversible limit, where all activity results in directed change of ϕ ($d_t\langle\phi\rangle \rightarrow a(\phi)$). In this regime, our TSL are stronger than conventional speed limits that are quadratic in $d_t\langle\phi\rangle$ [6], since those do not diverge in the limit of absolute irreversibility. At the same time, weaker quadratic TSLs can be derived from Eq. (90),

$$\sigma_{\text{ex}} \geq \frac{2(d_t\langle\phi\rangle)^2}{a(\phi)} \geq \frac{2(d_t\langle\phi\rangle)^2}{\mathfrak{a}}, \quad (92)$$

which follows from the inequality $x \tanh^{-1} x \geq x^2$.

There is an important connection between our TSL (91) and the 1-Wasserstein distance from optimal transport [108]. Given two states $\mathbf{x}(t)$ and $\mathbf{x}(t')$, the 1-Wasserstein distance is defined as

$$W(t, t') = \min_{\mathbf{m} \in \mathbb{R}_+^m} \|\mathbf{m}\|_1 \quad \text{where} \quad \nabla^\top \mathbf{m} = \mathbf{x}(t') - \mathbf{x}(t). \quad (93)$$

In words, $W(t, t')$ is the minimal activity (number of reactions) required to drive the system from state $\mathbf{x}(t)$ to state $\mathbf{x}(t')$, using reactions permitted by the stoichiometric matrix ∇ . Because it depends on the stoichiometric matrix, this distance is sensitive to the system's intrinsic topology. For example, the Wasserstein distance between the same states is typically larger on a 1-dimensional lattice than on a fully connected network.

To relate Wasserstein distance to our short-time TSLs, we define the Wasserstein speed as the infinitesimal distance per unit time,

$$\dot{W}(t) := \frac{1}{dt} W(t, t + dt). \quad (94)$$

An important duality shows that \dot{W} can be expressed as an optimization over normalized state observables:

$$\dot{W}(t) = \max_{\phi \in \mathbb{R}^d} \dot{\mathbf{x}}(t)^\top \phi \quad \text{where} \quad \|\nabla\phi\|_\infty \leq 1. \quad (95)$$

In optimal transport, this relation is called Kantorovich duality; a self-contained derivation is provided in SM5 [44].

Since the optimal observable in Eq. (95) satisfies the constraint (89), it obeys our short-time TSL (91). Plugging in gives the Wasserstein short-time TSL,

$$\sigma_{\text{ex}} \geq 2\dot{W} \tanh^{-1} \frac{\dot{W}}{\mathfrak{a}}. \quad (96)$$

From Eq. (95), we may verify that this provides the tightest version of the bound (91).

The Wasserstein TSL (96) was previously derived for EPR in MJPs in Ref. [108]. Our result tightens this bound by relating it to the excess EPR, in this way making it more useful for active systems. It also generalizes it beyond MJPs, making it applicable to arbitrary nonlinear CRNs.

In general, the HS excess EPR does not satisfy the Wasserstein TSL (96), as will be seen in the unicyclic system considered in Section VIII [109]. Instead, for MJPs, the HS excess EPR obeys the TSL [8],

$$\sigma_{\text{ex}}^{\text{HS}} \geq \frac{\|\dot{\mathbf{x}}\|_1^2}{2\mathfrak{a}}. \quad (97)$$

The quantity $\|\dot{\mathbf{x}}\|_1/2$ is the total variation (TV) speed, a measure which is not sensitive to system topology. For MJPs, Wasserstein speed is larger than TV speed [108], thus Eq. (96) also implies

$$\sigma_{\text{ex}} \geq \|\dot{\mathbf{x}}\|_1 \tanh^{-1} \frac{\|\dot{\mathbf{x}}\|_1}{2\mathfrak{a}}. \quad (98)$$

This far-from-equilibrium TV bound does not hold for $\sigma_{\text{ex}}^{\text{HS}}$, although some intermediate bounds have been shown [37, 73].

B. Finite-time speed limits

We now derive a finite-time TSLs for time-extended processes. For simplicity, we focus on the finite-time analogue of the Wasserstein TSL (96), though similar results can be derived for arbitrary observables using Eqs. (90) and (91).

Consider a time-extended process over $t \in [0, T]$, during which the state evolves from $\mathbf{x}(0)$ to $\mathbf{x}(T)$. The total excess EP is given by $\Sigma_{\text{ex}} = \int_0^T \sigma_{\text{ex}}(t) dt$. We define the total dynamical activity, the overall expected number of reactions, as

$$A := \int_0^T \mathfrak{a}(t) dt.$$

Finally, we use the Wasserstein speed $\dot{W}(t)$ to define the Wasserstein length of the state trajectory,

$$\mathcal{L}_W = \int_0^T \dot{W}(t) dt. \quad (99)$$

Using the triangle inequality for Wasserstein distance [108], we can bound the trajectory length using the overall Wasserstein distance from the initial to the final state,

$$\mathcal{L}_W \geq W(0, T).$$

Our short-time TSL (96) can be written as $\sigma_{\text{ex}}(t) \geq \mathbf{a}(t)g[\dot{W}(t)/\mathbf{a}(t)]$, where for convenience we introduced the function $g(x) := 2x \tanh^{-1} x$. Integrating both sides of this inequality gives

$$\Sigma_{\text{ex}} \geq \int_0^T \mathbf{a}(t) g \left[\frac{\dot{W}(t)}{\mathbf{a}(t)} \right] dt \geq Ag \left[\frac{\mathcal{L}_W}{A} \right],$$

where the second bound follows by applying Jensen's inequality to the convex function $g(x)$. Rearranging gives the finite-time Wasserstein TSL for excess EP,

$$\Sigma_{\text{ex}} \geq 2\mathcal{L}_W \tanh^{-1} \frac{\mathcal{L}_W}{A} \quad (100)$$

$$\geq 2W(0, T) \tanh^{-1} \frac{W(0, T)}{A}. \quad (101)$$

We may also derive a more familiar form of the TSL, as a bound on the minimal time required to traverse a given distance. Consider the time-averaged dynamical activity, defined as the number of reactions per time, $\bar{\mathbf{a}} := A/T$. We rearrange Eq. (100) to give

$$T \geq \frac{\mathcal{L}_W}{\bar{\mathbf{a}}} \coth \frac{\Sigma_{\text{ex}}}{2\mathcal{L}_W} \geq \frac{W(0, T)}{\bar{\mathbf{a}}} \coth \frac{\Sigma_{\text{ex}}}{2W(0, T)}. \quad (102)$$

Since $\coth(x) \geq 1$, there is a finite minimal time needed to undergo a trajectory of a given length,

$$T \geq \mathcal{L}_W / \bar{\mathbf{a}} \geq W(0, T) / \bar{\mathbf{a}}.$$

These bounds become relevant in the highly irreversible limit, since they hold even when Σ_{ex} diverges. Conversely, these TSL imply that Σ_{ex} diverges as $-\ln(T - \mathcal{L}_W / \bar{\mathbf{a}})$ as $T \rightarrow \mathcal{L}_W / \bar{\mathbf{a}}$. This is stronger than the $1/T$ scaling reported in conventional TSLs [6, 9, 15, 18, 20, 110, 111], which only become tight in the limit of slow driving [112–114].

C. Information-theoretic speed limit for relaxing MJPs

Our final result is a finite-time TSL that relates excess EP and the speed of relaxation. This result is quite different from the TSLs derived above, in that it only applies to MJPs, only to certain kinds of protocols, and it does not reference Wasserstein distance. Nonetheless, it provides a useful bound based on an interpretable and empirically-accessible information-theoretic notion of distance.

Consider an MJP that undergoes a process over $t \in [0, T]$, during which the system goes from state $\mathbf{x}(0)$ to state $\mathbf{x}(T)$. Suppose that the process involves an autonomous relaxation (time-independent control parameters), or more generally that the driving is time-symmetric, such that the control parameters at time t are the same as at time $T-t$. Given these assumptions, we show in SM3 [44] that the variational principle for excess EPR (42) can be expressed as

$$\sigma_{\text{ex}} = \max_{\mathbf{y}} \left[- \frac{d}{dt} D(\mathbf{x}(t) \| \mathbf{y}(-t)) \right]. \quad (103)$$

where the maximization is over all probability distributions over the microstates. The notation $\mathbf{y}(-t)$ indicates that \mathbf{y} evolves “backwards in time”,

$$-\frac{d}{dt} y_i(-t) = \sum_{j(\neq i), \alpha} (y_j(-t) R_{ij}^\alpha - y_i(-t) R_{ji}^\alpha). \quad (104)$$

Thus, σ_{ex} is the fastest rate of contraction of relative entropy between the actual state \mathbf{x} evolving forward-in-time and any other state evolving backward-in-time. The optimum in Eq. (103) is achieved by the pseudo-canonical state $\mathbf{x}^* \propto \mathbf{x} \circ e^{-\phi^*}$ defined by the generalized free energy ϕ^* .

Eq. (103) gives the following information-theoretic bound,

$$\Sigma_{\text{ex}}(T) \geq D(\mathbf{x}(0) \| \mathbf{x}(T)), \quad (105)$$

The relative entropy $D(\mathbf{x}(0) \| \mathbf{x}(T))$ is an information-theoretic measure of the distance traversed by system's state over time $t \in [0, T]$. It is interpretable and practically accessible by measuring the state at two timepoints.

Eq. (103) and (105) generalize the main results of Ref. [79], which derived the same expressions for EPR in passive MJPs. In particular, the derivation of Eq. (105) proceeds in the same way as [Eq. (3), 79]. Specifically, we choose $\mathbf{y}(0) = \mathbf{x}(T)$ in Eq. (103) and then integrate over $t \in [0, T/2]$. Under the assumption of time-symmetric driving, $\mathbf{y}(t) = \mathbf{x}(T-t)$ is a solution to Eq. (104), so the time integral gives

$$\begin{aligned} \Sigma_{\text{ex}}(T/2) &\geq - \int_0^{T/2} \frac{d}{dt} D[\mathbf{x}(t) \| \mathbf{x}(T-t)] dt \\ &= D[\mathbf{x}(0) \| \mathbf{x}(T)] - D[\mathbf{x}(T/2) \| \mathbf{x}(T/2)] \\ &= D[\mathbf{x}(0) \| \mathbf{x}(T)]. \end{aligned}$$

Since $\sigma_{\text{ex}}(t) \geq 0$ for $t \in [T/2, T]$, we have the sequence of bounds:

$$\Sigma_{\text{ex}}(T) \geq \Sigma_{\text{ex}}(T/2) \geq D[\mathbf{x}(0) \| \mathbf{x}(T)].$$

Note that the bound (105) was conjectured to hold for HS excess EP [115]. However, that conjecture is not valid, as we will see in the unicyclic system considered in the next section.

VIII. EXAMPLES

We now illustrate our approach on two examples: a unicyclic MJP and the Brusselator, a nonlinear CRN.

A. Unicyclic MJP

In our first example, we consider a uniform cyclic MJP. This example will be useful to illustrate the difference between our approach and the HS one.

The MJP is parameterized by transition rates

$$R_{i+1,i} = \frac{1}{1 + e^{-\gamma}}, \quad R_{i-1,i} = \frac{e^{-\gamma}}{1 + e^{-\gamma}}, \quad (106)$$

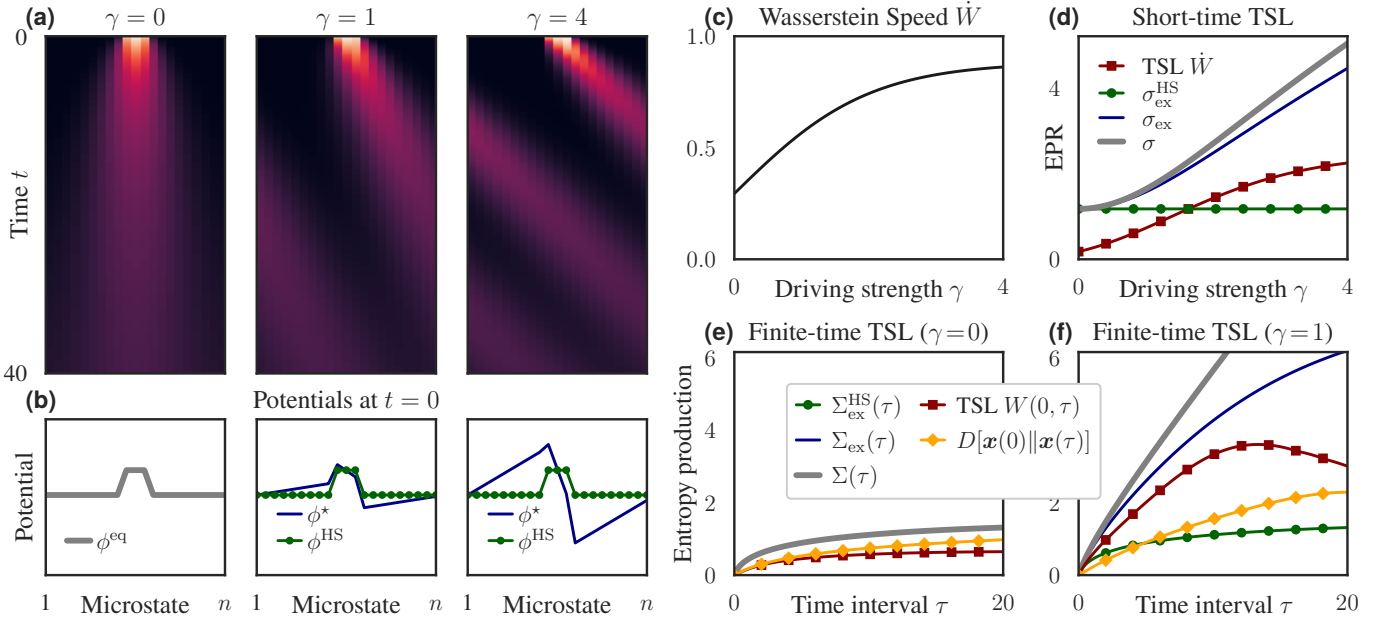


Figure 5. **Illustration of results on unicyclic MJP with $d = 21$ states.** (a): Time evolution of the probability distribution for three driving strengths ($\gamma = 0, 1, 4$). The initial distribution is concentrated on three initial microstates $i \in \{10, 11, 12\}$. (b) Generalized free energy ϕ^* and steady-state potential ϕ^{ss} for different driving strengths, evaluated at $t = 0$. (c) Wasserstein speed at $t = 0$ increases with driving strength. (d) EPR, excess EPR, and HS excess EPR shown as a function of driving strength. The Wasserstein short-time TSL (96) is also shown. The HS excess EPR and steady-state potential are not sensitive to the driving strength γ nor the Wasserstein speed. (e) Time-integrated EP, excess EP, and HS excess EP for a passive system ($\gamma = 0$) over time $t \in [0, \tau]$. All three quantities obey the Wasserstein TSL (101) and information-theoretic bound (105). (f) EP, excess EP and HS excess EP for an active driven system ($\gamma = 1$). The Wasserstein and information-theoretic bounds only hold for our excess EP, not the HS excess EP.

where the indexing of microstates i is taken mod d . The parameter γ determines the strength of nonconservative driving around the cycle. The overall timescale is normalized, in that the escape rates do not depend on γ ($-R_{ii} = 1$ for all i). Therefore, the dynamical activity is $\alpha = 1$, regardless of the γ or the distribution \mathbf{x} .

In Figure 5, we show a cycle with $d = 21$ microstates. For the initial probability distribution, we assume three microstates have elevated probability, $x_{10}(0) = x_{11}(0) = x_{12}(0) = 0.3$, while the other 18 microstates split the remainder, $x_i(0) = 0.1/18$. In Figure 5(a), we plot the time evolution of the system's state for three values of the driving strength: $\gamma = 0$ (no driving), $\gamma = 1$, and $\gamma = 4$. For $\gamma = 0$, the system is passive and it relaxes to equilibrium by diffusing symmetrically. For $\gamma = 1$ and $\gamma = 4$, the system increasingly exhibits a decaying oscillation around the cycle.

In Figure 5(b), we show the steady-state potential $\phi^{ss} = \ln(\mathbf{x}/\mathbf{x}^{ss})$ and the generalized free energy potential ϕ^* (found by numerical optimization) for the three driving strengths, evaluated at the initial time point $t = 0$. For $\gamma = 0$, the potentials are all equal to each other and to the free energy potential, $\phi^* = \phi^{ss} = \phi^{eq} = \ln(\mathbf{x}/\mathbf{x}^{eq})$. For stronger driving, ϕ^* becomes increasingly asymmetric and “cliff-like”, corresponding to the increasingly asymmetric evolution of the system's state. On the other hand, since the steady state is the uniform distribution for all γ , the steady-state potential ϕ^{ss} is always symmetric and does not vary with γ .

Figure 5(c) shows the Wasserstein speed \dot{W} (94) as a func-

tion of the driving strength, evaluated at the initial time. The Wasserstein speed increases with driving strength, showing that the system's state evolves faster when it undergoes a directed force around the cycle, compared to when it undergoes an undriven symmetric diffusion.

Figure 5(d) shows the values of EPR, our excess EPR, and HS excess EPR for different values of the driving. The EPR and our excess EPR increase with stronger driving. However, the HS excess EPR remains constant, being insensitive to the driving strength. We also plot the short-time Wasserstein TSL (96) for excess EPR. The TSL provides a lower-bound on our excess EPR, but no such bound holds for HS excess EPR.

To summarize, Figure 5(b)-(d) show that our generalized free energy and excess EPR are sensitive to the direction and speed of evolution of the system's state. This is not the case for the steady-state potential and HS excess EPR in this system, which are not sensitive to the strength of driving or speed of evolution.

In Figure 5(e)-(f), we show the time-integrated EP and excess EP for the time-extended processes shown in Figure 5(a)-(b). Specifically, we plot $\Sigma(\tau) = \int_0^\tau \sigma(t) dt$ as a function of the time interval τ , and similarly for $\Sigma_{ex}(\tau)$ and $\Sigma_{ex}^{HS}(\tau)$. We also plot our finite-time Wasserstein TSL (101) and the information-theoretic bound (105). For the passive system, Figure 5(e), $\Sigma(\tau) = \Sigma_{ex}(\tau) = \Sigma_{ex}^{HS}(\tau)$ and the Wasserstein and information-theoretic bounds are always obeyed. Figure 5(f) shows the active system with $\gamma = 1$, where we verify that $\Sigma(\tau) \geq \Sigma_{ex}(\tau) \geq \Sigma_{ex}^{HS}(\tau)$. We also see that the Wasser-

stein and information-bound bounds are violated by the HS excess EPR. Note that $D[x(0)||x(\tau)]$ tends to be larger in the active system, showing that stronger driving leads to faster dynamics under that information-theoretic measure of speed.

B. Brusselator CRN

In our second example, we consider the Brusselator CRN [51], a well-known model of a chemical oscillator, shown above in Figure 2.

To analyze the Brusselator, we use the fact that two of the reactions, $X_1 \rightleftharpoons X_2$ and $3X_1 \rightleftharpoons 2X_1 + X_2$, have the same stoichiometry. We may then introduce the reaction-level coarse-graining described in Section VC, which gives the following coarse-grained stoichiometric matrix and forward/reverse fluxes:

$$\nabla = \begin{bmatrix} 1 & 0 \\ -1 & 0 \\ -1 & 1 \\ 1 & -1 \end{bmatrix} \quad \bar{\mathbf{j}} = \begin{bmatrix} k_1^+ \\ x_1 k_1^- \\ x_1(k_2^+ + x_1^2 k_3^-) \\ x_2(k_2^- + x_1^2 k_3^+) \end{bmatrix} \quad \bar{\mathbf{j}} = \begin{bmatrix} x_1 k_1^- \\ k_1^+ \\ x_2(k_2^- + x_1^2 k_3^+) \\ x_1(k_2^+ + x_1^2 k_3^-) \end{bmatrix}$$

The resulting coarse-grained forces are conservative,

$$\bar{\mathbf{f}} = \left(\ln \frac{\bar{j}_1}{\bar{j}_2}, \ln \frac{\bar{j}_2}{\bar{j}_1}, \ln \frac{\bar{j}_3}{\bar{j}_4}, \ln \frac{\bar{j}_4}{\bar{j}_3} \right) = -\nabla \phi^*,$$

where generalized free energy potential is

$$\begin{aligned} \phi^* &= \left(\ln \frac{\bar{j}_2}{\bar{j}_1}, \ln \frac{\bar{j}_2}{\bar{j}_1} + \ln \frac{\bar{j}_4}{\bar{j}_3} \right) \\ &= \left(\ln \frac{x_1 k_1^-}{k_1^+}, \ln \frac{x_1 k_1^-}{k_1^+} + \ln \frac{x_2(k_2^- + x_1^2 k_3^+)}{x_1(k_2^+ + x_1^2 k_3^-)} \right). \end{aligned} \quad (107)$$

Since the coarse-fluxes are conservative, the excess EPR is equal to the EPR of the coarse-grained fluxes (see Section VC):

$$\sigma_{\text{ex}} = \sigma(\bar{\mathbf{j}}) = -\dot{\mathbf{x}}^\top \phi^*. \quad (109)$$

The housekeeping EPR is given by the remainder, $\sigma_{\text{hk}} = \sigma(\mathbf{j}) - \sigma(\bar{\mathbf{j}})$.

For concreteness, we take the rate constants as $k_1^+ = k_1^- = k_2^- = k_3^- = 1$, $k_2^+ = 17$ while k_3^+ is varied in the range of $k_3^+ \in [6, 11]$. For these parameter values, the system exhibits limit-cycle oscillations. Time-dependent concentrations $x_1(t), x_2(t)$ for three different choices of k_3^+ are shown in Figure 6(b)-(d). In addition, Figure 6(a) shows the EPR $\sigma_{\text{ex}}(t)$ and excess EPR $\sigma_{\text{ex}}(t)$ for $k_3^+ = 6$. Excess EPR tends to be large when the concentrations are changing rapidly. The grey boxes indicate single cycle period of the oscillator (considered in more detail below).

Figure 6(e) shows the decomposition of EPR into excess and housekeeping components, as a function of the two concentrations $\mathbf{x} = (x_1, x_2)$. Here we focus on the $k_3^+ = 6$ system, whose state evolution and dissipation over time is shown in

Figure 6(a)-(b). Streamlines show the dynamical evolution $\dot{\mathbf{x}}$ at each point in concentration space, with the actual trajectory from Figure 6(b) shown as a green line.

There is a clear relationship between the excess EPR and important features of the state dynamics. Lighter regions (higher excess EPR) correspond to regions of faster evolution, while darker regions (smaller excess EPR) correspond to slower regions, such as the limit cycle itself. Also, excess EPR vanishes at the unstable fixed point, located at the middle of the cycle. At the same time, there is no clear relationship between state dynamics and the overall EPR or the housekeeping EPR.

We do not compare our analysis to the HS decomposition because, for the parameters considered here, the Brusselator does not have a steady state (no stable fixed point). Formally, the HS decomposition could be defined by taking \mathbf{x}^{ss} as the unstable fixed point, however this is not physically meaningful and it leads to negative values of $\sigma_{\text{ex}}^{\text{HS}}$ (see [Fig. 7, 20]).

Next, we illustrate our finite-time TSL as a bound on the dissipation and time needed to complete one oscillator cycle. For a trajectory that enters a limit cycle, we measure the cycle time T_{cyc} as well as the activity A , excess EP Σ_{ex} , and EP Σ incurred during one cycle. In addition, we measure the Wasserstein length of the cycle, $\mathcal{L}_W = \int_0^{T_{\text{cyc}}} \dot{W}(t) dt$. We remind the reader that \mathcal{L}_W can be understood as the minimal dynamical activity required to traverse the cycle's trajectory in concentration space. Our finite-time TSL (100) then gives following bounds on the EP and excess EP:

$$\Sigma \geq \Sigma_{\text{ex}} \geq 2\mathcal{L}_W \tanh^{-1} \frac{\mathcal{L}_W}{A}. \quad (110)$$

For the Brusselator, the Wasserstein speed of evolution $\dot{\mathbf{x}} = (\dot{x}_1, \dot{x}_2)$ can be written in closed form as

$$\dot{W} = |\dot{x}_1 + \dot{x}_2| + |\dot{x}_2|. \quad (111)$$

To see why, note that only the (coarse-grained) reactions $X_1 \rightleftharpoons X_2$ affect the concentration of X_2 , so either the forward or reverse direction must have a flux of at least $|\dot{x}_2|$ (which one depending on the sign of \dot{x}_2). One of the two remaining reactions must have a minimal flux $|\dot{x}_1 + \dot{x}_2|$ to induce the correct evolution of X_1 . Eq. (111) implies that the Brusselator's Wasserstein length \mathcal{L}_W is given by the ‘‘taxicab-geometry’’ in coordinates $(x_1 + x_2, x_2)$.

To illustrate this, Figure 6(f) plots the three cycles from Figure 6(b)-(d) in this coordinate system. In this ‘‘Wasserstein space,’’ \mathcal{L}_W is equal to the perimeter of the minimal bounding box. Comparing Figure 6(b)-(d) and (f), we see that larger k_3^+ leads to shorter cycle times and smaller Wasserstein lengths. We plot the line width in Figure 6(f) proportionally to the time-averaged dynamical activity $\bar{a} = A/T_{\text{cyc}}$, though it does not change significantly across these k_3^+ values.

We illustrate our finite-time Wasserstein TSL (110) in Figure 6(g) for $k_3^+ \in [6, 11]$. The bound is relatively tight, capturing about a third of the excess EP at $k_3^+ \approx 6$, and about half around $k_3^+ \approx 11$. EP is many orders of magnitude larger than excess EP (shown in the inset in semi-logarithmic scale) and it does not lead to a useful TSL.

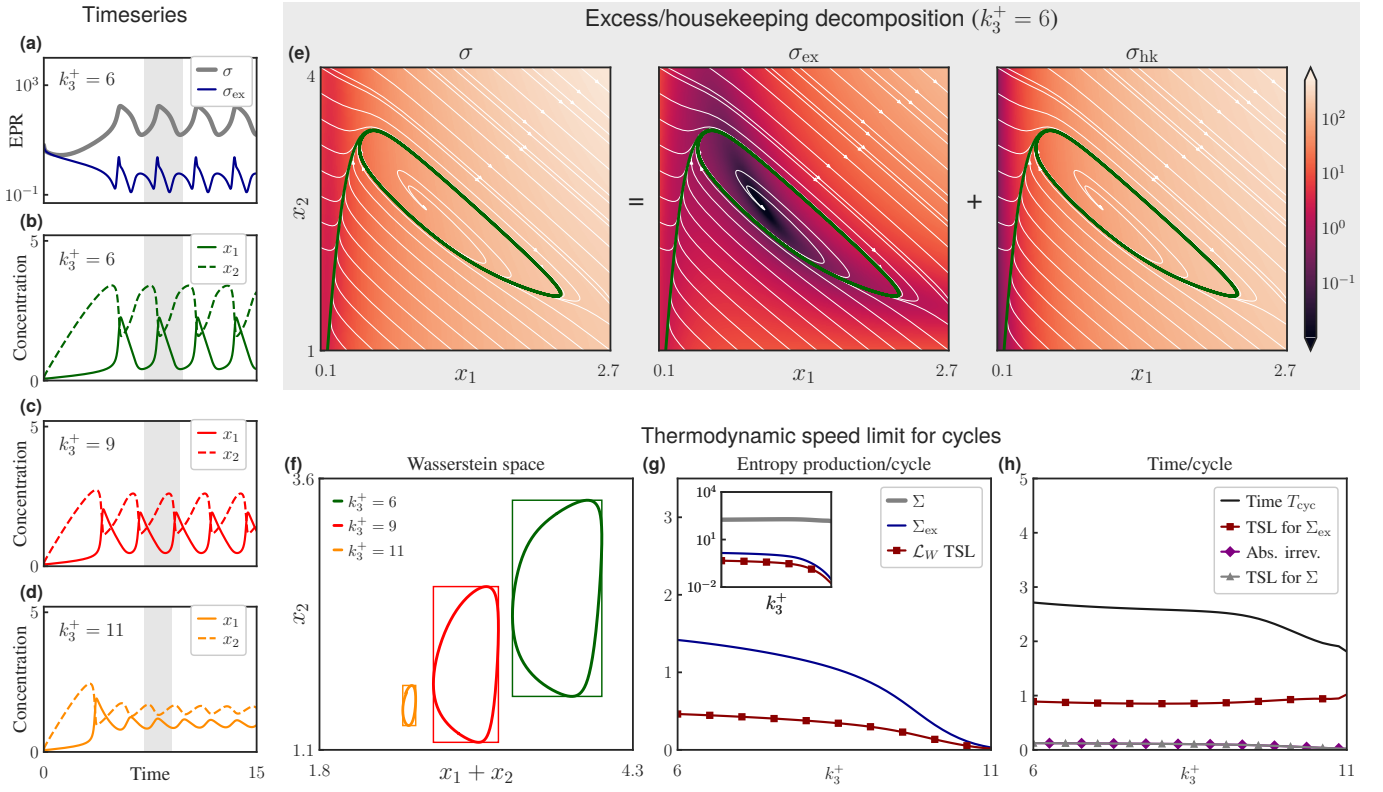


Figure 6. **Illustration of our approach on the Brusselator**, a nonlinear CRN previously shown Figure 2. (a) EPR σ and excess EPR σ_{ex} over time a typical trajectory (other parameters: $k_1^+ = k_1^- = k_2^- = k_3^- = 1$, $k_2^+ = 17$, $k_3^+ = 6$); excess EPR is larger during fast evolution. (b)-(d) Evolution of concentrations $x_1(t), x_2(t)$ for $k_3^+ \in \{6, 9, 11\}$ (other parameters as above). Single cycles are marked in gray. (e) EPR σ decomposed into excess EPR σ_{ex} and housekeeping EPR σ_{hk} , as a function of the two concentrations for the system shown in (a)-(b). Streamlines (white) and actual evolution (green) are overlaid. The excess EPR is sensitive to dynamics features, such as the limit cycles and fixed points. (f)-(g) Illustration of TSLs on the Brusselator. The cycles from (b)-(d) are shown in coordinates $(x_1 + x_2, x_2)$ in Wasserstein space (f). In this space, the Wasserstein length \mathcal{L}_W of the cycles corresponds to the perimeter length of bounding boxes (see text for details). TSL for entropy production (110) is shown in (g); TSLs for cycle time (112)-(113) are shown in (h).

We may use Eq. (102) to bound the minimal time needed to complete a cycle as

$$T_{cyc} \geq \frac{\mathcal{L}_W}{\bar{a}} \coth \frac{\Sigma_{ex}}{2\mathcal{L}_W} \quad (112)$$

$$\geq \frac{\mathcal{L}_W}{\bar{a}} \coth \frac{\Sigma}{2\mathcal{L}_W} \geq \frac{\mathcal{L}_W}{\bar{a}}. \quad (113)$$

The last bound (113) applies in the absolutely irreversible regime where σ_{ex} diverges. These bounds are illustrated in Figure 6(h) for $k_3^+ \in [6, 11]$. The excess EP bound is relatively tight across the range of k_3^+ values. The EP bound and absolute irreversibility bounds (113) are essentially equivalent, since EP is very large for this system.

IX. DISCUSSION

In this paper, we propose a generalized notion of free energy applicable to a broad class of linear and nonlinear active systems.

It is worth remarking that, when considering the thermodynamics of passive systems, free energy can be seen from

two different perspectives. The first perspective is state-based: free energy is considered as distance between the actual state and equilibrium, and it draws attention to aspects like stationary fluctuations, Lyapunov stability, and work availability. The second perspective is dynamical (flux-based): free energy is considered as the potential in conservative thermodynamic forces, and it draws attention to aspects like dynamical fluctuations, gradient flow dynamics, and entropy production rate. Many aspects of the dynamical perspective originated in the visionary work of Onsager [85, 116, 117].

These two perspectives lead to different generalizations to active systems, which lack equilibrium states and have nonconservative forces. Until now, most research has extended the first (static) perspective. Here, the generalized potential is defined as the distance between the actual state and (nonequilibrium) steady state. The excess EPR, the nonstationary contribution to dissipation, is defined as the decrease of this distance over time. This approach is undoubtedly useful, but also faces several conceptual and practical limitations. Moreover, it cannot be applied to many nonlinear systems of interest.

Here, we propose an alternative generalization of the concept of free energy, based on the second (dynamical) perspec-

tive. Here, the generalized potential is defined variationally as most irreversible state observable, and the excess EPR is defined as its degree of irreversibility. The generalized potential can be understood as offering the best “conservative approximation” to the forces. As we show, our approach is physical meaningful and experimentally accessible, and provides a generalization of Onsager’s theory to the far-from-equilibrium regime. Furthermore, because our approach makes no explicit reference to steady states, it can be applied to a large class of systems, including nonlinear systems without steady states. We use it to derive various thermodynamic bounds on dynamical evolution, showing that it gives meaningful bounds even in cases where the steady-state approach is insensitive to the dynamics or simply inapplicable.

We mention several possible directions for future work.

First, as we showed, excess EPR in the linear-response regime defines a Riemannian geometry over the set of thermodynamic states. It would be interesting to explore thermodynamic length and optimal protocols using this geometry, in both linear and nonlinear active systems.

Second, here we considered the excess/housekeeping decomposition applied to the EPR at a given instant in time. Our variational principle may be considered for time-extended stochastic processes, where entropy production is quantified as the relative entropy between trajectory distributions. This may lead to fluctuation theorems for excess/housekeeping EPR, as well as generalizations to non-Markovian stochastic processes. There are also interesting connections to other trajectory-level variational principles, such as Schrödinger-bridge problems [118, 119] and Maximum Caliber inference [120].

Third, in this paper, we focused mostly on the generalized free energy and the excess EPR. However, we also showed that the housekeeping EPR, the non-excess contribution to dissipation, quantifies the nonconservative nature of the forces. Future work may study the housekeeping EPR in more depth, e.g., from the perspective of large deviations, thermodynamic uncertainty relations and speed limits, as well as decompositions into elementary cycles [20].

Finally, it is interesting to consider our information-geometric formulation in other types of physical systems — such as reaction-diffusion systems [21], hydrodynamic systems [121], and quantum systems [122] — where EPR decompositions have recently been developed using Euclidean geometry.

ACKNOWLEDGMENTS

S. I. thanks Masafumi Oizumi for fruitful discussions. A. D. is supported by JSPS KAKENHI Grants No. 19H05795, and No. 22K13974. K. Y. is supported by Grant-in-Aid for JSPS Fellows (Grant No. 22J21619). S. I. is supported by JSPS KAKENHI Grants No. 21H01560, No. 22H01141, No. 23H00467, and No. 24H00834, JST ERATO Grant No. JP-MJER2302, and UTEC-UTokyo FSI Research Grant Program. A. K. received funding from the European Union’s Horizon 2020 research and innovation programme under the Marie Skłodowska-Curie Grant Agreement No. 101068029.

Appendix A: CRNs with external flows

We show how our formalism generalizes to deterministic CRN with external inflows or outflows, e.g., as in a flow reactor. In this case, the continuity equation (1) is written as

$$\dot{\mathbf{x}}(t) = \nabla^\top \mathbf{j}(\mathbf{x}, t) + \mathbf{I}(\mathbf{x}, t),$$

where the vector $\mathbf{I}(\mathbf{x}, t) \in \mathbb{R}^d$ indicates the net flows (inflow minus outflow), one for each species.

External flows do not contribute directly to the EPR σ , thus its definition in Eq. (6) remains the same. Also, the definitions of thermodynamic forces and EPR remain the same, since they are stated purely in terms of reaction fluxes \mathbf{j} . The expression of excess EPR (42) and the generalized free energy (43) also remains the same. The dual expression of the excess EPR (46), as an information-theoretic optimal transport problem, should be written in the more general form:

$$\sigma_{\text{ex}} = \min_{\mathbf{j}' \in \mathbb{R}_+^m} \mathcal{D}(\mathbf{j}' \| \tilde{\mathbf{j}}) \quad \text{where} \quad \nabla^\top \mathbf{j}' = \nabla^\top \mathbf{j}. \quad (\text{A1})$$

Thus, the excess EPR quantifies the minimal relative entropy required to generate $\nabla^\top \mathbf{j} = \dot{\mathbf{x}} - \mathbf{I}$, the state evolution induced by the reaction fluxes \mathbf{j} (not the flows). In the absence of flows, this reduces to the expression in the main text.

The bounds $0 \leq \sigma_{\text{ex}} \leq \sigma$ continue to hold. Furthermore, we still have a decomposition of EPR into nonnegative excess and housekeeping terms:

$$\sigma = \sigma_{\text{ex}} + \sigma_{\text{hk}}.$$

The housekeeping EPR still obeys (62), and it quantifies the nonconservative nature of the forces.

In the presence of external flows, excess EPR does not necessarily vanish in steady state. As an example, imagine a passive system (i.e., with conservative forces) that is maintained in a nonequilibrium steady state by external flows. In this case, $\sigma_{\text{hk}} = 0$ and $\sigma_{\text{ex}} = \sigma > 0$. Basically, in the presence of external flows, the excess EPR is associated with the non-stationarity of the reaction fluxes ($\nabla^\top \mathbf{j}' \neq \nabla^\top \tilde{\mathbf{j}}$), not of the state as a whole.

Appendix B: Systems with odd variables

1. Entropy production rate

We show how our formalism generalizes to MJPs with odd variables, such as velocity or momentum, whose sign changes under time reversal.

We first write the expression of EPR. Consider an MJP coupled to a single heat bath that evolves over a small time interval $[t, t + dt]$. The conditional probability that the system is in state j at time $t + dt$, given state i at time t , is

$$T_{j|i} = dt R_{ji} + O(dt^2).$$

The EP is the relative entropy between the forward and backward joint distributions,

$$\Sigma = D(x_i T_{j|i} \| x_j T_{\epsilon i|\epsilon j}), \quad (\text{B1})$$

where ϵi indicates the conjugation of microstate i (odd-parity variables flipped in sign). The conjugation of the reverse conditional probability $T_{\epsilon i|\epsilon j}$ follows from the principle of local detailed balance for systems with odd variables (see Refs. [68, 69, 123], also Section 5.3.4 in [124]). We may write Eq. (B1) more explicitly as

$$\Sigma = \underbrace{\sum_{i \neq j} x_i T_{j|i} \ln \frac{x_i T_{j|i}}{x_j T_{\epsilon i|\epsilon j}}}_{\text{Transitions}} + \underbrace{\sum_i x_i T_{i|i} \ln \frac{x_i T_{i|i}}{x_i T_{\epsilon i|\epsilon i}}}_{\text{Diagonals}}.$$

The second term, labeled ‘‘Diagonals’’, is the contribution to EP due to different escape rates under the forward and reverse dynamics. This contribution only appears in systems with odd variables, since it vanishes when $i = \epsilon i$.

The EPR is the time derivative of EP, $\sigma = \frac{d}{dt} \Sigma$. With a bit of algebra, this derivative can be found as

$$\sigma = \sum_{j \neq i} \left(x_i R_{ji} \ln \frac{x_i R_{ji}}{x_j R_{\epsilon i \epsilon j}} - x_i R_{ji} + x_j R_{\epsilon i \epsilon j} \right). \quad (\text{B2})$$

For derivations, see [Eq. (4.10), 125] or [Eq. (23), 126]. For a system coupled to multiple heat baths (or other reservoirs) indexed by α , this may be generalized as

$$\sigma = \sum_{j \neq i, \alpha} \left(x_i R_{ji}^\alpha \ln \frac{x_i R_{ji}^\alpha}{x_j R_{\epsilon i \epsilon j}^\alpha} - x_i R_{ji}^\alpha + x_j R_{\epsilon i \epsilon j}^\alpha \right). \quad (\text{B3})$$

The EPR can be expressed as a relative entropy between flux vectors. We define a reaction ρ for each one-way transition ($i \rightarrow j, \alpha$) with flux $j_\rho = x_i R_{ji}^\alpha$ and reverse flux $\tilde{j}_\rho = x_j R_{\epsilon i \epsilon j}^\alpha$. Importantly, unlike in systems without odd variables, the reverse flux does not have to correspond to the forward flux of any reaction. The force across reaction ρ is

$$f_\rho = \ln \frac{j_\rho}{\tilde{j}_\rho} = \ln \frac{x_i R_{ji}^\alpha}{x_j R_{\epsilon i \epsilon j}^\alpha}, \quad (\text{B4})$$

as in Eq. (2). Finally, the EPR (B3) can be written as the relative entropy between forward and reverse fluxes, as in Eq. (16):

$$\sigma = \mathcal{D}(j || \tilde{j}).$$

Note that Eq. (B3) may not have the usual ‘‘flux-force’’ form $\sigma = \sum_\rho j_\rho f_\rho$, as it does in systems without odd variables. This reflects the irreversibility due to different forward and reverse escape rates.

2. Generalized free energy and excess/housekeeping decomposition

Many of our results continue to hold for systems with odd variables, including the definition of the generalized free energy and the excess/housekeeping decomposition. One important caveat is that we do not simplify our expressions by using Eq. (3), the relationship between forward and reverse fluxes

that holds without odd variables. Without using this equation, excess EPR (42) should be defined in the more general way as

$$\sigma_{\text{ex}} = \max_{\phi \in \mathbb{R}^d} \left[-\dot{\mathbf{x}}^\top \phi - \tilde{\mathbf{j}}^\top (e^{-\nabla \phi} - \mathbf{1}) \right], \quad (\text{B5})$$

which is the analogue of Eq. (35). The optimality condition that defines ϕ^* is given by

$$\dot{\mathbf{x}} = \nabla^\top (\tilde{\mathbf{j}} \circ e^{-\nabla \phi^*}), \quad (\text{B6})$$

rather than Eq. (43). The expression of excess EPR as information-theoretic optimal transport, as in Eq. (46), remains unchanged. In the special case where Eq. (3) holds, Eq. (B5) reduces to Eq. (42), and Eq. (B6) reduces to Eq. (43).

Some results must be qualified in the presence of odd variables. For instance, with odd variables, excess EPR does not necessarily vanish in stationarity, unless the steady state is symmetric under conjugation: $x_i^{\text{ss}} = x_{\epsilon i}^{\text{ss}}$. Similarly, we do not have the inequality between our excess EPR and HS excess EPR, Eq. (66), unless the steady-state distribution is symmetric under conjugation. Finally, our thermodynamic speed limits do not hold in general for systems with odd variables. These differences arise because, for systems with odd variables and asymmetric escape rates, the steady state may be nonequilibrium even when the thermodynamic forces are conservative. However, the steady state will be equilibrium if the forces are conservative and the steady state is symmetric under conjugation of odd variables. (See Ref. [69] for further discussion.)

We note that odd variables are problematic for the HS decomposition, for instance they can lead to negative values of HS housekeeping EPR [67–69]. To our knowledge, no universally-applicable housekeeping/excess decomposition has been previously proposed for systems with odd variables.

3. Example: particle on a ring

We provide an example to illustrate our excess/housekeeping decomposition on a system with odd variables. We also compare to the HS decomposition, where the housekeeping EPR can take unphysical negative values [67–69].

We use a standard model from the literature on the stochastic thermodynamics of systems with odd variables [67–69], illustrated in Figure 7 (left). There is a particle on a ring with k locations; the particle also has an odd ‘‘velocity’’ degree of freedom, indicating whether it is moving clockwise or counterclockwise. The system’s microstate is specified by $i = (r, v)$, where $r \in \{1, \dots, k\}$ is the position of the particle on the ring and $v \in \{-1, +1\}$ is the velocity. Conjugation involves flipping the sign of the velocity variables,

$$\epsilon(r, v) = (r, -v).$$

The rate matrix contains two types of transitions: movements around the ring $(r, v) \rightarrow (r+v, v)$ and velocity flips $(r, v) \rightarrow (r, -v)$.

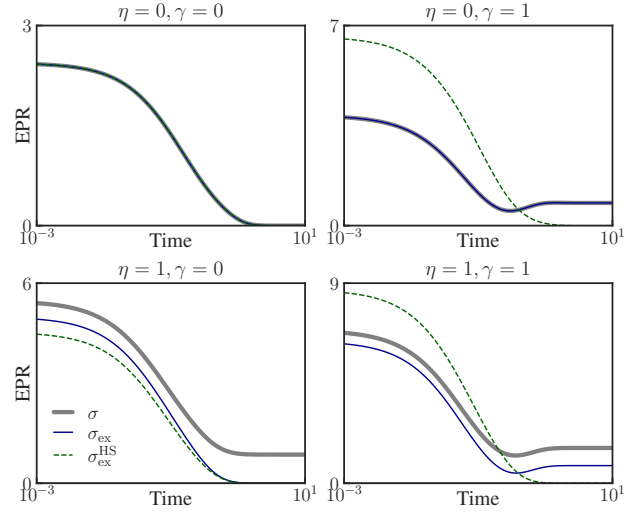
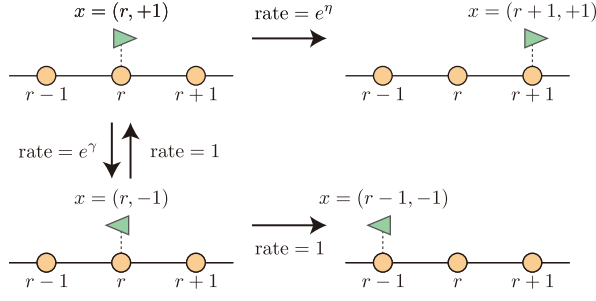


Figure 7. *Left*: a model of a discrete system with odd variables, consisting a particle on a ring with position $r \in \{1, \dots, k\}$ and odd velocity $v \in \{-1, +1\}$ [67–69]. *Right*: overall EPR σ , our excess EPR σ_{ex} , and HS excess EPR $\sigma_{\text{ex}}^{\text{HS}}$ for this model. $\eta \neq 0$ means forces are nonconservative, $\gamma \neq 0$ means steady-state distribution is not symmetric under conjugation of odd variables. HS decomposition can give unphysical values ($\sigma_{\text{ex}}^{\text{HS}} > \sigma, \sigma_{\text{hk}}^{\text{HS}} < 0$) when $\gamma \neq 0$.

The transition rates are parameterized as

$$R_{(r+v,v) \leftarrow (r,v)} = e^{\delta_{v,1}\eta}$$

$$R_{(r,-v) \leftarrow (r,v)} = e^{\delta_{v,1}\gamma}.$$

In words, the particle moves in the direction of its velocity with rate e^η when $v = +1$ and rate 1 when $v = -1$; the velocity flips with rate e^γ when $v = +1$ and rate 1 when $v = -1$. The steady state is given by

$$x_{r,v}^{\text{ss}} = \frac{\delta_{v,1} + \delta_{v,-1}e^\gamma}{k(e^\gamma + 1)}. \quad (\text{B7})$$

The parameter η controls driving around the ring, leading to nonconservative forces when $\eta \neq 0$. The parameter γ controls the breaking of symmetry of velocity flips, leading to a steady-state distribution that is asymmetric under conjugation of odd variables ($x_{r,v}^{\text{ss}} \neq x_{r,-v}^{\text{ss}}$) when $\gamma \neq 0$. The steady state is in equilibrium only when $\eta = 0$ and $\gamma = 0$. Using Eq. (B4), the forces across the two types of transitions are

$$f_{(r+v,v) \leftarrow (r,v)} = \ln \frac{x_{r,v} R_{(r+v,v) \leftarrow (r,v)}}{x_{r+v,v} R_{(r,-v) \leftarrow (r+v,-v)}}$$

$$= \ln \frac{x_{r,v}}{x_{r+v,v}} + \delta_{v,1}\eta - \delta_{-v,1}\eta$$

$$= \ln \frac{x_{r,v}}{x_{r+v,v}} + v\eta \quad (\text{B8})$$

$$f_{(r,-v) \leftarrow (r,v)} = \ln \frac{x_{r,v} R_{(r,-v) \leftarrow (r,v)}}{x_{r,-v} R_{(r,-v) \leftarrow (r,v)}} = \ln \frac{x_{r,v}}{x_{r,-v}} \quad (\text{B9})$$

In Figure 7 (right), we visualize the time-dependent values of EPR σ , our excess EPR σ_{ex} , and the HS excess EPR $\sigma_{\text{ex}}^{\text{HS}}$.

We consider a system with $k = 4$ positions and the non-steady-state initial distribution $x_{r,v} \propto 10\delta_{r,0}\delta_{v,1} + 1$. We consider four parameter values.

In the first condition (top left), $\eta = 0$ and $\gamma = 0$, so all transitions are symmetric. Here the forces are conservative, $f = -\nabla\phi$ for $\phi = \ln x$ and the steady-state distribution is symmetric under conjugation of odd variables. The steady state is in equilibrium and $\sigma = \sigma_{\text{ex}} = \sigma_{\text{ex}}^{\text{HS}}$ at all times.

In the second condition (top right), $\eta = 0$ and $\gamma = 1$, so velocity flips $(r, -1) \rightarrow (r, +1)$ occur more frequently than $(r, +1) \rightarrow (r, -1)$. The forces are conservative, $f = -\nabla\phi$ for $\phi = \ln x$, but the steady state is not symmetric under conjugation of odd variables. For this reason, the steady state is nonequilibrium ($\sigma > 0$ in steady state). Since the forces are conservative, our housekeeping EPR vanishes and $\sigma = \sigma_{\text{ex}}$ at all times. The HS decomposition gives different results, and it can produce unphysical negative values: $\sigma_{\text{ex}}^{\text{HS}} > \sigma, \sigma_{\text{hk}}^{\text{HS}} < 0$.

In the third condition (bottom left), $\eta = 1$ and $\gamma = 0$, so movements along the ring with positive velocity are faster than those with negative velocity. The steady state is symmetric under time-reversal but the forces $f_{(r+v,v) \leftarrow (r,v)}$ are not conservative, so the steady state is nonequilibrium. Our decomposition and HS decomposition both obey $0 \leq \sigma_{\text{ex}} \leq \sigma$ and $0 \leq \sigma_{\text{ex}}^{\text{HS}} \leq \sigma$. We verify that, in systems with time-reversal-symmetric steady states, $\sigma_{\text{ex}} \geq \sigma_{\text{ex}}^{\text{HS}}$ and $\sigma_{\text{ex}} = \sigma_{\text{ex}}^{\text{HS}} = 0$ in steady state.

In the fourth condition, $\eta = 1$ and $\gamma = 1$, so the forces are not conservative and the steady state is not symmetric under conjugation of odd variables. The HS decomposition again gives unphysical values $\sigma_{\text{ex}}^{\text{HS}} > \sigma, \sigma_{\text{hk}}^{\text{HS}} < 0$. Under our decomposition, neither σ_{ex} nor $\sigma_{\text{hk}}^{\text{HS}}$ vanish in steady state.

- [1] I. Procaccia and R. Levine, Potential work: A statistical-mechanical approach for systems in disequilibrium, *The Journal of Chemical Physics* **65**, 3357 (1976).
- [2] M. Esposito and C. Van den Broeck, Second law and Landauer principle far from equilibrium, *EPL (Europhysics Letters)* **95**, 40004 (2011).
- [3] F. Horn and R. Jackson, General mass action kinetics, *Archive for Rational Mechanics and Analysis* **47**, 81 (1972).
- [4] F. Schlögl, Fluctuations in thermodynamic non equilibrium states, *Zeitschrift für Physik A Hadrons and nuclei* **244**, 199 (1971).
- [5] H. Qian, Relative entropy: Free energy associated with equilibrium fluctuations and nonequilibrium deviations, *Physical Review E* **63**, 042103 (2001).
- [6] N. Shiraishi, K. Funo, and K. Saito, Speed limit for classical stochastic processes, *Physical review letters* **121**, 070601 (2018).
- [7] S. Ito, Stochastic thermodynamic interpretation of information geometry, *Physical Review Letters* **121**, 030605 (2018).
- [8] V. T. Vo, T. Van Vu, and Y. Hasegawa, Unified approach to classical speed limit and thermodynamic uncertainty relation, *Phys. Rev. E* **102**, 062132 (2020).
- [9] K. Yoshimura and S. Ito, Thermodynamic uncertainty relation and thermodynamic speed limit in deterministic chemical reaction networks, *Physical Review Letters* **127**, 160601 (2021).
- [10] N. Shiraishi, Wasserstein distance in speed limit inequalities for markov jump processes, *Journal of Statistical Mechanics: Theory and Experiment* **2024**, 074003 (2024).
- [11] P. Salamon, J. D. Nulton, and R. S. Berry, Length in statistical thermodynamics, *The Journal of chemical physics* **82**, 2433 (1985).
- [12] P. Salamon and R. S. Berry, Thermodynamic length and dissipated availability, *Physical Review Letters* **51**, 1127 (1983).
- [13] G. E. Crooks, Measuring Thermodynamic Length, *Physical Review Letters* **99** (2007).
- [14] D. A. Sivak and G. E. Crooks, Thermodynamic Metrics and Optimal Paths, *Physical Review Letters* **108** (2012).
- [15] E. Aurell, C. Mejía-Monasterio, and P. Muratore-Ginanneschi, Optimal protocols and optimal transport in stochastic thermodynamics, *Physical Review Letters* **106**, 250601 (2011).
- [16] E. Aurell, K. Gawędzki, C. Mejía-Monasterio, R. Mohayae, and P. Muratore-Ginanneschi, Refined second law of thermodynamics for fast random processes, *Journal of Statistical Physics* **147**, 487 (2012).
- [17] A. Dechant and Y. Sakurai, Thermodynamic interpretation of Wasserstein distance, *arXiv preprint arXiv:1912.08405* (2019).
- [18] M. Nakazato and S. Ito, Geometrical aspects of entropy production in stochastic thermodynamics based on Wasserstein distance, *Physical Review Research* **3**, 043093 (2021).
- [19] T. Van Vu and K. Saito, Thermodynamic unification of optimal transport: Thermodynamic uncertainty relation, minimum dissipation, and thermodynamic speed limits, *Physical Review X* **13**, 011013 (2023).
- [20] K. Yoshimura, A. Kolchinsky, A. Dechant, and S. Ito, Housekeeping and excess entropy production for general nonlinear dynamics, *Physical Review Research* **5**, 013017 (2023).
- [21] R. Nagayama, K. Yoshimura, A. Kolchinsky, and S. Ito, Geometric thermodynamics of reaction-diffusion systems: Thermodynamic trade-off relations and optimal transport for pattern formation, *arXiv preprint arXiv:2311.16569* (2023).
- [22] S. Ito, Geometric thermodynamics for the fokker–planck equation: stochastic thermodynamic links between information geometry and optimal transport, *Information Geometry* **7**, 441 (2024).
- [23] É. Fodor, R. L. Jack, and M. E. Cates, Irreversibility and biased ensembles in active matter: Insights from stochastic thermodynamics, *Annual Review of Condensed Matter Physics* **13**, 215 (2022).
- [24] R. Graham and T. Tél, Nonequilibrium potential for coexisting attractors, *Physical Review A* **33**, 1322 (1986).
- [25] B. Derrida, J. L. Lebowitz, and E. R. Speer, Free Energy Functional for Nonequilibrium Systems: An Exactly Solvable Case, *Physical Review Letters* **87**, 150601 (2001).
- [26] H. Ge and H. Qian, Dissipation, generalized free energy, and a self-consistent nonequilibrium thermodynamics of chemically driven open subsystems, *Physical Review E* **87** (2013).
- [27] Q. Li and W. E, The Free Action of Nonequilibrium Dynamics, *Journal of Statistical Physics* **161**, 300 (2015).
- [28] P. Glansdorff and I. Prigogine, Non-equilibrium stability theory, *Physica* **46**, 344 (1970), publisher: Elsevier.
- [29] J. Schnakenberg, Network theory of microscopic and macroscopic behavior of master equation systems, *Reviews of Modern physics* **48**, 571 (1976).
- [30] Y. Oono and M. Paniconi, Steady state thermodynamics, *Progress of Theoretical Physics Supplement* **130**, 29 (1998).
- [31] T. Hatano and S.-i. Sasa, Steady-state thermodynamics of Langevin systems, *Physical Review Letters* **86**, 3463 (2001).
- [32] M. Esposito, U. Harbola, and S. Mukamel, Entropy fluctuation theorems in driven open systems: Application to electron counting statistics, *Physical Review E* **76**, 031132 (2007).
- [33] T. S. Komatsu, N. Nakagawa, S.-i. Sasa, and H. Tasaki, Steady-state thermodynamics for heat conduction: microscopic derivation, *Physical Review Letters* **100**, 230602 (2008).
- [34] T. Sagawa and H. Hayakawa, Geometrical expression of excess entropy production, *Physical Review E* **84**, 051110 (2011).
- [35] C. Maes and K. Netočný, A nonequilibrium extension of the Clausius heat theorem, *Journal of Statistical Physics* **154**, 188 (2014).
- [36] E. Smith, Intrinsic and extrinsic thermodynamics for stochastic population processes with multi-level large-deviation structure, *Entropy* **22**, 1137 (2020).
- [37] J. S. Lee, S. Lee, H. Kwon, and H. Park, Speed limit for a highly irreversible process and tight finite-time Landauer’s bound, *Phys. Rev. Lett.* **129**, 120603 (2022).
- [38] L. Bertini, D. Gabrielli, G. Jona-Lasinio, and C. Landim, Clausius inequality and optimality of quasistatic transformations for nonequilibrium stationary states, *Physical Review Letters* **110**, 020601 (2013).
- [39] D. Mandal and C. Jarzynski, Analysis of slow transitions between nonequilibrium steady states, *Journal of Statistical Mechanics: Theory and Experiment* **2016**, 063204 (2016).
- [40] M. Esposito and C. Van den Broeck, Three detailed fluctuation theorems, *Physical Review Letters* **104**, 090601 (2010).
- [41] R. Rao and M. Esposito, Nonequilibrium thermodynamics of chemical reaction networks: wisdom from stochastic thermodynamics, *Physical Review X* **6**, 041064 (2016).
- [42] H. Ge and H. Qian, Nonequilibrium thermodynamic formalism of nonlinear chemical reaction systems with Waage–Guldberg’s law of mass action, *Chemical Physics* **472**, 241 (2016).
- [43] T. Van Vu and K. Saito, Topological speed limit, *Physical*

- review letters **130**, 010402 (2023).
- [44] See the supplemental material.
- [45] T. J. Kobayashi, D. Loutchko, A. Kamimura, and Y. Sughiyama, Hessian geometry of nonequilibrium chemical reaction networks and entropy production decompositions, *Physical Review Research* **4**, 033208 (2022).
- [46] T. J. Kobayashi, D. Loutchko, A. Kamimura, S. A. Horiguchi, and Y. Sughiyama, Information geometry of dynamics on graphs and hypergraphs, *Information Geometry* **7**, 97 (2024).
- [47] M. Feinberg, *Foundations of Chemical Reaction Network Theory*, Applied Mathematical Sciences, Vol. 202 (Springer International Publishing, Cham, 2019).
- [48] D. Kondepudi and I. Prigogine, *Modern thermodynamics: from heat engines to dissipative structures* (John Wiley & Sons, 2014).
- [49] D. A. Beard and H. Qian, Relationship between thermodynamic driving force and one-way fluxes in reversible processes, *PLoS one* **2**, e144 (2007).
- [50] C. Maes, Local detailed balance, *SciPost Physics Lecture Notes* , 032 (2021).
- [51] I. Prigogine and R. Lefever, Symmetry breaking instabilities in dissipative systems. II, *The Journal of Chemical Physics* **48**, 1695 (1968).
- [52] R. Rao and M. Esposito, Conservation laws shape dissipation, *New Journal of Physics* **20**, 023007 (2018).
- [53] H. Spohn, *Large Scale Dynamics of Interacting Particles* (Springer Berlin Heidelberg, Berlin, Heidelberg, 1991).
- [54] A. Mielke, R. I. A. Patterson, M. A. Peletier, and D. R. Michiel Renger, Non-equilibrium Thermodynamical Principles for Chemical Reactions with Mass-Action Kinetics, *SIAM Journal on Applied Mathematics* **77**, 1562 (2017).
- [55] H. Ge and H. Qian, Mesoscopic kinetic basis of macroscopic chemical thermodynamics: A mathematical theory, *Physical Review E* **94**, 052150 (2016).
- [56] H. Touchette, The large deviation approach to statistical mechanics, *Physics Reports* **478**, 1 (2009).
- [57] D. F. Anderson, G. Craciun, M. Gopalkrishnan, and C. Wiuf, Lyapunov Functions, Stationary Distributions, and Non-equilibrium Potential for Reaction Networks, *Bulletin of Mathematical Biology* **77**, 1744 (2015).
- [58] H. Ge and H. Qian, Mathematical Formalism of Nonequilibrium Thermodynamics for Nonlinear Chemical Reaction Systems with General Rate Law, *Journal of Statistical Physics* **166**, 190 (2017).
- [59] J. Wang, L. Xu, and E. Wang, Potential landscape and flux framework of nonequilibrium networks: robustness, dissipation, and coherence of biochemical oscillations, *Proceedings of the National Academy of Sciences* **105**, 12271 (2008).
- [60] F. Schlögl, On stability of steady states, *Zeitschrift für Physik A Hadrons and nuclei* **243**, 303 (1971).
- [61] T. Speck and U. Seifert, Integral fluctuation theorem for the housekeeping heat, *Journal of Physics A: Mathematical and General* **38**, L581 (2005).
- [62] M. Esposito and C. Van den Broeck, Three faces of the second law. I. Master equation formulation, *Physical Review E* **82**, 011143 (2010).
- [63] Hu Gang, Stationary solution of master equations in the large-system-size limit, *Physical Review A* **36**, 5782 (1987).
- [64] L. Bertini, A. De Sole, D. Gabrielli, G. Jona-Lasinio, and C. Landim, Macroscopic fluctuation theory, *Reviews of Modern Physics* **87**, 593 (2015).
- [65] G. Falasco and M. Esposito, Macroscopic Stochastic Thermodynamics (2023), arXiv:2307.12406 [cond-mat, physics:math-ph].
- [66] H. Ge and H. Qian, Thermodynamic Limit of a Nonequilibrium Steady State: Maxwell-Type Construction for a Bistable Biochemical System, *Physical Review Letters* **103** (2009).
- [67] I. J. Ford and R. E. Spinney, Entropy production from stochastic dynamics in discrete full phase space, *Physical Review E* **86**, 021127 (2012).
- [68] R. E. Spinney and I. J. Ford, Nonequilibrium thermodynamics of stochastic systems with odd and even variables, *Physical Review Letters* **108**, 170603 (2012).
- [69] H. K. Lee, C. Kwon, and H. Park, Fluctuation theorems and entropy production with odd-parity variables, *Physical Review Letters* **110**, 050602 (2013).
- [70] R. García-García, Nonadiabatic entropy production for non-Markov dynamics, *Physical Review E* **86**, 031117 (2012).
- [71] A. Dechant, S.-i. Sasa, and S. Ito, Geometric decomposition of entropy production in out-of-equilibrium systems, *Physical Review Research* **4**, L012034 (2022).
- [72] A. Dechant, S.-i. Sasa, and S. Ito, Geometric decomposition of entropy production into excess, housekeeping, and coupling parts, *Phys. Rev. E* **106**, 024125 (2022).
- [73] J.-C. Delvenne and G. Falasco, Thermokinetic relations, *Physical Review E* **109**, 014109 (2024).
- [74] D.-K. Kim, Y. Bae, S. Lee, and H. Jeong, Learning entropy production via neural networks, *Physical Review Letters* **125**, 140604 (2020).
- [75] S. Otsubo, S. K. Manikandan, T. Sagawa, and S. Krishnamurthy, Estimating time-dependent entropy production from non-equilibrium trajectories, *Communications Physics* **5**, 1 (2022).
- [76] S. Boyd and L. Vandenberghe, *Convex optimization* (Cambridge university press, 2004).
- [77] I. Gentil, C. Léonard, and L. Ripani, About the analogy between optimal transport and minimal entropy, *Annales de la Faculté des sciences de Toulouse : Mathématiques* **26**, 569 (2017).
- [78] C. Villani, *Optimal transport: old and new*, Vol. 338 (Springer, 2009).
- [79] N. Shiraishi and K. Saito, Information-theoretical bound of the irreversibility in thermal relaxation processes, *Physical Review Letters* **123**, 110603 (2019).
- [80] S.-i. Amari, *Information geometry and its applications*, Vol. 194 (Springer, 2016).
- [81] I. Csiszár, I-Divergence geometry of probability distributions and minimization problems, *The Annals of Probability* , 146 (1975).
- [82] S. Ito, M. Oizumi, and S.-i. Amari, Unified framework for the entropy production and the stochastic interaction based on information geometry, *Physical Review Research* **2**, 033048 (2020).
- [83] The equation $\dot{x} = -H\phi^*$ only determines ϕ^* up to the nullspace of ∇ . The choice $\phi^* = -H^+ \dot{x}$ satisfies the conservation laws (38) in the linear-response regime.
- [84] M. Doi, Onsager principle in polymer dynamics, *Progress in Polymer Science* **112**, 101339 (2021).
- [85] L. Onsager, Reciprocal relations in irreversible processes. i., *Physical review* **37**, 405 (1931).
- [86] I. Gyarmati *et al.*, *Non-equilibrium thermodynamics*, Vol. 184 (Springer, 1970).
- [87] L. M. Martyushev and V. D. Seleznev, Maximum entropy production principle in physics, chemistry and biology, *Physics reports* **426**, 1 (2006).
- [88] J. Verhás, Gyarmati's variational principle of dissipative processes, *Entropy* **16**, 2362 (2014).
- [89] G. E. Crooks, On the drazin inverse of the rate matrix (2018).

- [90] J. R. Sawchuk and D. A. Sivak, Dynamical and spectral decompositions of the generalized friction tensor for optimal control, arXiv preprint arXiv:2409.18065 (2024).
- [91] E. Helfand, Transport coefficients from dissipation in a canonical ensemble, *Physical Review* **119**, 1 (1960).
- [92] D. Frenkel, B. Smit, and M. A. Ratner, *Understanding Molecular Simulation: From Algorithms to Applications*, Vol. 50 (1997).
- [93] M. J. Saxton and K. Jacobson, Single-particle tracking: applications to membrane dynamics, Annual review of biophysics and biomolecular structure **26**, 373 (1997).
- [94] For physical relevance, we should assume that even short time intervals are longer than the hydrodynamic timescale, so that assumptions of Markovian and overdamped dynamics are justified.
- [95] D. T. Gillespie, Stochastic simulation of chemical kinetics, *Annu. Rev. Phys. Chem.* **58**, 35 (2007).
- [96] A. Vulpiani, F. Cecconi, M. Cencini, A. Puglisi, and D. Vergni, eds., *Large Deviations in Physics*, Lecture Notes in Physics, Vol. 885 (Springer Berlin Heidelberg, Berlin, Heidelberg, 2014).
- [97] Eq. (85) can be derived from Ref. [Thm. 3.4, 54], by considering the short-time limit. Note that σ_{ex} (42) is equal to $L(c, s)$ from [Eq. (3.7), 54], evaluated at $c = \mathbf{x}$ and $s = -\dot{\mathbf{x}}$.
- [98] L. Peliti, Path integral approach to birth-death processes on a lattice, *Journal de Physique* **46**, 1469 (1985).
- [99] M. I. Dykman, E. Mori, J. Ross, and P. Hunt, Large fluctuations and optimal paths in chemical kinetics, *The Journal of chemical physics* **100**, 5735 (1994).
- [100] M. Assaf and B. Meerson, Wkb theory of large deviations in stochastic populations, *Journal of Physics A: Mathematical and Theoretical* **50**, 263001 (2017).
- [101] A. Mielke, D. R. M. Renger, and M. A. Peletier, On the relation between gradient flows and the large-deviation principle, with applications to Markov chains and diffusion, *Potential Analysis* **41**, 1293 (2014).
- [102] A. Mielke, D. M. Renger, and M. A. Peletier, A generalization of onsager’s reciprocity relations to gradient flows with nonlinear mobility, *Journal of Non-Equilibrium Thermodynamics* **41**, 141 (2016).
- [103] D. M. Renger, Flux large deviations of independent and reacting particle systems, with implications for macroscopic fluctuation theory, *Journal of Statistical Physics* **172**, 1291 (2018).
- [104] R. I. Patterson, D. M. Renger, and U. Sharma, Variational structures beyond gradient flows: a macroscopic fluctuation-theory perspective (2024).
- [105] R. Zakine and E. Vanden-Eijnden, Minimum-action method for nonequilibrium phase transitions, *Physical Review X* **13**, 041044 (2023).
- [106] S. K. Manikandan, D. Gupta, and S. Krishnamurthy, Inferring entropy production from short experiments, *Physical review letters* **124**, 120603 (2020).
- [107] A. Dechant and S.-i. Sasa, Fluctuation–response inequality out of equilibrium, *Proceedings of the National Academy of Sciences* **117**, 6430 (2020).
- [108] A. Dechant, Minimum entropy production, detailed balance and Wasserstein distance for continuous-time Markov processes, *Journal of Physics A: Mathematical and Theoretical* (2022).
- [109] A slightly-weaker version of the TSL (96) was recently proposed for HS excess EPR in Ref. [73]. Unfortunately, that result is not valid in general, as may be shown using the unicyclic system from Section VIII A as a counter-example.
- [110] T. Van Vu and Y. Hasegawa, Geometrical bounds of the irreversibility in Markovian systems, *Physical Review Letters* **126**, 010601 (2021).
- [111] R. Hamazaki, Speed limits for macroscopic transitions, *PRX Quantum* **3**, 020319 (2022).
- [112] A. Bérut, A. Arakelyan, A. Petrosyan, S. Ciliberto, R. Dillenschneider, and E. Lutz, Experimental verification of Landauer’s principle linking information and thermodynamics, *Nature* **483**, 187 (2012).
- [113] Y.-Z. Zhen, D. Egloff, K. Modi, and O. Dahlsten, Universal bound on energy cost of bit reset in finite time, *Physical Review Letters* **127**, 190602 (2021).
- [114] Y.-Z. Zhen, D. Egloff, K. Modi, and O. Dahlsten, Inverse linear versus exponential scaling of work penalty in finite-time bit reset, *Physical Review E* **105**, 044147 (2022).
- [115] J. Gu, Speed limit, dissipation bound, and dissipation-time trade-off in thermal relaxation processes, *Physical Review E* **108**, L052103 (2023).
- [116] L. Onsager, Reciprocal relations in irreversible processes. ii., *Physical review* **38**, 2265 (1931).
- [117] L. Onsager and S. Machlup, Fluctuations and irreversible processes, *Physical Review* **91**, 1505 (1953).
- [118] A. Baradat and C. Léonard, Minimizing relative entropy of path measures under marginal constraints, arXiv preprint arXiv:2001.10920 (2020).
- [119] O. Movilla Miangolarra, A. Eldesoukey, and T. T. Georgiou, Inferring potential landscapes: A schrödinger bridge approach to maximum caliber, *Physical Review Research* **6**, 033070 (2024).
- [120] P. D. Dixit, J. Wagoner, C. Weistuch, S. Pressé, K. Ghosh, and K. A. Dill, Perspective: Maximum caliber is a general variational principle for dynamical systems, *The Journal of chemical physics* **148**, 010901 (2018).
- [121] K. Yoshimura and S. Ito, Two applications of stochastic thermodynamics to hydrodynamics, *Physical Review Research* **6**, L022057 (2024).
- [122] K. Yoshimura, Y. Maekawa, R. Nagayama, and S. Ito, Force-current structure in markovian open quantum systems and its applications: geometric housekeeping-excess decomposition and thermodynamic trade-off relations, arXiv preprint arXiv:2410.22628 (2024).
- [123] R. E. Spinney and I. J. Ford, Entropy production in full phase space for continuous stochastic dynamics, *Physical Review E* **85**, 051113 (2012).
- [124] C. Gardiner, *Handbook of Stochastic Methods: for Physics, Chemistry and the Natural Sciences*, 3rd ed. (Springer, Berlin ; New York, 2004).
- [125] R. E. Spinney, *The use of stochastic methods to explore the thermal equilibrium distribution and define entropy production out of equilibrium*, Ph.D. thesis, UCL (University College London) (2012).
- [126] F. Liu and H. Lei, Splitting of the rate matrix as a definition of time reversal in master equation systems, *Journal of Physics A: Mathematical and Theoretical* **45**, 125004 (2012).
- [127] D. G. Luenberger, *Optimization by Vector Space Methods*, 1969th ed. (Wiley-Interscience, New York, 1997).
- [128] K. Yoshimura and S. Ito, Two applications of stochastic thermodynamics to hydrodynamics, *Physical Review Research* **6**, L022057 (2024).

Supplemental Material

SM1: Generalized free energy with conservation laws (38)

Here we show how to numerically find the generalized potential ϕ^* that optimizes our variational principle (42) while obeying the conservation laws (38).

Recall that Eq. (42) is a convex optimization problem (maximization of a concave objective). It can be solved using standard algorithms to find the potential ϕ^* , which is uniquely determined up to the nullspace of ∇ . To find the potential within this nullspace that satisfies the conservation laws (38), we introduce another convex optimization problem:

$$\min_{\mathbf{y} \in \mathbb{R}_+^d} D(\mathbf{y} \parallel \mathbf{x} \circ e^{-\phi^*}) \quad \text{where} \quad P_{\emptyset} \mathbf{y} = P_{\emptyset} \mathbf{x}. \quad (\text{S1})$$

Here ϕ^* is the optimal potential found in the first step and D is the generalized relative entropy (14). Also, P_{\emptyset} refers to the projector onto the nullspace of ∇ , defined as

$$P_{\emptyset} = I - \nabla^+ \nabla, \quad (\text{S2})$$

where ∇^+ is the pseudo-inverse. The optimization over states $\mathbf{y} \in \mathbb{R}_+^d$ looks for the ‘‘canonical’’ distribution that satisfy the conservation laws (38).

The generalized free energy potential that satisfies the conservation laws (38) is given by

$$\phi^{**} = -\ln \frac{\mathbf{y}^*}{\mathbf{x}}, \quad (\text{S3})$$

where \mathbf{y}^* is the optimizer of Eq. (S1). To see why, we write the Lagrangian of the optimization (S1) as

$$\sum_i y_i \left[\ln \frac{y_i}{x_i e^{-\phi_i^*}} - y_i + x_i e^{-\phi_i^*} \right] + \boldsymbol{\lambda} (P_{\emptyset} \mathbf{y} - P_{\emptyset} \mathbf{x}).$$

Taking derivatives with respect to each y_i , setting to 0, and rearranging gives

$$-\ln \frac{\mathbf{y}^*}{\mathbf{x}} = \phi^* + P_{\emptyset} \boldsymbol{\lambda}^*, \quad (\text{S4})$$

where the value of the optimal Lagrange multipliers $\boldsymbol{\lambda}^*$ is determined by the constraint $P_{\emptyset} \mathbf{y} = P_{\emptyset} \mathbf{x}$. It is clear that $\phi^{**} = -\ln(\mathbf{y}^*/\mathbf{x})$ differs from ϕ^* by a vector in the image of P_{\emptyset} , i.e., a null vector of ∇ , therefore ϕ^{**} achieves the same objective in the variational principle (42). Also, by construction, $\mathbf{y}^* = \mathbf{x} \circ e^{-\phi^{**}}$ satisfies $P_{\emptyset} \mathbf{y}^* = P_{\emptyset} \mathbf{x}$, which is the conservation law (38).

SM2: Statistical fluctuations and the cumulant generating function

As we discuss in Section VI of the main text, our generalized free energy and excess/housekeeping decomposition is related to the cumulant generating function (CGF) of dynamical fluctuations. Here we derive the form of the CGF for (1) stochastic MJPs and (2) stochastic chemical systems with Poisson rates.

Recall from the main text that the random variable N_{ρ} indicates the number of reactions ρ that occur during a short time interval $t \in [t, t + dt]$. In addition, for any reaction observables $\boldsymbol{\theta} \in \mathbb{R}^m$ (e.g., θ_{ρ} might indicate the heat generated by reaction ρ), we use the random variable $Z_{\boldsymbol{\theta}} = \sum_{\rho} N_{\rho} \theta_{\rho}$ to indicate the total amount of $\boldsymbol{\theta}$ incurred over the time interval. The fluctuations of $Z_{\boldsymbol{\theta}}$ are encoded in the CGF,

$$\ln \mathbb{E} e^{\lambda Z_{\boldsymbol{\theta}}} = \ln \sum_{\mathbf{N}} \Pr(\mathbf{N}) e^{\lambda \sum_{\rho} N_{\rho} \theta_{\rho}}, \quad (\text{S5})$$

Here we will show that to first order in dt , the cumulant generating function can be expressed as

$$\ln \mathbb{E} e^{\lambda Z_{\boldsymbol{\theta}}} \approx dt \mathbf{j}^{\top} (e^{\lambda \boldsymbol{\theta}} - 1). \quad (\text{S6})$$

For the special case of reaction observables that have the form $\boldsymbol{\theta} = \nabla \phi$ for some state potential ϕ , the random variable $Z_{\nabla \phi}$ quantifies the fluctuating change of ϕ over the time interval. In this case, the random variable $Z_{\nabla \phi}$ is equivalent to the random variable $\Delta \phi$ defined in Eq. (75) in the main text, and the CGF expression (S6) reduces to Eq. (76) in the main text.

To derive the CGF expression (S6), we first consider a stochastic system described by an MJP. Suppose that the time interval $[t, t + dt]$ is much shorter than the timescale of any escape rate. Consider some reaction ρ associated with the transition $i \rightarrow j$ and reservoir α , with transition rate R_{ji}^{α} . The probability that the transition happens during the time integral is

$$(1 - e^{dt R_{ii}}) x_i \frac{R_{ji}^{\alpha}}{-R_{ii}} \sim x_i R_{ji}^{\alpha} dt = j_{\rho} dt,$$

where \sim indicates equality up to first order in dt . The probability that two or more jumps occur is of order $(dt)^2$, so it can be ignored. Thus, we can approximate the probability of count vector $\mathbf{N} \in \mathbb{N}^m$ as $\Pr(\mathbf{N}) \sim 1 + dt \sum_{\rho} (\delta_{1, N_{\rho}} - \delta_{0, N}) j_{\rho}$. Plugging into (S5) and rearranging allows us to approximate the CGF with Eq. (S6),

$$\ln \mathbb{E} e^{\lambda Z_{\boldsymbol{\theta}}} \sim \ln \left[1 + dt \sum_{\rho} j_{\rho} (e^{\lambda \theta_{\rho}} - 1) \right] \quad (\text{S7})$$

$$\sim dt \sum_{\rho} j_{\rho} (e^{\lambda \theta_{\rho}} - 1) \quad (\text{S8})$$

where we expanded in the logarithm to first order in dt .

Next, we consider a stochastic chemical system. Under standard assumptions [95], fluctuating reaction counts can be related to deterministic fluxes via ‘‘propensity functions’’. Specifically, at a very short timescales, the probability of a single reaction ρ in a unit volume is $\sim j_\rho dt$, while the probability of two or more reactions is of order $(dt)^2$. In this case, the analysis described above for MJPs also holds for CRNs.

In many systems, however, it is impractical to access timescales so small that only single reaction has an appreciable chance of happening in a unit volume. In this case, we may treat reaction counts N_ρ as independent Poisson random variables, each with expectation $j_\rho dt$. The Poisson approximation is frequently used in the literature, and it can be motivated by standard assumptions (e.g., well-mixed reactor with sufficiently large concentrations) [95]. The CGF can be written as

$$\ln \mathbb{E} e^{\lambda Z_\theta} = dt \sum_\rho j_\rho (e^{\lambda \theta_\rho} - 1) \quad (\text{S9})$$

Here we used that the CGF of the scaled Poisson $N_\rho \theta_\rho$ is $dt j_\rho (e^{\lambda \theta_\rho} - 1)$, and that the CGFs of a sum of independent random variables is the sum of their CGFs. Interestingly, no short-time approximations are used explicitly in the derivation of (S9). However, implicitly, the time interval should be sufficiently short so that fluxes do not change much over dt , but long enough so that reactions can occur multiple times.

SM3: Relation to variational principle from Ref. [79]

In previous work, Shiraishi and Saito [79] proposed a variational principle for EPR in passive MJPs. They showed that

$$\sigma = \max_{\mathbf{y}} \left[-\frac{d}{dt} D(\mathbf{x}(t) \| \mathbf{y}(-t)) \right]. \quad (\text{S10})$$

where D is the relative entropy between probability distributions and the maximization is over all probability distributions \mathbf{y} . The notation $\mathbf{y}(-t)$ indicates that this distribution evolves backwards in time under the reverse rates,

$$-\frac{d}{dt} y_i(-t) = \sum_{j(\neq i), \alpha} (y_j(-t) R_{ij}^\alpha - y_i(-t) R_{ji}^\alpha). \quad (\text{S11})$$

Here we show that this variational principle is a special case of the variational principle for excess EPR (42), in this way recovering Eq. (103) in the main text. We first rewrite the optimization (103) as

$$\max_{\mathbf{y}} \left[\sum_i \dot{x}_i \ln \frac{y_i}{x_i} + \sum_i x_i \frac{d}{dt} \ln y_i(-t) \right]. \quad (\text{S12})$$

Next, we define a reaction ρ for each transition ($j \rightarrow i, \alpha$), with forward and reverse fluxes $j_\rho = x_j R_{ij}^\alpha$ and $\bar{j}_\rho = x_i R_{ji}^\alpha$. We then write the variational principle (42) as

$$\sigma_{\text{ex}} = \max_{\phi \in \mathbb{R}^d} \left[-\sum_i \dot{x}_i \phi_i - \sum_{i \neq j, \alpha} x_j R_{ij}^\alpha (e^{\phi_i - \phi_j} - 1) \right].$$

We change the optimization variable from potentials to probability distributions \mathbf{y} via $\ln y_i = \ln x_i - \phi_i + \text{const}$. Using this replacement, we can write

$$\sigma_{\text{ex}} = \max_{\mathbf{y}} \left[\sum_i \dot{x}_i \ln \frac{y_i}{x_i} - \sum_{i \neq j, \alpha} x_j R_{ij}^\alpha \left(\frac{x_i y_j}{y_i x_j} - 1 \right) \right]. \quad (\text{S13})$$

We rewrite the second sum as

$$\sum_{j \neq i, \alpha} \left(\frac{x_i}{y_i} y_j R_{ij}^\alpha - x_j R_{ij}^\alpha \right) \quad (\text{S14})$$

$$= \sum_{j \neq i, \alpha} \left(\frac{x_i}{y_i} y_j R_{ij}^\alpha - x_i R_{ji}^\alpha \right) \quad (\text{S15})$$

$$= \sum_i \frac{x_i}{y_i} \sum_{j(\neq i), \alpha} (y_j R_{ij}^\alpha - y_i R_{ji}^\alpha) \\ = -\sum_i \frac{x_i}{y_i} \frac{d}{dt} y_i(-t) = -x_i \frac{d}{dt} \ln y_i(-t), \quad (\text{S16})$$

where in the last line we used the definition (S11). Combining shows the equivalence to (S12).

SM4: Derivation of Eq. (90)

We first derive the TSL in Eq. (90) in the main text. From the variational expression of excess EPR (42), we have

$$\sigma_{\text{ex}} = \max_{\lambda \in \mathbb{R}, \phi \in \mathbb{R}^d} \left[-\lambda d_t \langle \phi \rangle - \sum_\rho j_\rho (e^{\lambda [\nabla \phi]_\rho} - 1) \right] \quad (\text{S17})$$

where we used the definition $d_t \langle \phi \rangle = \dot{\mathbf{x}}^\top \phi = \mathbf{j}^\top \nabla \phi$. For any state observable $\phi \in \mathbb{R}^d$, this implies

$$\sigma_{\text{ex}} \geq \max_{\lambda \in \mathbb{R}} \left[-\lambda d_t \langle \phi \rangle - \sum_\rho j_\rho (e^{\lambda [\nabla \phi]_\rho} - 1) \right]. \quad (\text{S18})$$

Note that $[\nabla \phi]_\rho \in [-1, 1]$ by assumption (89). Note also that

$$e^{\lambda x} - 1 \leq x e^\lambda - |x| \quad \text{for } x \in [0, 1] \\ e^{\lambda x} - 1 \leq -x e^{-\lambda} - |x| \quad \text{for } x \in [-1, 0]$$

Plugging these inequalities into Eq. (S18) for $x = [\nabla \phi]_\rho$ leads to the bound

$$\sigma_{\text{ex}} \geq \max_\lambda \left[-\lambda d_t \langle \phi \rangle + a(\phi) - a_+(\phi) e^\lambda - a_-(\phi) e^{-\lambda} \right] \quad (\text{S19})$$

where we defined the positive $a_+(\phi)$ and negative $a_-(\phi)$ activity of the observable as

$$a_+(\phi) := \sum_{\rho: [\nabla \phi]_\rho > 0} j_\rho [\nabla \phi]_\rho = \frac{1}{2} (a(\phi) + d_t \langle \phi \rangle)$$

$$a_-(\phi) := \sum_{\rho: [\nabla \phi]_\rho < 0} j_\rho [-\nabla \phi]_\rho = \frac{1}{2} (a(\phi) - d_t \langle \phi \rangle).$$

The optimization Eq. (S19) can be solved by taking derivatives, which gives the optimal λ as

$$\lambda^* = \ln \frac{a_-(\phi)}{a_+(\phi)} = \ln \frac{a(\phi) - d_t \langle \phi \rangle}{a(\phi) + d_t \langle \phi \rangle} = 2 \tanh^{-1} \frac{d_t \langle \phi \rangle}{a(\phi)}$$

where we used $a(\phi) = a_+(\phi) + a_-(\phi)$ and $d_t \langle \phi \rangle = a_+(\phi) - a_-(\phi)$. Plugging into Eq. (S19) gives Eq. (90).

SM5: Duality for 1-Wasserstein distance

The 1-Wasserstein distance between states $\mathbf{x}(t)$ and $\mathbf{x}(t')$ is defined as

$$W(t, t') = \min_{\mathbf{m} \in \mathbb{R}_+^m} \|\mathbf{m}\|_1 \quad \text{where} \quad \nabla^\top \mathbf{m} = \mathbf{x}(t') - \mathbf{x}(t). \quad (\text{S20})$$

as in Eq. (93) in the main text. Observe that the problem is always feasible, since the actual integrated fluxes $\mathbf{J} = \int_t^{t'} \mathbf{j}(s) ds$ satisfy $\mathbf{J} \in \mathbb{R}_+^m$ and the evolution constraint:

$$\nabla^\top \mathbf{J} = \int_t^{t'} \nabla^\top \mathbf{j}(s) ds = \int_t^{t'} \dot{\mathbf{x}}(s) ds = \mathbf{x}(t') - \mathbf{x}(t).$$

Here we derive the dual expression of W as an optimization over state observables:

$$W(t, t') = \max_{\phi \in \mathbb{R}^d} (\mathbf{x}(t') - \mathbf{x}(t))^\top \phi \quad \text{where} \quad \|\nabla \phi\|_\infty \leq 1. \quad (\text{S21})$$

Using the dual expression, we may verify that we recover the Wasserstein speed (95) in the limit of short times:

$$\lim_{dt \rightarrow 0} \frac{1}{dt} W(t, t + dt) \approx dt \max_{\phi: \|\nabla \phi\|_\infty \leq 1} \dot{\mathbf{x}}(t)^\top \phi.$$

Here we moved the limit $\lim_{dt \rightarrow 0} [\mathbf{x}(t + dt) - \mathbf{x}(t)]/dt = \dot{\mathbf{x}}(t)$ inside the linear program (S21). This is justified because the maximum of this optimization is bounded and convex in $\mathbf{x}(t') - \mathbf{x}(t)$, therefore it is continuous in $\mathbf{x}(t') - \mathbf{x}(t)$.

To derive Eq. (S21), we first drop the positivity constraint in (S20). To do so, observe that for any real-valued $\mathbf{m} \in \mathbb{R}^m$ that satisfies the evolution constraint in (S21), we can define a non-negative vector $\mathbf{g} \in \mathbb{R}_+^m$ via

$$g_\rho = (m_\rho - m_{\bar{\rho}})^+,$$

where we introduced the notation $x^+ := \max\{0, x\}$. This vector also satisfies the evolution constraint:

$$\nabla^\top \mathbf{g} = \frac{1}{2} \nabla^\top (\mathbf{g} - \tilde{\mathbf{g}}) = \frac{1}{2} \nabla^\top (\mathbf{m} - \tilde{\mathbf{m}}) = \nabla^\top \mathbf{m}.$$

The middle step follows from anti-symmetry $\nabla_{\rho i} = -\nabla_{\bar{\rho} i}$ and the identity $x^+ - (-x)^+ = x$, so

$$g_\rho - g_{\bar{\rho}} = (m_\rho - m_{\bar{\rho}})^+ - (m_{\bar{\rho}} - m_\rho)^+ = m_\rho - m_{\bar{\rho}}.$$

Also, \mathbf{g} achieves no worse objective value as \mathbf{m} ,

$$\begin{aligned} \|\mathbf{g}\|_1 &= (\mathbf{m} - \tilde{\mathbf{m}})^+ \\ &= \frac{1}{2} [(\mathbf{m} - \tilde{\mathbf{m}})^+ + (\tilde{\mathbf{m}} - \mathbf{m})^+] \\ &= \frac{1}{2} \|\mathbf{m} - \tilde{\mathbf{m}}\|_1 \leq \frac{1}{2} (\|\mathbf{m}\|_1 + \|\tilde{\mathbf{m}}\|_1) = \|\mathbf{m}\|_1. \end{aligned}$$

To summarize, since the optimum in (S20) can always be achieved by a nonnegative vector, we do not need to impose nonnegativity as an additional constraint. Thus, W can be equivalently defined as

$$W(t, t') = \min_{\mathbf{g} \in \mathbb{R}_+^m} \|\mathbf{g}\|_1 \quad \text{where} \quad \nabla^\top \mathbf{g} = \mathbf{x}(t') - \mathbf{x}(t).$$

The expression (S21) follows from a standard duality result in linear algebra. To apply it, we use $\mathbf{x}(t') - \mathbf{x}(t) = \nabla^\top \mathbf{J}$, then change variables as $\mathbf{u} = \mathbf{J} - \mathbf{g}$, so that

$$W(t, t') = \min_{\mathbf{u} \in \ker \nabla^\top} \|\mathbf{J} - \mathbf{u}\|_1.$$

This is the minimization of the 1-norm subject to \mathbf{u} being in the kernel of ∇^\top , which enforces $\nabla^\top \mathbf{J} = \nabla^\top \mathbf{g}$. The duality of norm minimization [127, p. 119] then gives

$$W(t, t') = \max_{\mathbf{v} \in (\ker \nabla^\top)^\perp} \mathbf{v}^\top \mathbf{J} \quad \text{where} \quad \|\mathbf{v}\|_\infty \leq 1. \quad (\text{S22})$$

The condition $\mathbf{v} \in (\ker \nabla^\top)^\perp$ means that \mathbf{v} is in the orthogonal complement of $\ker \nabla^\top$, which is the image of ∇ . Thus, \mathbf{v} can always be written as $\mathbf{v} = \nabla \phi$ for some $\phi \in \mathbb{R}^d$. Plugging into (S22), and using $\mathbf{J}^\top \nabla \phi = (\mathbf{x}(t') - \mathbf{x}(t))^\top \phi$, gives (S21).

SM6: Comparison to other decompositions

Here we compare our approach to several excess/housekeeping decompositions that have been previously proposed in the literature.

1. Hatano-Sasa (HS) decomposition

We derive an inequality between our excess/housekeeping EPR and the HS excess/housekeeping EPR:

$$\sigma_{\text{hk}} \leq \sigma_{\text{hk}}^{\text{HS}} \quad \sigma_{\text{ex}} \geq \sigma_{\text{ex}}^{\text{HS}} \quad (\text{S23})$$

Our derivations apply to (1) MJPs without odd variables, (2) MJPs with odd variables and time-symmetric steady states, and (3) deterministic CRNs with complex balance and mass-action kinetics. In all cases, we show that the HS housekeeping EPR can be written as the generalized relative entropy,

$$\sigma_{\text{hk}}^{\text{HS}} = \mathcal{D}(\mathbf{f} \| -\nabla \phi^{\text{ss}}), \quad (\text{S24})$$

where $\phi_i^{\text{ss}} := \ln(x_i/x_i^{\text{ss}})$ is defined via the steady-state distribution \mathbf{x}^{ss} . Since our housekeeping EPR satisfies the variational principle in (59), Eq. (S24) implies Eq. (S23).

We first consider the simplest case, MJPs without odd variables. The HS excess and housekeeping terms are given by [32, 62]

$$\sigma_{\text{ex}}^{\text{HS}} = \sum_{j \neq i, \alpha} x_i R_{ji}^\alpha \ln \frac{x_i x_j^{\text{ss}}}{x_j x_i^{\text{ss}}} \quad (\text{S25})$$

$$\sigma_{\text{hk}}^{\text{HS}} = \sigma - \sigma_{\text{ex}}^{\text{HS}} = \sum_{j \neq i, \alpha} x_i R_{ji}^\alpha \ln \frac{x_i R_{ji}^\alpha}{x_i R_{ij}^\alpha x_j^{\text{ss}} / x_i^{\text{ss}}}. \quad (\text{S26})$$

Within our exponential family Eq. (61), the conservative force $-\nabla \phi^{\text{ss}}$ specifies the fluxes

$$[\tilde{\mathbf{j}} \circ e^{-\nabla \phi^{\text{ss}}}]_{i \rightarrow j; \alpha} = x_j R_{ij}^\alpha e^{\ln(x_i/x_i^{\text{ss}}) - \ln(x_j/x_j^{\text{ss}})} = x_i R_{ij}^\alpha \frac{x_j^{\text{ss}}}{x_i^{\text{ss}}}$$

In the notation (60), this leads to Eq. (S24),

$$\begin{aligned} \mathcal{D}(\mathbf{f} \| -\nabla \phi^{\text{ss}}) &= \sum_{j \neq i, \alpha} \left(x_i R_{ji}^\alpha \ln \frac{x_i R_{ji}^\alpha}{x_i R_{ij}^\alpha x_j^{\text{ss}} / x_i^{\text{ss}}} - x_i R_{ji}^\alpha + x_i R_{ij}^\alpha \frac{x_j^{\text{ss}}}{x_i^{\text{ss}}} \right) \\ &= \sum_{j \neq i, \alpha} x_i R_{ji}^\alpha \ln \frac{x_i R_{ji}^\alpha}{x_i R_{ij}^\alpha x_j^{\text{ss}} / x_i^{\text{ss}}} = \sigma_{\text{hk}}^{\text{HS}}, \end{aligned} \quad (\text{S27})$$

where in the second line we used that

$$\begin{aligned} \sum_{j \neq i, \alpha} \left(x_i R_{ji}^\alpha \frac{x_j^{\text{ss}}}{x_i^{\text{ss}}} - x_i R_{ij}^\alpha \right) \\ = \sum_i \frac{x_i}{x_i^{\text{ss}}} \sum_{j(\neq i), \alpha} \left(x_j^{\text{ss}} R_{ij}^\alpha - x_i^{\text{ss}} R_{ji}^\alpha \right) = 0, \end{aligned}$$

which follows since \mathbf{x}^{ss} is a steady-state distribution.

Next, we consider MJPs with odd variables, under the assumption that the steady-state distribution is symmetric under conjugation of odd variables,

$$x_i^{\text{ss}} = x_{\epsilon i}^{\text{ss}}. \quad (\text{S28})$$

(Note that this condition is violated in our example of the particle on a ring from Appendix B 3 whenever $\gamma \neq 0$.) The EPR is given by

$$\sigma = \sum_{j \neq i, \alpha} \left(x_i R_{ji}^\alpha \ln \frac{x_i R_{ji}^\alpha}{x_j R_{\epsilon i \epsilon j}^\alpha} - x_i R_{ji}^\alpha + x_j R_{\epsilon i \epsilon j}^\alpha \right), \quad (\text{S29})$$

as discussed near Eq. (B3) above. The HS excess EPR is still defined as in Eq. (S25), while the HS housekeeping EPR is the remainder [68, 69], $\sigma_{\text{hk}}^{\text{HS}} = \sigma - \sigma_{\text{ex}}^{\text{HS}}$. Rearranging gives

$$\sigma_{\text{hk}}^{\text{HS}} = \sum_{j \neq i, \alpha} \left(x_i R_{ji}^\alpha \ln \frac{x_i R_{ji}^\alpha}{x_i R_{\epsilon i \epsilon j}^\alpha x_j^{\text{ss}} / x_i^{\text{ss}}} - x_i R_{ji}^\alpha + x_j R_{\epsilon i \epsilon j}^\alpha \right). \quad (\text{S30})$$

In parameterized family of fluxes, we have

$$[\tilde{\mathbf{j}} \circ e^{-\nabla \phi^{\text{ss}}}]_{i \rightarrow j; \alpha} = x_j R_{\epsilon i \epsilon j}^\alpha e^{\ln x_i / x_i^{\text{ss}} - \ln x_j / x_j^{\text{ss}}} = x_i R_{\epsilon i \epsilon j}^\alpha \frac{x_j^{\text{ss}}}{x_i^{\text{ss}}}$$

This leads to the following value of the relative entropy:

$$\begin{aligned} \mathcal{D}(\mathbf{f} \| -\nabla \phi^{\text{ss}}) &= \sum_{j \neq i, \alpha} \left(x_i R_{ji}^\alpha \ln \frac{x_i R_{ji}^\alpha}{x_i R_{\epsilon i \epsilon j}^\alpha x_j^{\text{ss}} / x_i^{\text{ss}}} - x_i R_{ji}^\alpha + x_i R_{\epsilon i \epsilon j}^\alpha \frac{x_j^{\text{ss}}}{x_i^{\text{ss}}} \right) \end{aligned} \quad (\text{S31})$$

Finally, we have

$$\begin{aligned} \sum_{j \neq i, \alpha} \left(x_i R_{\epsilon i \epsilon j}^\alpha \frac{x_j^{\text{ss}}}{x_i^{\text{ss}}} - x_j R_{\epsilon i \epsilon j}^\alpha \right) \\ = \sum_{j \neq i, \alpha} \left(x_i R_{\epsilon i \epsilon j}^\alpha \frac{x_j^{\text{ss}}}{x_i^{\text{ss}}} - x_i R_{\epsilon j \epsilon i}^\alpha \right) \\ = \sum_i \frac{x_i}{x_i^{\text{ss}}} \sum_{j(\neq i), \alpha} \left(R_{\epsilon i \epsilon j}^\alpha x_j^{\text{ss}} - R_{\epsilon j \epsilon i}^\alpha x_i^{\text{ss}} \right) \\ = \sum_i \frac{x_i}{x_i^{\text{ss}}} \sum_{j(\neq i), \alpha} \left(R_{\epsilon i \epsilon j}^\alpha x_{\epsilon j}^{\text{ss}} - R_{\epsilon j \epsilon i}^\alpha x_{\epsilon i}^{\text{ss}} \right) = 0, \end{aligned}$$

where we used the symmetry (S28). Plugging $\sum_{j \neq i, \alpha} x_i R_{\epsilon i \epsilon j}^\alpha x_j^{\text{ss}} / x_i^{\text{ss}} = \sum_{j \neq i, \alpha} x_j R_{\epsilon j \epsilon i}^\alpha$ into Eq. (S31) shows it is the same as the expression for $\sigma_{\text{hk}}^{\text{HS}}$ in Eq. (S30), thus giving Eq. (S24).

Finally, we consider deterministic CRNs that obey complex balance, which means that the net current entering and leaving each chemical complex vanishes in steady state [47]. We also assume mass-action kinetics, as in Eq. (13). In that case, the HS excess and housekeeping EPR are given by [41, 42]

$$\sigma_{\text{ex}}^{\text{HS}} = - \sum_{\rho} j_{\rho} \sum_i \nabla_{\rho i} \ln \frac{x_i}{x_i^{\text{ss}}}. \quad (\text{S32})$$

$$\sigma_{\text{hk}}^{\text{HS}} = \sigma - \sigma_{\text{ex}}^{\text{HS}} = \sum_{\rho} j_{\rho} \left(\ln \frac{j_{\rho}}{\tilde{j}_{\rho}} + \sum_i \nabla_{\rho i} \ln \frac{x_i}{x_i^{\text{ss}}} \right) \quad (\text{S33})$$

Using the steady-state potential $\phi_i^{\text{ss}} := \ln(x_i/x_i^{\text{ss}})$, Eq. (S33) can be written as

$$\sigma_{\text{hk}}^{\text{HS}} = \mathbf{j}^{\top} (\mathbf{f} + \nabla \phi^{\text{ss}}). \quad (\text{S34})$$

We also have the expression of the relative entropy as

$$\mathcal{D}(\mathbf{f} \| -\nabla \phi^{\text{ss}}) = \mathbf{j}^{\top} (\mathbf{f} + \nabla \phi^{\text{ss}}) - \sum_{\rho} (j_{\rho} - \tilde{j}_{\rho} e^{[-\nabla \phi^{\text{ss}}]_{\rho}}).$$

Using this result and Eq. (S34), we prove Eq. (S24) by showing

$$\sum_{\rho} (j_{\rho} - \tilde{j}_{\rho} e^{[-\nabla \phi^{\text{ss}}]_{\rho}}) = 0. \quad (\text{S35})$$

To begin, we split Eq. (S35) into contributions from the forward and backward direction of each reversible reaction r ,

$$\sum_r (j_r^+ - j_r^- e^{[-\nabla \phi^{\text{ss}}]_r}) + \sum_r (j_r^- - j_r^+ e^{[\nabla \phi^{\text{ss}}]_r}). \quad (\text{S36})$$

For mass-action kinetics Eq. (13), each term in the first sum can be written as

$$\begin{aligned} & j_r^+ - j_r^- e^{[-\nabla\phi^{\text{ss}}]_r} \\ &= k_r^{\rightarrow} \prod_i x_i^{\nu_{ir}} - k_r^{\leftarrow} \prod_i x_i^{\kappa_{ir}} \prod_i \left(\frac{x_i}{x_i^{\text{ss}}} \right)^{\nu_{ir} - \kappa_{ir}} \\ &= \prod_i \left(\frac{x_i}{x_i^{\text{ss}}} \right)^{\nu_{ir}} \left(k_r^{\rightarrow} \prod_i (x_i^{\text{ss}})^{\nu_{ir}} - k_r^{\leftarrow} \prod_i (x_i^{\text{ss}})^{\kappa_{ir}} \right) \\ &\equiv \prod_i \left(\frac{x_i}{x_i^{\text{ss}}} \right)^{\nu_{ir}} \mathcal{J}_\rho^{\text{ss}}, \end{aligned}$$

where $\mathcal{J}_\rho^{\text{ss}}$ is the current (net flux) across reversible reaction r in steady state. In similar way, we write each term in the second sum in Eq. (S36) as

$$j_r^- - j_r^+ e^{[\nabla\phi^{\text{ss}}]_r} = - \prod_i \left(\frac{x_i}{x_i^{\text{ss}}} \right)^{\kappa_{ir}} \mathcal{J}_\rho^{\text{ss}}. \quad (\text{S37})$$

Combining, we rewrite Eq. (S35) as

$$\sum_r \left[\prod_i \left(\frac{x_i}{x_i^{\text{ss}}} \right)^{\nu_{ir}} \mathcal{J}_\rho^{\text{ss}} - \prod_i \left(\frac{x_i}{x_i^{\text{ss}}} \right)^{\kappa_{ir}} \mathcal{J}_\rho^{\text{ss}} \right]. \quad (\text{S38})$$

Now split this sum into contributions from each reactant complex and each product complex. Let \mathcal{C} indicate the set of reactant and product complexes, where each element of \mathcal{C} is a vector $\boldsymbol{\eta} \in \mathbb{N}_0^d$ with η_i is the number of species i in complex $\boldsymbol{\eta}$. Let $A(\boldsymbol{\eta}) = \{r : \nu_{ir} = \eta_i \forall i\}$ and $B(\boldsymbol{\eta}) = \{r : \kappa_{ir} = \eta_i \forall i\}$ indicate the sets of reactions that complex $\boldsymbol{\eta}$ as reactant and product, respectively. Then, we can rewrite Eq. (S38) as

$$\begin{aligned} & \sum_{\boldsymbol{\eta} \in \mathcal{C}} \left[\sum_{r \in A(\boldsymbol{\eta})} \prod_i \left(\frac{x_i}{x_i^{\text{ss}}} \right)^{\nu_{ir}} \mathcal{J}_\rho^{\text{ss}} - \sum_{r \in B(\boldsymbol{\eta})} \prod_i \left(\frac{x_i}{x_i^{\text{ss}}} \right)^{\kappa_{ir}} \mathcal{J}_\rho^{\text{ss}} \right] \\ &= \sum_{\boldsymbol{\eta} \in \mathcal{C}} \left[\sum_{r \in A(\boldsymbol{\eta})} \prod_i \left(\frac{x_i}{x_i^{\text{ss}}} \right)^{\eta_i} \mathcal{J}_\rho^{\text{ss}} - \sum_{r \in B(\boldsymbol{\eta})} \prod_i \left(\frac{x_i}{x_i^{\text{ss}}} \right)^{\eta_i} \mathcal{J}_\rho^{\text{ss}} \right] \\ &= \sum_{\boldsymbol{\eta} \in \mathcal{C}} \prod_i \left(\frac{x_i}{x_i^{\text{ss}}} \right)^{\eta_i} \left[\sum_{r \in A(\boldsymbol{\eta})} \mathcal{J}_\rho^{\text{ss}} - \sum_{r \in B(\boldsymbol{\eta})} \mathcal{J}_\rho^{\text{ss}} \right]. \quad (\text{S39}) \end{aligned}$$

By the definition of complex balance, $\sum_{r \in A(\boldsymbol{\eta})} \mathcal{J}_\rho^{\text{ss}} = \sum_{r \in B(\boldsymbol{\eta})} \mathcal{J}_\rho^{\text{ss}}$ for each $\boldsymbol{\eta}$ [47]. Therefore, Eq. (S39), hence also Eq. (S35), vanishes, which implies Eq. (S24).

2. Euclidean-Onsager decomposition

In this paper, we considered the excess/housekeeping decomposition based on relative entropy between flux vectors. In our previous work, we explored a similar decomposition based on Euclidean distance.

In particular, the distance between forces \mathcal{D} , defined using relative entropy in Eq. (60), was instead defined using a generalized squared Euclidean norm,

$$\mathcal{D}'(\boldsymbol{\theta} \|\boldsymbol{\theta}') := \|\boldsymbol{\theta} - \boldsymbol{\theta}'\|_L^2 := \frac{1}{2}(\boldsymbol{\theta} - \boldsymbol{\theta}')^\top L(\boldsymbol{\theta} - \boldsymbol{\theta}'), \quad (\text{S40})$$

where $L \in \mathbb{R}_+^{m \times m}$ is a diagonal matrix with entries $L_{\rho\rho} = (j_\rho - \tilde{j}_\rho)/f_\rho$. L can be understood as a Onsager-type matrix that specifies a linear relationship between forces and net fluxes, $\boldsymbol{j} - \tilde{\boldsymbol{j}} = L\boldsymbol{f}$, thus we may term the decomposition as the *Euclidean-Onsager decomposition*. Note that the factor 1/2 appears in our definition of L , but not in Ref. [20], due to a minor change of convention (in this paper we consider reversible reactions as two separate reactions).

Using Eq. (S40), the overall EPR can be written as $\sigma = \|\boldsymbol{f} - \mathbf{0}\|_L^2$. The housekeeping EPR and generalized potential may be defined via a Euclidean projection,

$$\sigma_{\text{hk}}^{\text{ons}} = \min_{\boldsymbol{\phi}} \|\boldsymbol{f} - (-\nabla\boldsymbol{\phi})\|_L^2 \equiv \|\boldsymbol{f} - (-\nabla\boldsymbol{\phi}_{\text{ons}}^*)\|_L^2. \quad (\text{S41})$$

This is Euclidean analogue to Eq. (62), also the (Euclidean version of the) Pythagorean relation (65) applies in a similar way. However, the values of the generalized potential $\boldsymbol{\phi}_{\text{ons}}^*$, the housekeeping $\sigma_{\text{hk}}^{\text{ons}}$ and the excess EPR $\sigma_{\text{ex}}^{\text{ons}}$ are different when defined in terms of the Euclidean-Onsager distance rather than the relative entropy.

As discussed in Ref. [20], the Euclidean-Onsager excess EPR can be physically interpreted as the minimal EPR achievable by manipulating forces while keeping the Onsager-type coefficients L fixed. Our information-geometric decomposition is not interpreted in terms of a minimal EPR principle, but rather in terms of dynamical large deviations and thermodynamic uncertainty relations. The information-geometric approach is arguably more natural in the far-from-equilibrium regime, where the relationship between forces and net fluxes becomes nonlinear. Unlike the bounds derived in Ref. [20], our approach leads to speed limits that may be tight far-from-equilibrium and far-from-stationarity.

We now show that the two approaches agree to third order in the linear-response regime near equilibrium. We also show that our excess EPR is always smaller than the Euclidean-Onsager excess EPR.

Recall that for systems without odd variables, each reaction ρ is paired with a unique reverse reaction $\tilde{\rho}$ such that $f_{\tilde{\rho}} = -f_\rho$. Consider the relative entropy between the forward fluxes $\boldsymbol{j} = \tilde{\boldsymbol{j}} \circ e^{\boldsymbol{f}}$ and any other $\tilde{\boldsymbol{j}} \circ e^{\boldsymbol{\theta}}$, where $\boldsymbol{\theta}$ is anti-symmetric ($\theta_\rho = -\theta_{\tilde{\rho}}$):

$$\begin{aligned} \mathcal{D}(\boldsymbol{f} \|\boldsymbol{\theta}) &= \sum_{\rho} j_\rho (e^{-(f_\rho - \theta_\rho)} + (f_\rho - \theta_\rho) - 1) \\ &= \sum_{\rho} \tilde{j}_\rho (e^{f_\rho - \theta_\rho} - (f_\rho - \theta_\rho) - 1). \end{aligned}$$

In the second line, we used anti-symmetry of \boldsymbol{f} and $\boldsymbol{\theta}$. Combining these expressions, and using $j_\rho = e^{f_\rho} \tilde{j}_\rho$, gives

$$\begin{aligned} \mathcal{D}(\boldsymbol{f} \|\boldsymbol{\theta}) &= \frac{1}{2} \sum_{\rho} \tilde{j}_\rho ((e^{f_\rho - \theta_\rho} - (f_\rho - \theta_\rho) - 1) \\ &\quad + e^{f_\rho} (e^{-(f_\rho - \theta_\rho)} + (f_\rho - \theta_\rho) - 1)). \end{aligned}$$

We now rewrite the right hand side as

$$\begin{aligned} \mathcal{D}(\mathbf{f} \parallel \boldsymbol{\theta}) &= \frac{1}{2} \sum_{\rho} \tilde{j}_{\rho} h(f_{\rho} - \theta_{\rho}, f_{\rho}) + \frac{e^{f_{\rho}} - 1}{f_{\rho}} (f_{\rho} - \theta_{\rho})^2 \\ &= \frac{1}{2} \sum_{\rho} \tilde{j}_{\rho} h(f_{\rho} - \theta_{\rho}, f_{\rho}) + \|\mathbf{f} - \boldsymbol{\theta}\|_L^2, \end{aligned} \quad (\text{S42})$$

where for convenience we defined the following function:

$$h(a, b) = \left[\frac{(e^a - a - 1) + e^b(e^{-a} + a - 1)}{a^2} - \frac{e^b - 1}{b} \right] a^2.$$

It can be verified that the term inside the brackets is always nonnegative. Thus, h is nonnegative, therefore $\mathcal{D}(\mathbf{f} \parallel \boldsymbol{\theta}) \geq \|\mathbf{f} - \boldsymbol{\theta}\|_L^2$ given Eq. (S42). Finally, since $\boldsymbol{\theta} = -\nabla\phi$ is anti-symmetric, we arrive at the inequality between the information-geometric and Euclidean-Onsager housekeeping EPR:

$$\sigma_{\text{hk}} = \min_{\boldsymbol{\phi}} \mathcal{D}(\mathbf{f} \parallel -\nabla\phi) \geq \min_{\boldsymbol{\phi}} \|\mathbf{f} - (-\nabla\phi)\|_L^2 = \sigma_{\text{hk}}^{\text{ons}}. \quad (\text{S43})$$

For a numerical comparison, see Section SM6.4.

We now consider the limit in which the two decompositions agree. Using the derivations above, we have the bounds

$$0 \leq \sigma_{\text{hk}} - \sigma_{\text{hk}}^{\text{ons}} \leq \frac{1}{2} \sum_{\rho} \tilde{j}_{\rho} h(f_{\rho} + [\nabla\phi_{\text{ons}}^*]_{\rho}, f_{\rho}). \quad (\text{S44})$$

The function $h(a, b)$ vanishes to first order around $a = b$ and $a = 0$ (in general, $h(a, b)$ is symmetric under the transformation $a \mapsto b - a$). Given Eq. (S44), considering $a = b$ implies that σ_{hk} and $\sigma_{\text{hk}}^{\text{ons}}$ agree to first order around $\nabla\phi_{\text{ons}}^* = 0$ (steady state) while considering $a = 0$ implies that they agree to first order around $\mathbf{f} = -\nabla\phi_{\text{ons}}^*$ (conservative forces in a passive systems). We can ask if they also agree to second order there. A Taylor expansion of $h(a, b)$ shows that second order terms do not vanish except in the limit $b \rightarrow 0$. Given Eq. (S44), this is the equilibrium limit $f_{\rho} \rightarrow 0$, where the force across each reaction vanishes. Note that

$$c_1 \|\mathbf{f}\|^2 \geq \|\mathbf{f}\|_L^2 \geq \|\mathbf{f} + \nabla\phi_{\text{ons}}^*\|_L^2 \geq c_2 \|\mathbf{f} + \nabla\phi_{\text{ons}}^*\|^2$$

where $c_1 = \max(j_{\rho} + \tilde{j}_{\rho})/2$, $c_2 = \min_{\rho} \sqrt{j_{\rho}\tilde{j}_{\rho}}$, and $\|\cdot\|$ is the usual Euclidean norm. The middle inequality comes from Eq. (S41), the others from bounds between the arithmetic, geometric, and logarithmic mean. Thus, if $f_{\rho} \rightarrow 0$, then $f_{\rho} + [\nabla\phi_{\text{ons}}^*]_{\rho}$, the first argument of h in Eq. (S44), also vanishes. We expand h in each argument and rearrange to give

$$h(\gamma, f) = \frac{1}{12} \gamma^2 (\gamma - f)^2 + \mathcal{O}(\epsilon^5) = \mathcal{O}(\epsilon^4) \quad (\text{S45})$$

for $f, \gamma \sim \epsilon$. Plugging into Eq. (S44) shows that σ_{hk} and $\sigma_{\text{hk}}^{\text{ons}}$ agree to third order in the equilibrium limit.

3. Maes-Netočný decomposition

Maes and Netočný (MN) proposed an excess/housekeeping decomposition for Langevin systems [35]. In later work, the

MN decomposition was shown to have a geometric interpretation in terms of Euclidean projections and optimal transport [71]. Recently, it has also been generalized to hydrodynamic systems [128].

Actually, the MN decomposition is recovered by the Euclidean-Onsager decomposition in the continuum limit of an MJP [20, Appendix B]. The continuum limit corresponds to the linear-response regime near equilibrium, where the information-geometric decomposition of this paper agrees with the Euclidean-Onsager one. Therefore, we may understand our decomposition (as well as the Euclidean-Onsager decomposition) as a generalization of the MN decomposition beyond linear response and beyond Langevin systems.

4. Numerical comparison with Refs. [20] and [45]

We numerically compare the excess/housekeeping decomposition from this paper with two others: the Euclidean-Onsager decomposition described in Section SM6.2, the ‘‘Hessian decomposition’’ recently proposed in Ref. [45] (see also Ref. [46]). While an inequality exists between the Euclidean-Onsager decomposition and our decomposition, Eq. (S43), no inequality between the Hessian decomposition and the others has been proved analytically. Nonetheless, our numerical results prove that they are different. They also suggest that the Hessian decomposition gives intermediate values between the other two decompositions, at least in one simple example.

To be self-contained, we briefly review the Hessian decomposition presented in Ref. [45]. Consider a system without odd variables that has reversible m reactions, having forward and reverse fluxes j_{ρ} and \tilde{j}_{ρ} . We use $r \in \{1, 2, \dots, M/2\}$ to label each pair of one-way reactions ρ and $\tilde{\rho}$, where the forward/reverse fluxes of the pair are indicated as $j_r^+ = j_{\rho}$ and $j_r^- = \tilde{j}_{\rho}$. We define a vector of currents (net fluxes) $\mathcal{J} \in \mathbb{R}^{M/2}$ as $\mathcal{J}_r := j_r^+ - j_r^-$, a vector of ‘‘frenetic activities’’ $\boldsymbol{\omega} \in \mathbb{R}_+^{M/2}$ as $\omega_r := 2\sqrt{j_r^+ j_r^-}$, and a vector of (half)forces $\mathcal{F} \in \mathbb{R}^{M/2}$ as $\mathcal{F}_r = \frac{1}{2} \ln(j_r^+ / j_r^-)$. We use the notation $\check{\nabla}^{\top}$ to indicate the $d \times m/2$ matrix that only has columns for the forward reaction (ρ) in each pair $(\rho, \tilde{\rho})$. $\check{\nabla}^{\top}$ maps currents to state evolution: $\dot{\mathbf{x}} = \check{\nabla}^{\top} \mathcal{J} = \nabla^{\top} \mathbf{j}$. Note that Ref. [45] uses the convention that forces $\mathcal{F}_r = \frac{1}{2} \ln(j_r^+ / j_r^-)$ are scaled by $1/2$ relative to the forces as defined in this paper, $f_r = \ln(j_r^+ / j_r^-)$.

The currents can be expressed as

$$\mathcal{J}_r = \omega_r \sinh(\mathcal{F}_r) = \sqrt{j_r^+ j_r^-} \left(\sqrt{\frac{j_r^+}{j_r^-}} - \sqrt{\frac{j_r^-}{j_r^+}} \right) = j_r^+ - j_r^-.$$

This equation can be solved for \mathcal{F}_r as

$$\mathcal{F}_r = \sinh^{-1}(\mathcal{J}_r / \omega_r).$$

These relations can also be derived from a canonical structure. Define two dual convex functions which are the Legendre conjugate of each other: for a fixed $\boldsymbol{\omega}$, the convex function

$$\Psi_{\boldsymbol{\omega}}(\mathcal{J}') := \sum_r \left[\mathcal{J}'_r \sinh^{-1} \frac{\mathcal{J}'_r}{\omega_r} - \omega_r \left[\sqrt{1 + \left(\frac{\mathcal{J}'_r}{\omega_r} \right)^2} - 1 \right] \right]$$

is the Legendre conjugate of

$$\Psi_\omega^*(\mathcal{F}') = \sum_r \omega_r \left[\cosh(\mathcal{F}'_r) - 1 \right],$$

and they specify the current and force across reaction r as

$$\mathcal{J}_r = \partial_{\mathcal{F}_r} \Psi_\omega^*(\mathcal{F}), \quad \mathcal{F}_r = \partial_{\mathcal{J}_r} \Psi_\omega(\mathcal{J}).$$

Note that for any ω , the minima of these functions is achieved at $\Psi_\omega(\mathbf{0}) = \Psi_\omega^*(\mathbf{0}) = 0$.

In general, a convex function $\varphi(\mathbf{x})$ induces the Bregman divergence $D_\varphi(\mathbf{x}, \mathbf{x}') := \varphi(\mathbf{x}) - \varphi(\mathbf{x}') - \langle \mathbf{x} - \mathbf{x}', \text{grad } \varphi(\mathbf{x}') \rangle \geq 0$, where $\langle \cdot, \cdot \rangle$ is the normal inner product and $\text{grad } \varphi(\mathbf{x}) = (\partial_{x_1} \varphi(\mathbf{x}), \partial_{x_2} \varphi(\mathbf{x}), \dots)^T$ is the gradient vector of the function [80]. For a fixed ω , we can define the Bregman divergences D_ω and the dual one D_ω^* by

$$\begin{aligned} D_\omega(\mathcal{J}', \mathcal{J}'') &:= \\ &\Psi_\omega(\mathcal{J}') - \Psi_\omega(\mathcal{J}'') - \langle \mathcal{J}' - \mathcal{J}'', \text{grad } \Psi_\omega(\mathcal{J}'') \rangle \\ D_\omega^*(\mathcal{F}', \mathcal{F}'') &:= \\ &\Psi_\omega^*(\mathcal{F}') - \Psi_\omega^*(\mathcal{F}'') - \langle \mathcal{F}' - \mathcal{F}'', \text{grad } \Psi_\omega^*(\mathcal{F}'') \rangle \end{aligned}$$

As a general property of Bregman divergences and the Legendre transformation, we have

$$D_\omega(\mathcal{J}', \mathcal{J}'') = D_\omega^*(\mathcal{F}', \mathcal{F}'') \quad (\text{S46})$$

when $(\mathcal{J}', \mathcal{F}')$ and $(\mathcal{J}'', \mathcal{F}'')$ are Legendre dual coordinates. In this situation, we also have

$$D_\omega(\mathcal{J}', \mathcal{J}'') = \Psi_\omega(\mathcal{J}') + \Psi_\omega^*(\mathcal{F}'') - \langle \mathcal{J}', \mathcal{F}'' \rangle, \quad (\text{S47})$$

which leads to

$$\sigma = \langle \mathcal{J}, \mathcal{F} \rangle = \Psi_\omega(\mathcal{J}) + \Psi_\omega^*(\mathcal{F}). \quad (\text{S48})$$

In general, these Bregman divergences cannot be expressed directly in terms of the relative entropy, because the current \mathcal{J}_r can be negative. Therefore, they do not relate to the EPR in the same direct way as the relative entropy \mathcal{D} in Eq. (16).

The Hessian decomposition [45] is defined by using two special points: $(\mathcal{J}_{\text{eq}}, \mathcal{F}_{\text{eq}})$, which represent conservative currents/forces, and $(\mathcal{J}_{\text{ss}}, \mathcal{F}_{\text{ss}})$, which represent steady-state currents/forces. Given these two pairs of currents/forces, we have

$$\sigma_{\text{hk}}^{\text{hess}} := \Psi_\omega(\mathcal{J}_{\text{eq}}) + D_\omega^*(\mathcal{F}, \mathcal{F}_{\text{ss}}), \quad (\text{S49})$$

$$\sigma_{\text{ex}}^{\text{hess}} := \Psi_\omega^*(\mathcal{F}_{\text{ss}}) + D_\omega(\mathcal{J}, \mathcal{J}_{\text{eq}}). \quad (\text{S50})$$

To explain how $(\mathcal{J}_{\text{eq}}, \mathcal{F}_{\text{eq}})$ and $(\mathcal{J}_{\text{ss}}, \mathcal{F}_{\text{ss}})$ are determined, we define two kinds of sets. $\mathcal{P}(\mathcal{J}')$ is the set of currents that induce the same dynamics as \mathcal{J}' ,

$$\mathcal{P}(\mathcal{J}') := \{ \mathcal{J}'' \in \mathbb{R}^{M/2} \mid \check{\nabla}^\top \mathcal{J}'' = \check{\nabla}^\top \mathcal{J}' \}. \quad (\text{S51})$$

$\mathcal{M}_\omega(\mathcal{F}')$ is defined as the set of currents that are given by \mathcal{F}' plus some conservative forces,

$$\mathcal{M}_\omega(\mathcal{F}') := \{ \text{grad } \Psi_\omega^*(\mathcal{F}'') \mid \mathcal{F}'' \in \mathcal{F}' + \text{im } \check{\nabla} \}, \quad (\text{S52})$$

where $\mathcal{F}' + \text{im } \check{\nabla} := \{ \mathcal{F}' + \check{\nabla} \phi \mid \phi \in \mathbb{R}^N \}$. Then, \mathcal{J}_{eq} and \mathcal{J}_{ss} are given as unique intersections as

$$\mathcal{J}_{\text{eq}} := \mathcal{P}(\mathcal{J}) \cap \mathcal{M}_\omega(\mathbf{0}), \quad \mathcal{J}_{\text{ss}} := \mathcal{P}(\mathbf{0}) \cap \mathcal{M}_\omega(\mathcal{F}), \quad (\text{S53})$$

while the corresponding forces \mathcal{F}_{eq} and \mathcal{F}_{ss} are given by $\text{grad } \Psi_\omega(\mathcal{J}_{\text{eq}})$ and $\text{grad } \Psi_\omega(\mathcal{J}_{\text{ss}})$. Therefore, holding the frenetic activity fixed, \mathcal{J}_{eq} is the current induced by a conservative force which recovers the original dynamics, while \mathcal{J}_{ss} is the steady-state current given by the force that has the same nonconservative contribution as the actual force.

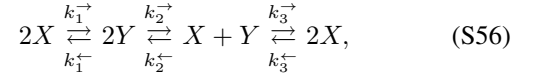
We note variational characterizations of $(\mathcal{J}_{\text{eq}}, \mathcal{F}_{\text{eq}})$ and $(\mathcal{J}_{\text{ss}}, \mathcal{F}_{\text{ss}})$, which simplify numerical calculation of the decomposition. \mathcal{J}_{eq} is given by

$$\mathcal{J}_{\text{eq}} = \underset{\mathcal{J}' \in \mathcal{P}(\mathcal{J})}{\text{argmin}} \Psi_\omega(\mathcal{J}'), \quad (\text{S54})$$

while \mathcal{F}_{ss} is obtained as

$$\mathcal{F}_{\text{ss}} = \underset{\mathcal{F}' \in \mathcal{F} + \text{im } \check{\nabla}}{\text{argmin}} \Psi_\omega^*(\mathcal{F}'). \quad (\text{S55})$$

Next, we consider a specific CRN as an example. In Ref. [45], the authors discuss the reaction network



with mass-action kinetics. We calculate our EPRs σ_{hk} , σ_{ex} , the Euclidean-Onsager EPRs $\sigma_{\text{hk}}^{\text{ons}}$, $\sigma_{\text{ex}}^{\text{ons}}$, and the Hessian EPRs $\sigma_{\text{hk}}^{\text{hess}}$, $\sigma_{\text{ex}}^{\text{hess}}$, with the same parameters as Ref. [45]. Concretely, we use the rate constants $k_1^+ = 1/2$, $k_1^- = 2$, $k_2^+ = 4$, $k_2^- = 47/4$, $k_3^+ = \sqrt{2}$, and $k_3^- = 15/2 + 2\sqrt{2}$ to obtain (a) in Figure S1, or $k_1^+ = 1/2$, $k_1^- = 2$, $k_2^+ = 1/17$, $k_2^- = 85/8$, $k_3^+ = 273/68$, and $k_3^- = 137/68$ to obtain (b). The three decompositions are exhibited in Figure S1, which reproduces numerical results obtained in Ref. [45]. The inequality $\sigma_{\text{ex}} \leq \sigma_{\text{ex}}^{\text{ons}}$ is also verified. In addition, we observe numerically that $\sigma_{\text{ex}} \leq \sigma_{\text{ex}}^{\text{hess}} \leq \sigma_{\text{ex}}^{\text{ons}}$, although we have not proved analytically that these inequalities hold in general.

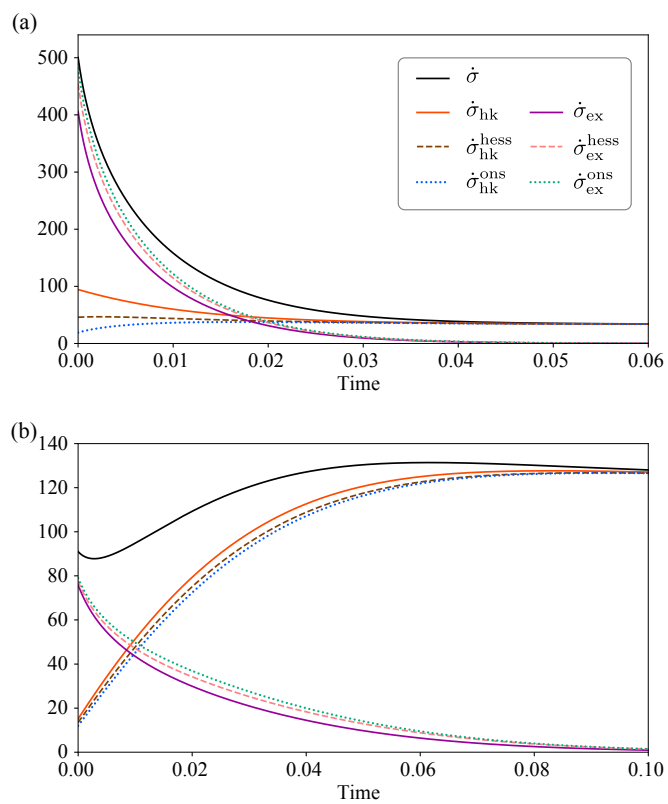


Figure S1. Comparison of three EPR decompositions. We calculate EPRs of the chemical reaction network in Eq. (S56) for two distinct rate constants (detailed values are given in the text).